

SARS CoV-2

Understanding the potential for enhanced disease

Marion F. Gruber, PhD Global Regulators Meeting Brussels March 18, 2020

Objectives

- Experience with other pathogens, e.g. RSV
Immunopathogenesis of Coronavirus vaccines
SARS-CoV MERS-CoV
Considerations for SARS-CoV-2 vaccine development
Topics for preclinical Roundtable

Respiratory syncytial virus (RSV) vaccine –enhanced disease

- In the 1960s, in clinical trials with a formalin inactivated RSV vaccine (FI-RSV) administered to children, vaccinated children experienced serious disease after acquiring a natural RSV infection Two of the vaccinees died and histological analysis of their lungs showed extensive mononuclear cell infiltration including pulmonary eosinophilia RSV challenge of FI-RSV vaccinated mice results in pulmonary eosinophilia mimicking the lung pathology observed in FI-RSV vaccinated children FI-RSV vaccinated mice challenged with RSV show increase levels of TH2 associated cytokines Increases of eosinophils are characteristic of Th2 –mediated immune responses Other contributing factors to FI-RSV vaccine-enhanced disease are immune complexes Castilow et al (2007) Understanding respiratory syncytial virus (RSV) vaccine-enhanced disease. Immunol. Res. 39:225-239

Immunopathogenesis of Coronavirus infections

Experience from SARS-CoV

- Severe acute respiratory syndrome (SARS) is an infectious disease caused by SARS-CoV. Originated in Guangdong province in China in late 2002, it spread around the globe resulting in > 8,000 cases and > 800 death in 33 countries. Outbreak controlled in 2003. Efforts to develop vaccines continued; however, studies in animal models suggested induction of enhanced disease and immunopathology in vaccinated animals that were subsequently challenged with infectious virus.

Immunopathogenesis of Coronavirus infections Experience from SARS-CoV (cont.)

- Ferrets and Cynomolgus monkeys administered an alum adjuvanted inactivated whole cell SARS vaccine followed by challenge with SARS CoV exhibited immunopathologic lung reaction characteristic of a Th2-type hypersensitivity that was similar to that described for respiratory syncytial virus in infants and animal models that were administered RSV vaccine and challenged with RSV due to either natural exposure or in the laboratory Perlman S (2005) Immunopathogenesis of coronavirus infections: Implications for SARS. Nature Rev. Immunol. 5:917-927 Haagmans BL et al (2005) Protective immunity induced by the inactivated SARS coronavirus vaccine. Abstract S 12-1 presented at the X International Nidovirus Symposium, Colorado, Springs, CO

Immunopathogenesis of Coronavirus infections

Experience from SARS-CoV (cont.)

- Tseng et al evaluated four vaccines with and without alum in a mouse model of SARS by immunizing animals IM on day 0 and 28 and challenge with live virus on day 56. A VLP vaccine, two whole virus vaccines, double-inactivated with formalin and UV, and inactivated with beta propiolactone. DNA-produced S protein. All vaccines induced antibody and protection against infection. All mice exhibited histopathologic changes in lungs 2 days after challenge. Histopathology in animals administered these SARS-CoV vaccines was uniformly a Th2-type immunopathology with eosinophil infiltration. Tseng C-T et al (2012) Immunization with SARS Coronavirus vaccines leads to pulmonary immunopathology on challenge with the SARS virus. Plos ONE Vol. 7 (4) e35421

Immunopathogenesis of Coronavirus infections

Experience from SARS-CoV (cont.)

- Additional reports described similar immunopathologic reactions in mice administered SARS-CoV vaccines and subsequently challenged with SARS-CoV Yasui F et al (2008) Prior immunization with severe acute respiratory syndrome (SARS) – associated coronavirus (SARS-CoV) nucleocapsid protein causes severe pneumonia in mice infected with SARS-CoV J. Immunol. 181: 6337-6348 Bolles et al (2011) A double-inactivated severe acute respiratory syndrome coronavirus vaccine provides incomplete protection in mice and induces increased eosinophilic proinflammatory pulmonary response upon challenge J. Virol. 85: 12201-12215

Immunopathogenesis of Coronavirus infections

Experience from MERS-CoV

- Middle East Respiratory Syndrome (MERS) emerged in 2012 underscoring the need for continued vaccine development against Coronaviruses Agrawal et al developed a transgenic mouse model containing the human DPP4 MERS-CoV receptor to evaluate whether Th2-type hypersensitivity immunopathology was observed upon vaccination with an inactivated MERS-CoV vaccine and subsequent challenge with MERS-CoV virus Neutralizing antibodies were induced and reduction in lung viral load was observed in vaccinated mice after challenge Lung mononuclear infiltrates occurred in all groups Increased infiltrates containing eosinophils in vaccinated groups only suggesting a Th2- type hypersensitivity lung pathology similar to that found with inactivated SARS-CoV vaccines Agrawal et al (2016) Immunization with inactivated Middle East Respiratory Syndrome coronavirus vaccine leads to lung immunopathology on challenge with live virus. Human Vaccines and Immunotherapeutics Vol. 12 (9): 2351-2356

Immunopathogenesis of Coronavirus infections

Experience from MERS-CoV (cont.)

- Other studies in transgenic mice models vaccinated with vaccine viral vectors, e.g., measles virus vector and modified vaccinia virus Ankara vector, encoding full-length MERS-CoV S induced neutralizing antibodies and T cell proliferation and protected against MERS-CoV challenge in these models without inducing lung pathology Volz et al (2015) Protective efficacy of recombinant modified vaccinia virus Ankara delivering Middle East respiratory syndrome Coronavirus Spike glycoprotein. J. Virol, 89: 8651-8656 Bodmer et al (2018) Live-attenuated bivalent measles virus-derived vaccines targeting Middle east respiratory syndrome coronavirus induce robust and multifunctional T cell responses against both viruses in an appropriate mouse model. Virology 2018, 521 99-107

Immunopathogenesis of Coronavirus infections

Experience from SARS-CoV & MERS-Cov (cont.)

- Additional studies in mice with inactivated SARS-CoV vaccines administered with a TH1-adjuvant did not exhibit a similar immunopathologic reaction following challenge with virus suggesting that the pulmonary immunopathology observed in vaccinated and challenged animals may represent an inadequate Th1 response Honda-Okubo et al (2015) Severe acute respiratory syndrome-associated coronavirus vaccines formulated with delta inulin adjuvants provide enhanced protection while ameliorating lung eosinophilic immunopathology J. Virol. 89: 2995-3007 Iwata-Yoshikawa et al (2014) Toll-like receptor stimulation on eosinophilic infiltration in lungs of BALB/c mice immunized with UV-inactivated severe acute respiratory syndrome-related coronavirus vaccine J. Virol. 88: 8597-614

Additional Immunological Mechanism that may potentially lead to Coronavirus Disease Enhancement

Observation of enhanced disease not vaccine related: Feline infectious peritonitis virus (FIPV) is a fatal disease characterized by antigen-antibody complex formation and complement activation in the late stage of disease. Induction of Anti-spike protein neutralizing antibodies which opsonize virus particles and facilitate their entry into macrophages through Fc receptor binding. Perlman S (2005) Immunopathogenesis of coronavirus infections: Implications for SARS. Nature Rev. Immunol. 5:917-927

WHO meeting Feb 11 & 12, 2020 - R & D Roadmap:

Evaluating potential for enhanced disease
Potential importance of cellular tropism (monocyte/macrophage)
Potential importance of CD8-mediated immune responses
Potential importance of high neutralizing responses
Animal models to study enhanced disease
Role of human clinical trials to evaluate enhanced disease

Considerations for SARS-CoV-2 vaccine development

Experience gained from Clinical trials conducted with FI-RSV
Studies with FI-RSV vaccinated mice subsequently challenged
with RSV
Studies with SARS-CoV and MERS-CoV vaccine-
immunized animal models subsequently challenged with CoV
underscores the need for careful and measured advances to
clinical trials with SARS-CoV-2 vaccine candidates in particular,
advancing to later stage clinical trials enrolling large numbers of
subjects

Considerations for SARS-CoV-2 vaccine development (cont.)

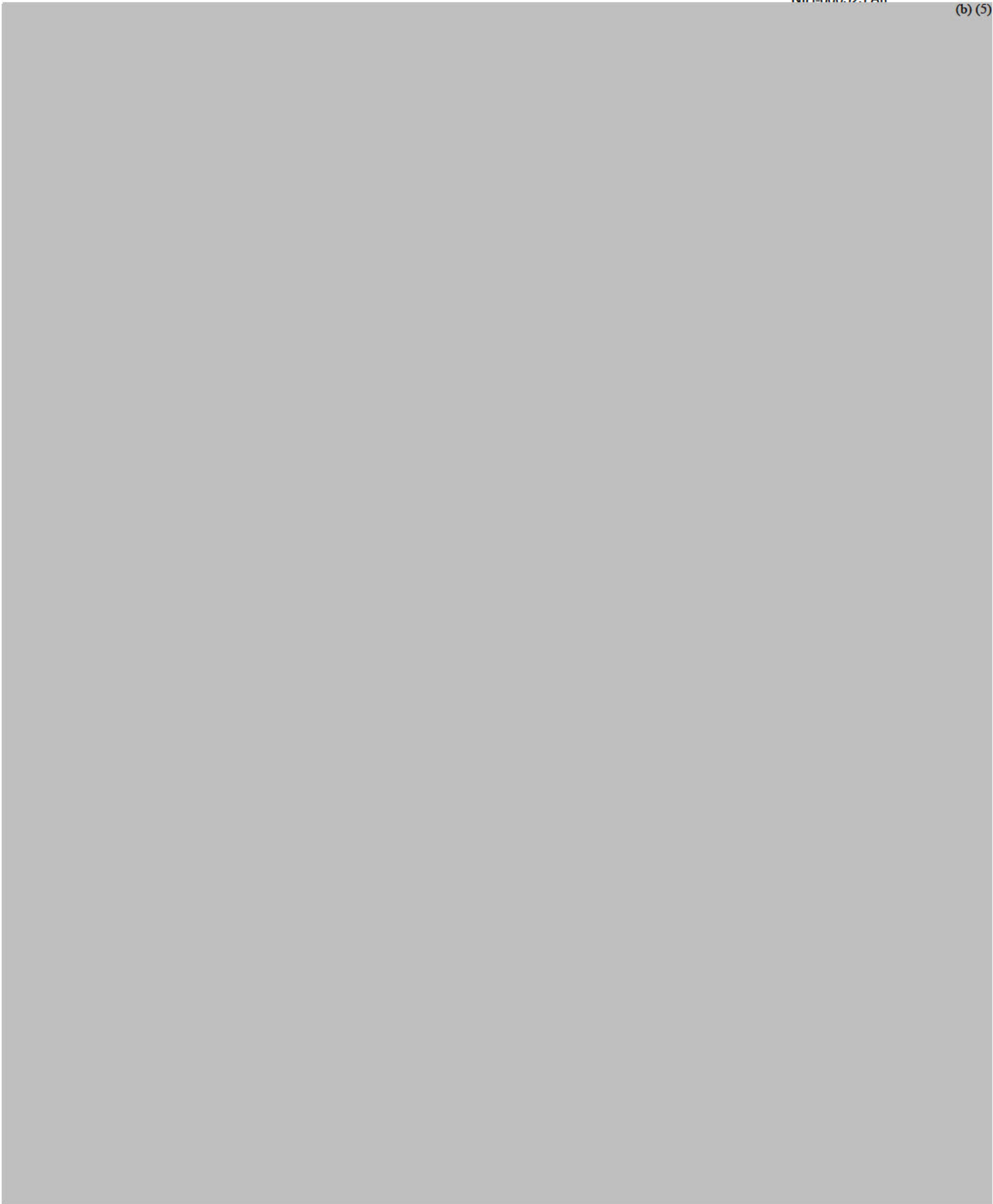
- Currently not known whether the findings observed in animal models vaccinated with SARS-CoV and MERS-CoV vaccine candidates will be replicated in animal models vaccinated with SARS-CoV-2 vaccine candidates
Currently not known whether the findings observed in animal models will occur in people vaccinated with SARS-CoV-2 vaccine candidates and then exposed to COVID-19
Depending on Vaccine characteristic ?Vaccine dose ?Prior exposure of subjects to same or other Coronaviruses ?Age of subjects ?Type of immune response induced ?The potential for disease enhancement induced by SARS-CoV -2 vaccine candidates will need to be addressed as part of vaccine development

Considerations for SARS-CoV-2 vaccine development (cont.)

- Of note, in the case of RSV vaccines, animal models of enhanced disease were set-up because of the clinical trial experience. For SARS-CoV and MERS-CoV, animal models were set-up in order to predict a possible safety issue with SARS-CoV and MERS-CoV vaccines without knowing whether such a problem will be seen in the clinic. Also it is not known whether the observation of enhanced disease observed in animal models of SARS-CoV and MERS-CoV will be observed with SARS-CoV-02

Discussion points for Pre-clinical Roundtable

- Proceeding with first in human clinical trials with SARS-CoV-2 vaccine candidates in the absence of animal data evaluating the potential for SARS-CoV-2 induced vaccine enhancement Will this decision depend on the characteristics of the vaccine (potential to induce TH1 type versus Th2 type immune response) Proceeding to larger Phase 2 and 3 clinical trials: What preclinical data need to be developed to address the potential for SARS-CoV-2 vaccine disease enhancement?



(b) (5)



Anti-spike IgG causes severe acute lung injury by skewing macrophage responses during acute SARS-CoV infection

Li Liu,^{1,2} Qiang Wei,³ Qingqing Lin,¹ Jun Fang,¹ Haibo Wang,¹ Hauyee Kwok,¹ Hangying Tang,¹ Kenji Nishiura,¹ Jie Peng,¹ Zhiwu Tan,¹ Tongjin Wu,¹ Ka-Wai Cheung,¹ Kwok-Hung Chan,¹ Xavier Alvarez,⁴ Chuan Qin,³ Andrew Lackner,⁴ Stanley Perlman,^{5,6} Kwok-Yung Yuen,¹ and Zhiwei Chen^{1,2}

¹AIDS Institute and Department of Microbiology, State Key Laboratory of Emerging Infectious Disease, Li Ka Shing Faculty of Medicine, The University of Hong Kong, Hong Kong, China. ²HKU-AIDS Institute Shenzhen Research Laboratory and AIDS Clinical Research Laboratory, Shenzhen Key Laboratory of Infection and Immunity, Shenzhen Key Clinical Department of Emerging Infectious Diseases, Shenzhen Third People's Hospital, Shenzhen, China. ³Institute of Laboratory Animal Science, Chinese Academy of Medical Sciences (CAMS) and Peking Union Medical College (PUMC), Beijing, China. ⁴Division of Comparative Pathology, Tulane National Primate Research Center, Covington, Louisiana, USA. ⁵Department of Microbiology and Immunology, University of Iowa, Iowa City, Iowa, USA. ⁶State Key Laboratory of Respiratory Disease, National Clinical Research Center for Respiratory Disease, Guangzhou Institute of Respiratory Health, the First Affiliated Hospital of Guangzhou Medical University, Guangzhou, China.

Newly emerging viruses, such as severe acute respiratory syndrome coronavirus (SARS-CoV), Middle Eastern respiratory syndrome CoVs (MERS-CoV), and H7N9, cause fatal acute lung injury (ALI) by driving hypercytokinemia and aggressive inflammation through mechanisms that remain elusive. In SARS-CoV/maaque models, we determined that anti-spike IgG (S-IgG), in productively infected lungs, causes severe ALI by skewing inflammation-resolving response. Alveolar macrophages underwent functional polarization in acutely infected macaques, demonstrating simultaneously both proinflammatory and wound-healing characteristics. The presence of S-IgG prior to viral clearance, however, abrogated wound-healing responses and promoted MCP1 and IL-8 production and proinflammatory monocyte/macrophage recruitment and accumulation. Critically, patients who eventually died of SARS (hereafter referred to as deceased patients) displayed similarly accumulated pulmonary proinflammatory, absence of wound-healing macrophages, and faster neutralizing antibody responses. Their sera enhanced SARS-CoV-induced MCP1 and IL-8 production by human monocyte-derived wound-healing macrophages, whereas blockade of FcγR reduced such effects. Our findings reveal a mechanism responsible for virus-mediated ALI, define a pathological consequence of viral specific antibody response, and provide a potential target for treatment of SARS-CoV or other virus-mediated lung injury.

Authorship note: AL is deceased.

Conflict of interest: This work was financially supported by grants from the US NIH R01HL080211 and HK RGC TRS T11-706/18-N to ZC, the TNPRC (base grant RR00164), R01060699 to SP, HMRF 16150662, and the University Development Fund/Li Ka Shing Faculty of Medicine Matching Fund of the University of Hong Kong to its AIDS Institute and Hong Kong RGV.

License: Copyright 2019, American Society for Clinical Investigation.

Submitted: July 23, 2018

Accepted: January 11, 2019

Published: February 21, 2019

Reference information:

JCI Insight. 2019;4(4):e123158.
<https://doi.org/10.1172/jci.insight.123158>.

Introduction

Severe acute respiratory syndrome coronavirus (SARS-CoV) causes fatal human respiratory disease (1–3). Patients with SARS (hereafter referred to as SARS patients) displayed the characteristics of acute lung injury (ALI), including diffuse alveolar damage (DAD), epithelial necrosis, and fibrin and hyaline deposition (4, 5). Most patients who die of SARS develop acute respiratory distress syndrome (ARDS), the most severe form of ALI (6, 7). Recent outbreaks of severe acute respiratory infections of emerging viruses, including Middle Eastern respiratory syndrome CoVs (MERS-CoV), highly pathogenic avian influenza viruses (e.g., H5N1 and H7N9), highlight the need to characterize the mechanisms responsible for virus-mediated ALI or ARDS.

Fundamental to ARDS is the acute onset of lung inflammation, which is intimately tied to monocyte/macrophage polarization and function (7, 8). Lung macrophages are highly plastic and heterogeneous cells that are resident in the lung interstitium and alveoli or recruited upon inflammatory stimuli. Inflammatory monocytes and resident tissue macrophages play critical roles in initiating and maintaining inflammation

during the acute stage of ARDS, as well as in the resolution phases of inflammation and recovery from ARDS. At steady state, resident macrophages are normally quiescent to prevent damaging the alveoli and are critically involved in normal tissue homeostasis. After tissue injury or during infection, resident macrophages become activated. Circulating monocytes can be efficiently recruited to the site of injury. Inflammatory monocytes/macrophages (IMMs) and resident macrophages undergo marked phenotypic and functional changes, and they can be classified into proinflammatory (M1 or classically activated) and inflammatory-resolving (M2, alternatively activated, wound-healing, or antiinflammatory) macrophages, with a continuum of macrophage polarization existing beyond these discrete categories (9). During acute infection, monocytes/macrophages often display a phenotype of classically activated macrophages. These cells mediate host defenses against viruses and also promote lung injury by producing nitric oxide (NO); ROS; IL-1, IL-6, and IL-8; and TNF. Simultaneously, some macrophages may become alternatively activated, exerting antiinflammatory function and regulating wound healing by producing matrix metalloproteinases (MMPs), growth factors, and antiinflammatory cytokines, particularly TGF- β . When the pathogen or inflammatory stimulus is eliminated, proinflammatory macrophages diminish. The predominant macrophage population assumes a wound-healing phenotype. At the final recovery stage, macrophages show a regulatory/suppressive phenotype, secreting increased levels of IL-10, which facilitates the resolution of wound healing and restores homeostasis. When the wound-healing response is well organized and controlled, the inflammatory response resolves quickly, and normal tissue architecture is restored. Disturbances in wound-healing response can lead to uncontrolled production of inflammatory mediators, contributing to a state of persistent injury (9–11). In patients who eventually died of SARS (hereafter referred to as deceased patients) and animal models, extensive lung damage is associated with high initial viral loads, increased IMM accumulation in the lungs, and elevated serum proinflammatory cytokine (IL-1, IL-6, IL-8, CXCL-10, and MCP1) levels (4, 5, 12, 13). While much is known about the terminal phase of SARS, little is known about the early immune events during the acute phase of infection. Studies defining macrophage heterogeneity and function during acute infection and ALI using nonhuman primate and patient specimens are limited, and the factors driving the hypercytokinemia and aggressive inflammation remain elusive.

During the SARS outbreak in Hong Kong, most patients (70%–80%) presented with abnormal chest radiographs, with approximately one-quarter of these individuals progressing to ALI. After 12 days, 80% of these SARS patients developed ARDS, coincident with IgG seroconversion (6). In a detailed analysis of antibody responses against SARS-CoV spike (S) glycoprotein, we reported that the anti-S neutralizing antibody (NAb) response developed significantly faster in deceased patients compared with recovered patients after the onset of clinical symptoms (14). It took an average of 20 days for the recovered patients to reach their peak of NAb activities, as opposed to only 14.7 days for the deceased patients. Moreover, the actual NAb titer is significantly higher in deceased patients compared with that in the recovered patients during the same time period (14). These findings suggest a role of anti-S antibodies in SARS-CoV-mediated ALI during acute infection. Consistently, preexisting serum antibodies against influenza antigens were found to associate with worse clinical severity and poor outcomes in patients during the 2009 influenza pandemic (15, 16). Moreover, multiple vaccine platforms and viral infection appeared to induce SARS-CoV-specific immune memory that enhanced lung inflammation following homologous challenge in mice and African green monkeys (17–19). The mechanism responsible for the immunopathologic reaction remains elusive. Recent studies suggested that T cells play a crucial role in protection of mice against lethal SARS-CoV infection (20–22). Enhanced pulmonary immunopathology in vaccinated and challenged animals reflects an inadequate Th1 response (22, 23). The role of virus-specific antibody response in SARS-CoV-induced lung injury has yet to be clearly defined. Therefore, we used vaccination and anti-S-IgG passive immunization strategies to evaluate the effects of anti-S antibodies on SARS-CoV-induced ALI in Chinese rhesus monkeys (*Macaca mulatta*). Our results now show that, in productively infected lungs, anti-S-IgG causes severe ALI by skewing inflammatory resolving responses during acute infection.

Results

Vaccine-induced S-specific immunity resulted in severe ALI in SARS-CoV infected Chinese macaques. We initially compared the pathological changes in the lungs of rhesus macaques vaccinated with a modified vaccinia Ankara (MVA) virus encoding full-length SARS-CoV S glycoprotein (ADS-MVA) or control at 7 and 35 days after pathogenic SARS-CoV_{PUMC} (1×10^5 tissue culture infectious dose of 50% [TCID₅₀]) challenge (24). Three healthy macaques were included as controls. Sixteen macaques were i.m. immunized twice: 8 animals with

ADS-MVA and another 8 animals with a control MVA (ADC-MVA) (Figure 1A) (24). Vaccination with ADS-MVA induced high levels of anti-SARS-CoV NABs in all 8 macaques, with sera IC_{50} values ranging from 10,232- to 28,703-fold dilutions (Figure 1B). None of the macaques developed fever during or after vaccination (normal body temperature 37.8°C–38.1°C). The IC_{50} values of these sera were maintained, with an over-2,000-fold reciprocal serum dilution at 4 weeks after the secondary immunization, a time when all of the animals were i.n. challenged (Figure 1B). After viral challenge, all macaques developed fever between 1 and 5 days after inoculation (dpi) ranging from 38.6°C–39.2°C, and sera from control vaccinated macaques showed increased neutralizing activity after 14 dpi, indicating establishment of infection (Figure 1B). SARS-CoV RNA was readily detected on oral swabs from all control macaques examined at multiple time points using real-time reverse transcription PCR (real-time RT-PCR) but only in 3 of the 8 ADS-MVA-vaccinated macaques with lower NAb titers at 2 dpi (SL11, SE13, and SL14) (Figure 1C), suggesting reduced productive viral infection in the immunized macaques through S-specific immunity.

However, histological examination revealed acute DAD with various degrees of severity in 6 ADS-MVA-vaccinated macaques at 7 and 35 dpi, whereas most control macaques in the ADC-MVA group showed minor to moderate inflammation (Figure 1D). To better characterize the pathological changes, we adopted a 6-grade scoring system to describe the severity of the lung damage from least severe to most severe: 0, -; 1, +; 2, ++; 3, +++; 4, ++++; and 5, +++++ (Supplemental Figure 1; supplemental material available online with this article; <https://doi.org/10.1172/jci.insight.123158DS1>). In the control vaccinated group, 5 macaques showed minor inflammation with slight septa broadening and inflammatory cells infiltration that we scored as + (CL23, CE25, CE20, CE21, and CL19; Figure 1D, Supplemental Figure 1B, and Supplemental Figure 2). Two macaques showed moderate inflammation with more interstitial mononuclear inflammatory infiltration and were scored as ++ (CL26, CE24; Supplemental Figure 1C and Supplemental Figure 2). Only 1 macaque showed typical symptoms of acute DAD with extensive exudation and cell infiltration at 35 dpi (CL22, scored as +++++; Supplemental Figure 2). In the ADS-MVA-vaccinated group, 4 macaques showed typical symptom of acute DAD with extensive exudation and many-cell infiltration in alveolar cavities (SL11, SE12, SL16, and SL18, scored as +++++; Supplemental Figure 1E and Supplemental Figure 2). One macaque showed severe acute DAD with exudation, hyaline membrane formation along the alveoli, pneumocyte desquamation, and damaged alveolus filled with hemorrhage and inflammatory cells (SL15, scored as +++++; Figure 1D). One macaque showed early symptom of acute DAD (SL14, scored as +++; Supplemental Figure 1D), and the remaining 2 macaques showed moderate inflammation (SE13 and SE17, scored as ++; Supplemental Figure 2). The comparison of lung histopathological scores of 2 groups showed significantly enhanced lung injury in the ADS-MVA-vaccinated group at both 7 and 35 dpi compared with the control ADC-MVA group, suggesting that S-specific — but not MVA-specific — immunity promotes ALI during SARS-CoV infection (Figure 1E). Moreover, there is a moderate correlation between lung pathological scores and sera NAB titers at 0 dpi (Figure 1F), suggesting a role of S-specific antibody in enhancing SARS-CoV-mediated lung injury.

Anti-S-IgG induced severe lung injury during acute SARS-CoV infection. In our previous study, i.n. inoculation of Chinese macaques with SARS-CoV_{PUMC} (1×10^5 TCID₅₀) led to lower respiratory tract infection in all animals within 2 days (25). However, most of them rapidly cleared infection in the lungs, and all of the animals ($n = 8$) exhibited mild lung lesions before 3 dpi (25). Severe lung injury in SARS-CoV-infected Chinese macaques has not been detected until 7 dpi (26, 27). To determine the effect of anti-S antibody on the extent of SARS-CoV-mediated lung injury, we adoptively transferred 5 mg (low dose) and 200 mg (high dose) purified anti-S-IgG from ADS-MVA-vaccinated but unchallenged macaques into 2 groups of unvaccinated macaques ($n = 6$ /group) via i.v. injection, and then i.n. challenged recipients with SARS-CoV_{PUMC} (1×10^5 TCID₅₀) (Figure 2A). As controls, another 2 macaques were administered 200 mg of control IgG (C-IgG) derived from ADC-MVA-vaccinated macaques. We sacrificed half of the macaques in each group at 2 dpi to avoid potential disruption by virus infection-induced antibodies against nucleocapsid protein (N) and other viral proteins — and prior to when induction of ALI was typically observed. The remaining half of the macaques in each group was sacrificed at 21 dpi to evaluate long-term impact (Figure 2A). At day 2, sera from macaques that received low- or high-dose S-IgG showed neutralizing activity, with IC_{50} values ranging from 10–260 and 1,000–10,000, corresponding to the dose of sera transfer; macaques that received C-IgG failed to show neutralizing activity (Figure 2B and Supplemental Table 1). While NAb titers in the sera of macaques in the high-dose group declined steadily between 2 and 21 dpi, macaques in the low-dose and control groups displayed increased NAB titers over time (Figure 2B), suggesting active viral replication.

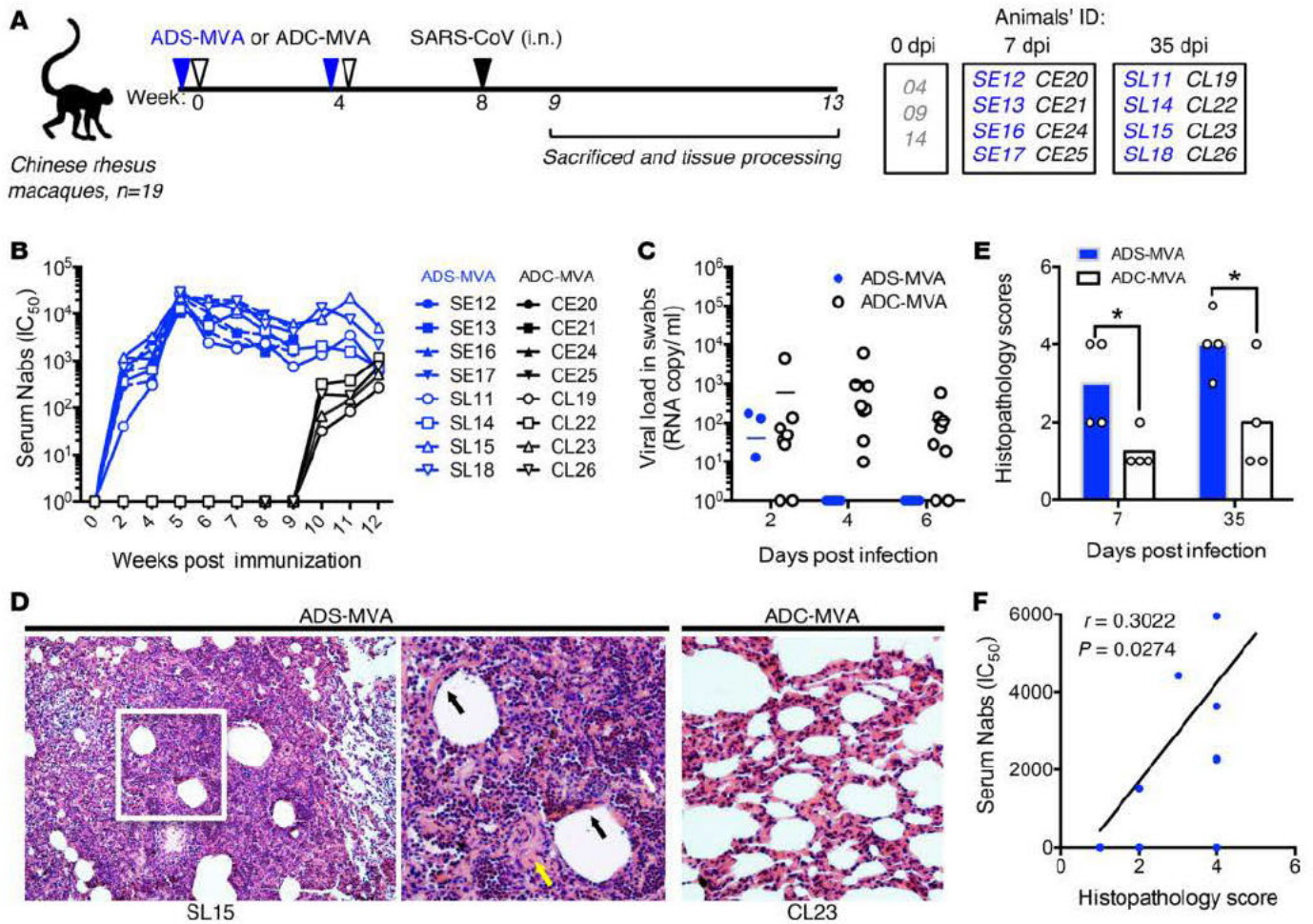


Figure 1. ADS-MVA–induced S-specific immune response enhanced pulmonary pathology in SARS-CoV-infected Chinese rhesus macaques. (A) Experimental design used to investigate the influence of S-specific immunity on SARS-CoV–induced lung injury. Two groups of Chinese rhesus macaques ($n = 8$ /group) were subjected to i.m. injections of ADS-MVA or control vaccine ADC-MVA at weeks 0 and 4, followed by i.n. challenge with live pathogenic SARS-CoV_{PUMC} (1×10^5 TCID₅₀) at 4 weeks after the second vaccination. Four animals each were sacrificed at 1 and 5 weeks after inoculation. Three healthy macaques were included as controls. (B) Serum neutralizing activity. Sera collected from macaques were tested for a capacity to neutralize SARS-CoV pseudotype virus. (C) Detection of viral RNA in oral swabs. SARS-CoV RNA was detected by nested RT-PCR in the swabs at the indicated time points relative to infection. (D) Pathology changes of the lung tissue. Sections were stained with H&E. D shows symptom of acute DAD exhibited in 6 of 8 ADS-MVA–vaccinated macaques with extensive exudation (yellow arrow), hyaline membranes lining the alveolar walls (black arrows), and massive cell infiltration in alveolar cavities (white arrow). Left image shows a low magnification overview (100 \times). Middle image shows higher magnification of the boxed area in left image (200 \times). Right image shows minor inflammation observed in 7 macaques received ADC-MVA ($n = 8$) with slight alveolar septa broadening and sparse monocyte infiltration (original magnification, 100 \times). (E) Histopathological scores of the ADS-MVA group, including lung samples collected at both 7 and 35 dpi, were compared against the ADC-MVA control group. See Supplemental Figure 1 for the scoring index based on severity of lung histopathology. Data represent mean \pm SEM values. Statistical analysis was undertaken using 2-tailed unpaired Student's *t* test. * $P < 0.05$, $n = 4$. (F) Correlation of lung histopathological scores of all macaques with sera NAb titers at 0 dpi. Solid lines denote the relationship between histopathology scores and serum neutralizing activity. Statistical analysis was performed using Spearman's rank correlation test.

Indeed, SARS-CoV RNA was detected using real-time RT-PCR on oral swabs, and/or virus was recovered from lung tissue in both control animals and 5 of 6 animals (83%) in the low-dose group. Only 2 of 6 animals (33%) in the high-dose group were viral RNA⁺ (Figure 2C and Supplemental Table 1), suggesting reduced viral production by high-dose S-IgG.

Consistent with the findings in the control ADC-MVA–vaccinated group, histopathological examination of the lungs indicated minor and moderate inflammation at day 2 and 21 in C-IgG recipients, respectively. In contrast, all S-IgG recipients exhibited symptoms of acute DAD with various degrees of exudation, hyaline membrane formation, and hemorrhage and inflammatory cells within alveolus at both day 2 and 21 (Figure 2, D and E, and Supplemental Table 2). Of note, despite the presence of high titer sera NAbs during the chronic stage of infection (Figure 1B and Figure 2B), only 1 of 5 C-IgG and control

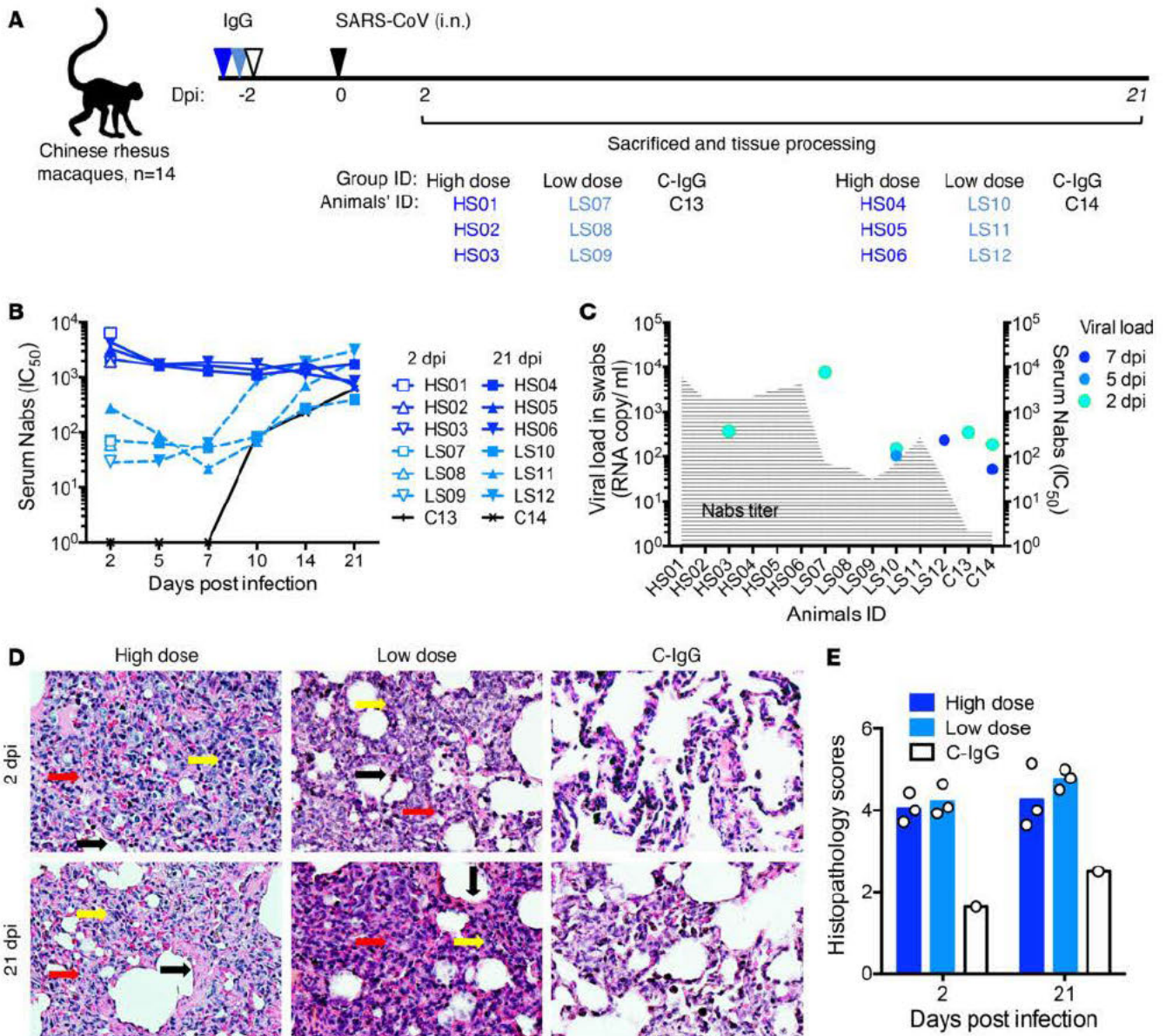


Figure 2. Anti-spike antibodies induced ALI in SARS-CoV-infected Chinese rhesus macaques. (A) Experimental design used to investigate the influence of S-IgG on SARS-CoV-induced lung injury. Two groups of Chinese rhesus macaques ($n = 6$ /group) were subjected to i.v. injection of high-dose (200 mg) or low-dose (5 mg) purified S-IgG from ADS-MVA-vaccinated but unchallenged macaques. As controls, another 2 macaques were administered 200 mg of C-IgG derived from ADC-MVA-vaccinated macaques. After 2 days, 3 groups of macaques were challenged i.n. with SARS-CoV_{PUMC} (1×10^5 TCID₅₀). Half of the animals from each group were sacrificed at 2 and 21 dpi. (B) Sera from macaques at the indicated time points were tested for the capacity to neutralize SARS-CoV pseudotype virus. (C) Detection of viral RNA in oral swabs. SARS-CoV RNA was detected by nested RT-PCR in the swabs from one of the high-dose S-IgG-treated macaques ($n = 6$), 3 low-dose S-IgG-treated macaques ($n = 6$), and 2 C-IgG-treated macaques ($n = 2$) at the indicated time points. Left y axis shows the viral RNA copy number per milliliter swab. Right y axis shows the serum NAB titers of each macaque at 2 dpi, which are highlighted by shaded area. (D) Pathology changes of the lung tissue (200x). Sections from macaques were stained with H&E. Images show symptom of acute DAD exhibited in macaques received high-dose and low-dose S-IgG ($n = 12$) with extensive exudation (red arrows), hyaline membranes (black arrows), and massive cell infiltration (yellow arrows) at 2 and 21 dpi. Right panel shows minor and moderate inflammation in the macaques received C-IgG with slight alveolar septa broadening and sparse monocyte infiltration at 2 and 21 dpi. (E) Histopathological scores of the high-dose and low-dose S-IgG groups, including lung samples collected at both 2 and 21 dpi, were compared against the C-IgG group. See Supplemental Figure 1 for the scoring index based on severity of lung histopathology.

ADC-MVA vaccine recipients showed acute DAD (Figure 1E and Figure 2E), indicating a time-restricted role for S-IgG, which mostly causes severe ALI in acutely infected macaques. Therefore, we conclude that, despite viral suppression, the presence of S-IgG at the acute stage of SARS-CoV infection caused severe ALI that persists until late stages.

S-IgG failed to prevent SARS-CoV lower respiratory tract infection and amplified IMM infiltration and accumulation in the lungs. To determine the potential cause of S-IgG-enhanced ALI, we measured viral infection and monocytes/macrophages infiltration in the lungs and serum cytokine profile at 2 dpi. We previously found that pulmonary infection of Chinese macaques could be rapidly controlled. Viral RNA⁺ cells were detectable in the lungs of only 2 of 4 animals at 2 dpi, although all of them were viral nucleoprotein-positive (NP⁺) in the lungs and the hilar lymph nodes (LNs), where the lymphatics of the lungs drain (25). Therefore, we measured viral RNA⁺ cells by in situ hybridization (ISH), as well as NP signals in the lungs and the hilar LNs by IHC staining to evaluate the actual pulmonary infection of each macaque. Consistent with the results by viral isolation (Supplemental Table 1), viral RNA was detected in pneumocytes of 1 macaque in the high-dose (HS02, 33%), 2 macaques in the low-dose (LS01, LS02; 66%), and the C-IgG-treated macaque (Figure 3A and Supplemental Table 3), suggesting reduced productive infection by S-IgG. However, an NP antibody identified positive signals in the lungs and hilar LNs of all S-IgG and C-IgG recipients (7 of 7 macaques) but not healthy controls (Figure 3B and Supplemental Table 3), suggesting that S-IgG failed to prevent SARS-CoV entry, and SARS-CoV established lower respiratory tract infection in all of the challenged animals.

Consistent with previous findings in SARS-CoV-inoculated naive Chinese macaques ($n = 4$) (25), double-immunostaining with the NP antibody and antibodies specific to the stages of macrophage differentiation and inflammation (MAC387, CD68, CD163) revealed significant infiltration of IMMs in the lungs of C-IgG recipients, consisting of newly infiltrated (MAC387⁺) and inflammatory (CD163⁺) monocytes/macrophages (Figure 3C and Supplemental Figure 3). The CD163⁺ cells greatly exceeded the CD68⁺ population and typically gathered around NP⁺ cells to form cell clusters (Figure 3C), showing an association between viral infection and IMM infiltration in these macaques.

Compared with C-IgG recipients, more robust signals for MAC387 and CD163 were identified in the lungs of S-IgG recipients (Figure 3C and Supplemental Figure 3), suggesting enhanced IMM infiltration by S-IgG. MAC387⁺ and CD163⁺ monocytes/macrophages not only gathered around NP⁺ cells, but also formed clusters in tissues with little NP signal (Figure 3C), suggesting that infection-induced recruitment from circulation continued after viral clearance and accumulated at the inflamed site. Moreover, more-concentrated CD68⁺ signals were found, indicating altered macrophages functional response by S-IgG treatment (Figure 3C). Consistently, elevated serum levels of IL-8 were observed in macaques treated with high-dose S-IgG at 2 dpi (Supplemental Figure 3), and the IL-8 levels are strongly correlated with anti-SARS-CoV NAb titers (Supplemental Figure 3). IL-8 is a macrophage-derived inflammatory cytokine important in initiating ALI. These results, therefore, suggest that S-IgG likely altered macrophage functional response in the lungs during acute infection, resulted in increase in IL-8 production, and enhanced ALI and IMM infiltration and accumulation.

Alveolar monocytes/macrophages assumed a wound-healing function as early as 2 dpi in macaques not treated with S-IgG. Macrophage activation is dynamic and plastic. Different monocyte/macrophage activation statuses have different specialized and critically timed roles, taking part in either the initiation and maintenance or resolution of inflammation (9). A well-organized wound-healing response leads to timely resolution of inflammation, whereas disturbance in wound-healing response results in persistent inflammation and injury. To understand the S-IgG-caused excessive inflammation, we further defined macrophage heterogeneity and activation statuses in the lung lesions of C-IgG ($n = 1$) and S-IgG recipients ($n = 3$) at 2 dpi. Three healthy macaques and 4 naive Chinese macaques challenged with the same dose of SARS-CoV_{PUMC} and scarified at 2 dpi from a previous study were included as controls (25).

By combining 5 macrophages markers (MAC387, CD68, CD163, HAM56, and CD206) (28–30), 2 subpopulations of resident macrophages were shown in the lungs of Chinese rhesus macaques at steady state as previously described (29). They are interstitial macrophages (IMs; MAC387⁺HAM56⁺CD206⁻) (Figure 4A) and resident alveolar macrophages (AMs; CD68⁺ HAM56⁻) expressing low levels of CD163 and CD206, a marker specific to the macrophage wound-healing response, corresponding to their intrinsic antiinflammatory function (Figure 4B) (29). In lung lesions of both C-IgG-treated and naive macaque groups challenged with SARS-CoV_{PUMC}, IMMs were further characterized and divided into 2 subpopulations. One subpopulation was the recently recruited MAC387⁺HAM56⁺CD68⁻ monocytes (Figure 4C) (29), which is like IM but is larger in size and primarily coexpressed CD163 (Supplemental Figure 4). The other subpopulation was single CD163⁺ inflammatory macrophages that had differentiated from newly recruited MAC387⁺ monocytes/macrophages (Figure 4D and Supplemental Figure 4) (29). Importantly, resident

AMs (CD68⁺) differentiated into HAM56⁺ cells, with a slight increase in numbers and increased size, with stronger CD163 and — more importantly — CD206 staining, suggesting that they are alternatively activated (Figure 4D). Strikingly, elevated levels of TGF- β expression were detected in all MAC387⁺ — and most enlarged CD163⁺ — as well as CD68⁺ macrophages in the lungs of both C-IgG-treated and unvaccinated macaques compared with healthy controls (Figure 4, G–I), indicating that many IMMs and activated resident AMs have assumed a wound-healing function in infected lungs within 2 days of infection.

S-IgG treatment skewed wound-healing macrophage response in the lungs during acute SARS-CoV infection. Compared with the macaques not treated with S-IgG, the number of IMMs (MAC387⁺ and CD163⁺HAM56⁻) significantly increased in S-IgG recipients (Figure 4, E and F). Moreover, many recently recruited MAC387⁺HAM56⁻ monocytes/macrophages did not coexpress CD163 (Supplemental Figure 4), representing the newest recruited blood monocytes, as a result of enhanced monocytes infiltration by S-IgG. Importantly, the majority of CD163⁺HAM56⁻ IMMs coexpressed CD68 (Supplemental Figure 4), suggesting a change of function of this subpopulation by S-IgG. Moreover, resident macrophages (CD68⁺HAM56⁺) in the lungs of S-IgG recipients no longer express CD206, which — being surrounded by many CD163⁺ IMMs (Figure 4F) — suggests a loss of wound-healing function and a role in recruiting blood monocytes. Consistently, S-IgG-treated macaques displayed a loss of TGF- β and high expression of IL-6 in all macrophage subpopulations (Figure 4, G, H, and J). IL-6 favors macrophage accumulation at the site of injury and is important for the development of persistent inflammation and ALI (31, 32). Therefore, we conclude that, while AMs underwent phenotypic and functional changes in acutely infected lungs, many monocytes/macrophages assumed a wound-healing function for inflammation resolution, but the presence of S-IgG skewed the wound-healing response, leading to uncontrolled inflammation and tissue injury.

Onset of an antibody response prior to viral clearance is associated with abrogated wound healing responses and increased IMM lung infiltration in unvaccinated Chinese rhesus macaques. To understand the mechanism underlying the time-restricted role of S-IgG in promoting ALI, we conducted a temporal analysis of the productive viral infection, antibody response, and macrophage functional changes in unvaccinated Chinese macaques during the first week of infection. Naive macaques were challenged i.n. with 1×10^5 TCID₅₀ SARS-CoV_{PUMC} and sacrificed at 2, 3, and 7 dpi (4 macaques/group) (Figure 5A) (25). Successful lower respiratory tract infection was confirmed by detection of viral NP using IHC staining in the lungs of all macaques (25). Viral RNA⁺ alveolar pneumocytes were primarily found at 2 dpi (2 of 4 macaques), and infrequently at 3 dpi (0 of 4 macaques; Figure 5B and Supplemental Table 4) (25). At 7 dpi, viral RNA was detectable in the lungs of 2 macaques, AD0516 and AD0518, suggesting productive infection there (Figure 5, B and C). Only few scattered NP⁺ cells were found in AD0517 (Figure 5D). Neither NP nor viral RNA was found in the lungs or swabs of AD0515, suggesting clearance of productive viral pulmonary infection in this macaque (Figure 5D and Supplemental Table 4). Serum NAb was not observed at 2 and 3 dpi until 7 dpi in 2 of 4 macaques, AD0515 and AD0516 (Supplemental Table 4 and Figure 5E).

In agreement with the findings in the C-IgG group, temporal analysis of macrophage heterogeneity revealed significantly increased number of IMMs (CD163⁺CD206⁻) in viral RNA⁺ lungs at 2 dpi (Figure 5F, right image). The IMMs diminished at 3 dpi (4 of 4 macaques) (Figure 5G) and became nearly completely absent at 7 dpi in macaques without productive pulmonary viral infection (2 of 4 macaques, AD0515 and AD0517) (Figure 5H), indicating that inflammatory response resolved with 7 days following the control of productive infection. Critically, wound-healing macrophages (CD163⁺CD206⁺ and CD163⁺TGF- β ⁺) were observed in the lungs of all macaques at 2 dpi, despite productive pulmonary viral infection in macaques AD0506 and AD0508 (Figure 5F). In contrast, macaque AD0516, with serum NAb and productive virus infection in the lungs, displayed a significantly enhanced proinflammatory macrophage response and reduced inflammatory-resolving macrophages (Figure 5I), which was not observed in macaques with productive viral infection but undetectable NAb responses (AD0518) or in macaques with detectable NAb but undetectable viral replication (AD0515) (Figure 5D and Supplemental Table 4). Therefore, persistent viral replication and concomitant NAb detection is associated with increased IMM lung infiltration and reduced wound-healing macrophage numbers.

S-IgG modifies functional response of alternatively but not classically activated macrophages to SARS-CoV infection. To determine whether S-IgG skews wound-healing response through modifying wound-healing macrophage functional response during SARS-CoV infection, we treated in vitro-polarized alternatively activated human monocyte-derived macrophages (MDM) for 20 hours with SARS-CoV pseudo-virus and heat-inactivated sera of high-dose S-IgG-treated macaques (S-IgG sera) collected at 2 dpi. We

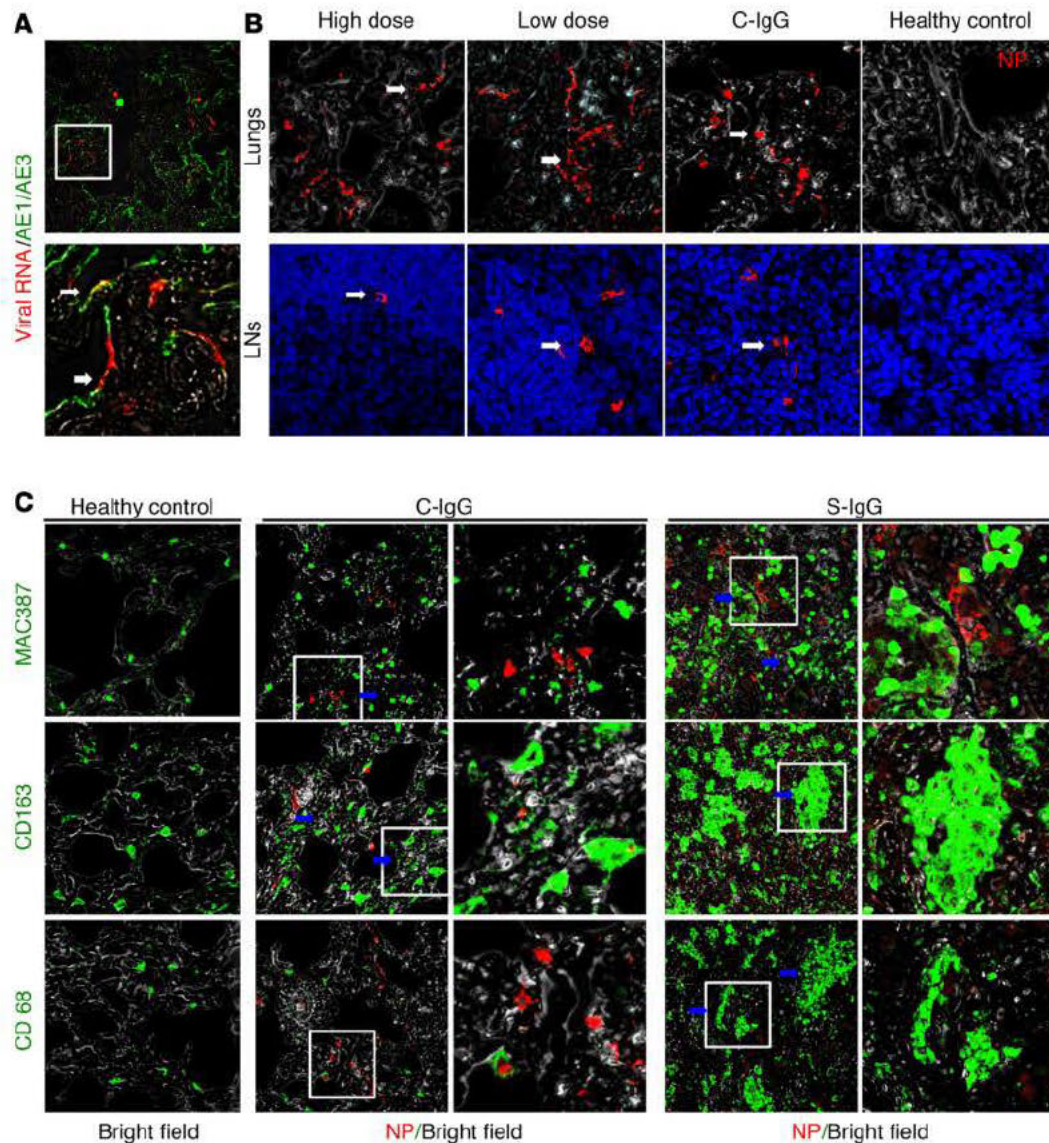


Figure 3. SARS-CoV infection and monocytes/macrophages infiltration in the lungs of C-IgG- and S-IgG-treated macaques at 2 dpi. (A) Representative images of SARS-CoV RNA⁺ (TRITC) and AE1/AE3⁺ (FITC) cells in the lungs of infected macaques (white arrows). The upper photo shows a low magnification overview (200 \times); the bottom photo shows the boxed area in the upper photo. (B) Representative images of viral protein (NP) immunostaining of the lungs and hilar lymph nodes (LN) of 7 infected and 3 uninfected animals (TRITC, white arrows) (original magnification, 200 \times). (C) Representative images of viral NP and monocytes/macrophages. These sections showed significantly increased IMM in the lungs of the S-IgG group compared with the C-IgG group (MAC387⁺, CD163⁺, or CD68⁺; blue arrows). Tissue samples are double-immunostained for the SARS-CoV NP (TRITC) and markers for macrophages, including MAC387 (FITC), CD163 (FITC), and CD68 (FITC). Within the panel of representative images for the C-IgG and S-IgG groups, the left panel shows a low magnification overview; the right panel shows the boxed area in the left panel (original magnification, 200 \times).

then measured the concentrations of 13 inflammatory cytokines in cell culture supernatants, including IL-1 β , IFN- α , IFN- γ , TNF- α , MCP1, IL-6, IL-8, IL-10, IL-12p70, IL-17A, IL-18, IL-23, and IL-33. Sera from C-IgG recipients or healthy macaques were included as controls. In vitro-polarized classically activated MDM was also studied and compared with alternatively activated MDM in parallel. Consistent with previous report, unstimulated classically activated MDM produced high levels of IL-8 and IL-6; alternatively activated MDM only produced minimal levels of those cytokines (Figure 6A). Addition of SARS-CoV pseudovirus induced IL-8 production in alternatively activated MDM to levels comparable with those found in unstimulated, classically activated MDM, as well as in low-level MCP1 and IL-6 production (Figure 6B). By contrast, SARS-CoV pseudovirus caused less than a 1-fold increase in IL-8 secretion, but not other cytokine secretion, by classically activated MDM (Figure 6C). Strikingly, while none of the sera samples induced cytokine production when they were administered into MDMs alone,

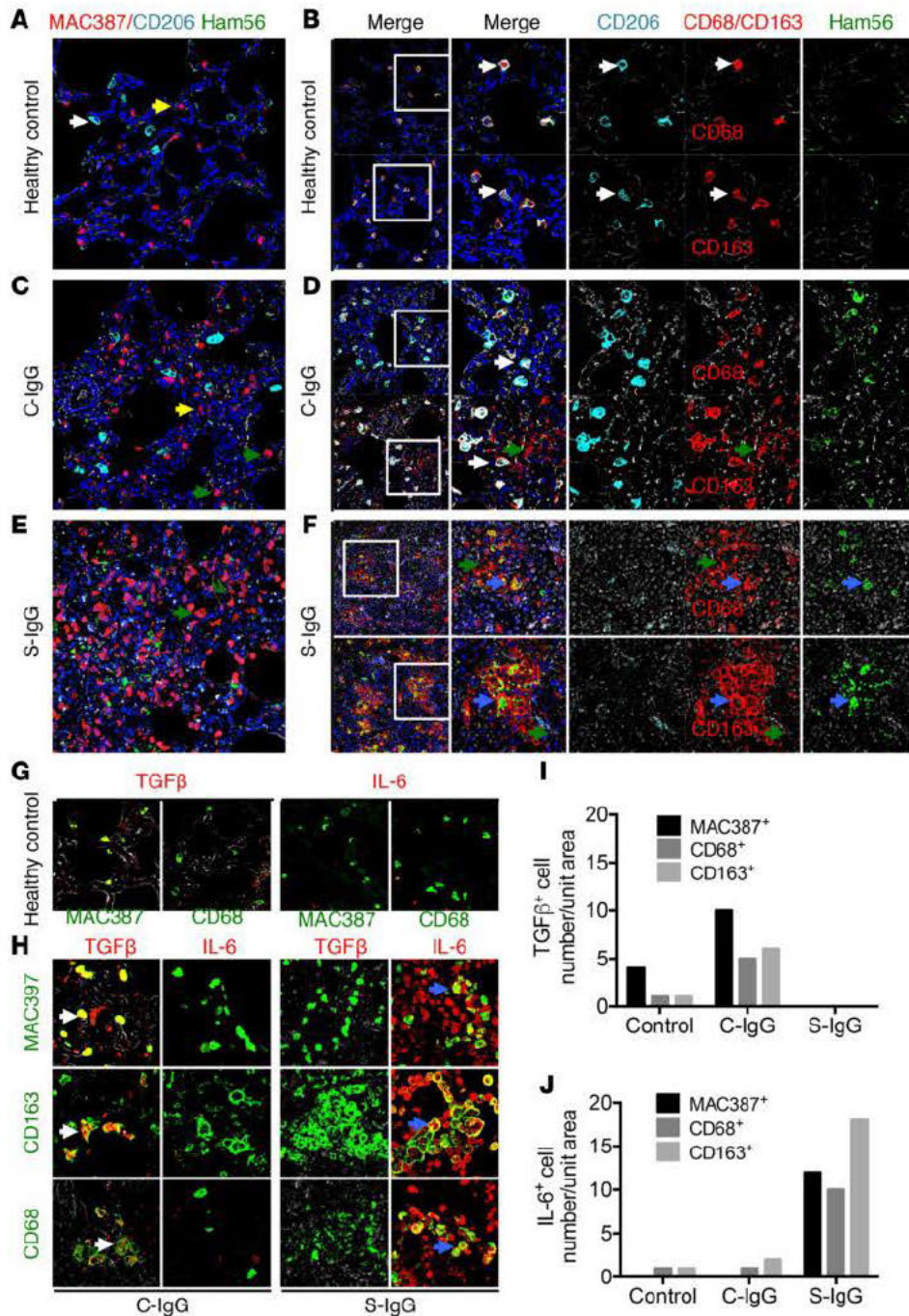


Figure 4. Comparison of monocyte/macrophage phenotype and function in the lungs of S-IgG- and C-IgG-treated macaques. (A-F) Phenotype of monocytes/macrophages subpopulations in the lungs of healthy, C-IgG-, and S-IgG-treated macaques (original magnification, 200×). These sections were triple-immunostained with antibodies for CD206 (cyan), HAM56 (FITC), and MAC387 (TRITC) (A, C, and E); CD206 (cyan), HAM56 (FITC) (B, D, and F), and CD68 (TRITC) (upper panel in B, D, and F); or CD163 (TRITC) (lower panel in B, D, and F). A and B show 2 subpopulations at steady states, including interstitial macrophages (IM) (MAC387⁺HAM56⁻CD206⁻) (yellow arrow), and resident alveolar macrophages (AM) (CD68⁺CD163^{hi}CD206^{lo}HAM56⁻) (white arrows). C and D show the presence of alternatively activated resident AM and accumulated IMs in the C-IgG group. Alternatively activated AMs are CD206^{hi}CD68⁻CD163^{hi}HAM56⁺ (D, white arrows). IM are MAC387⁺HAM56⁻CD206⁻ (C, yellow arrow). IMs include newly infiltrating monocytes/macrophages (MAC387⁺) (C, green arrow); and inflammatory macrophages (CD163⁺CD68⁻CD206⁻HAM56⁻) (D, green arrow). E and F show significantly increased number of IMs and decreased number of alternatively activated macrophages in the S-IgG group. IMs include newly infiltrating monocytes/macrophages (MAC387⁺) (E, green arrow) and inflammatory macrophages that are CD68⁺HAM56⁻ (green arrow, F, upper panel) and CD163⁺CD206⁻HAM56⁻ (green arrow, F, lower panel). Resident AMs are no longer expressing CD206 (CD68⁺HAM56⁻CD163^{hi}CD206⁻) (blue arrow, F, upper panel). (G-J) TGF-β and IL-6 expression in macrophages in the lungs. These sections were double-immunostained with antibodies for TGF-β or IL-6 (TRITC) and MAC387, CD163, or CD68 (FITC). G shows low expression levels of TGF-β and IL-6 in IMs (MAC387⁺) and AMs (CD68⁺) in healthy macaques. H shows increased TGF-β expression in the C-IgG group (white arrows) but increased IL-6 in the S-IgG group (blue arrows). I and J show the numbers of TGF-β⁺ and IL-6⁺ monocytes/macrophages in 3 groups in a 200× field.

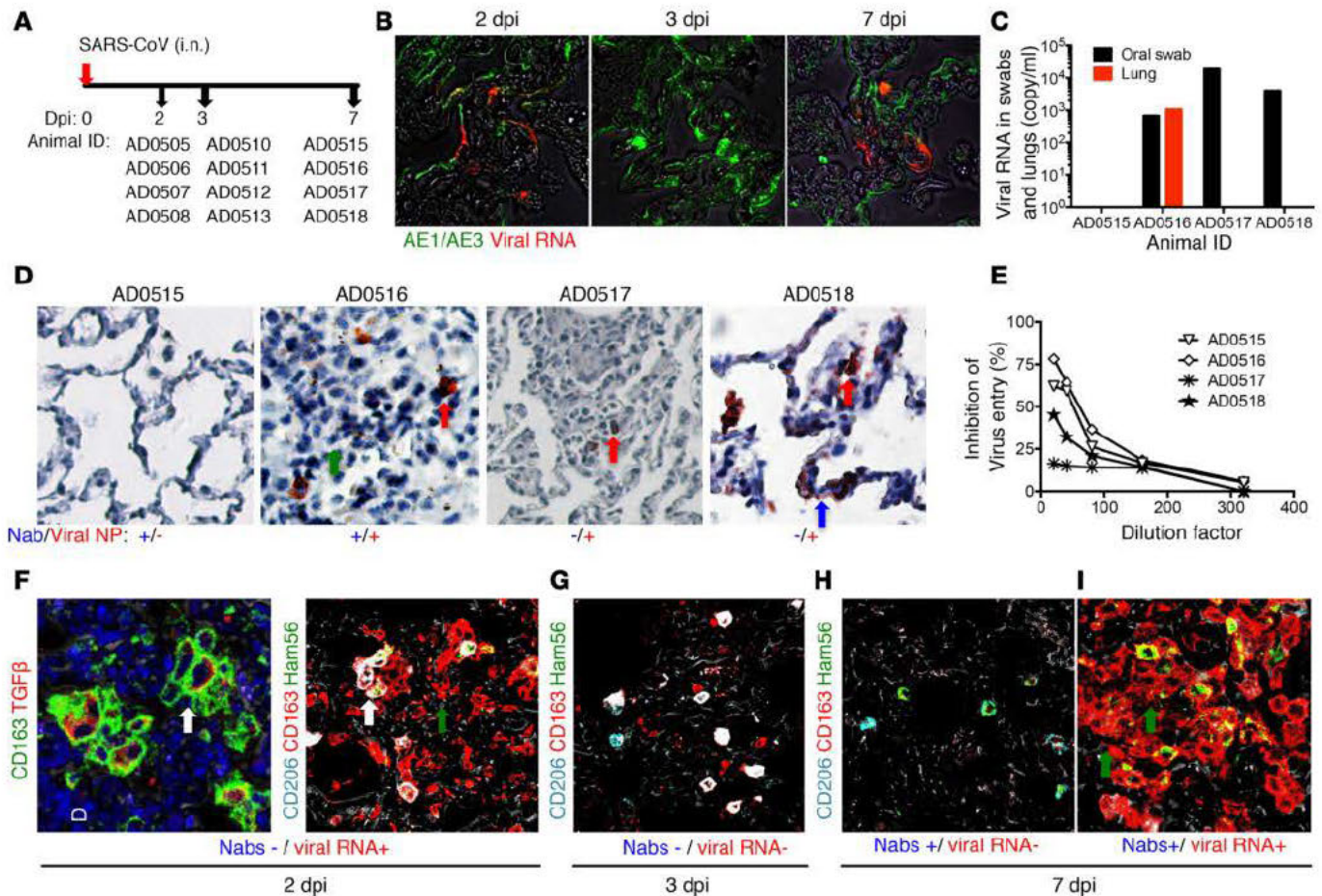


Figure 5. Dynamics of the viral replication, antibody response, and macrophage activation during acute SARS-CoV infection. (A) Experimental scheme. A total of 12 Chinese rhesus macaques were challenged i.n. with SARS-CoV_{PUMC} (1×10^5 TCID₅₀). Four animals each were sacrificed at 2, 3, and 7 dpi. (B) SARS-CoV RNA detection by ISH in the lungs at 2, 3, and 7 dpi (original magnification, 200 ×). Viral RNA* (TRITC) type I pneumocytes (FITC) was found at 2 dpi ($n = 2$) and 7 dpi ($n = 1$). (C) Viral RNA in the swabs and lung homogenates on 7 dpi. SARS-CoV RNA was detected using nested RT-PCR in swabs from 3 macaques (AD0516, AD0517, and AD0518) and lung homogenates from macaque AD0516. (D) Viral antigen and inflammatory infiltrates in the lungs at 7 dpi (200×). These sections were stained for SARS-CoV NP (red) and nucleus (blue) by IHC, showing NP signal in macrophage-like cells in AD0516 and AD0517 (red arrows), and type I pneumocytes in AD0518 (blue arrows), but substantial inflammatory infiltrates were only observed in AD0516 (green arrows). (E) Serum neutralizing activity. Serum neutralizing activity was detected in macaques AD0515 and AD0516 at 7 dpi. (F–I) Decreased wound-healing response in macaques with productive pulmonary viral infection and serum neutralizing activity (200×). These sections were double-immunostained for TGF-β (TRITC) and CD163 (FITC) or triple stained for CD206 (cyan), HAM56 (FITC), and CD163 (TRITC). The figure shows that wound-healing response took place within 2 dpi, with alternatively activated pneumocytes/macrophages (TGF-β⁺ and CD206⁺, white arrows) and IMMs (CD163⁺CD206⁻, green arrows) coexisting in the lungs (F). After viral clearance, IMMs diminish at 3 dpi (G), and the homeostasis was restored at 7 dpi (AD0515) (H). When pulmonary viral infection persists, IMM (CD163⁺CD206⁻, green arrows) infiltration and accumulation is enhanced, and wound-healing macrophages (CD206⁺) are reduced in macaques that have faster NAb response (AD0516) (I).

administration of S-IgG sera caused a dose-dependent increase in the production of all 3 inflammatory cytokines in SARS-CoV-stimulated alternatively activated MDM, resulted in a greater than 10-fold increase in IL-6, an 8-fold increase in MCP1, and a 5-fold increase in IL-8 (Figure 6, D and E). This enhancement, however, was not observed when S-IgG sera were replaced with sera from C-IgG recipients or healthy macaques (Figure 6, F, G, and H), suggesting that S-IgG, but not other sera components, enhanced SARS-CoV-stimulated cytokine production by alternatively activated MDM. Administration of S-IgG sera had no effect on cytokine production by SARS-CoV-treated classically activated MDM (Figure 6, I, J, and K), indicating that S-IgG do not modulate virus-mediated classically activated macrophage functional response. MCP1 and IL-8 are key cytokines that regulate monocytes/macrophages migration and promote neutrophils infiltration, while IL-6 promotes persistent inflammation and injury. These results suggest that, in response to SARS-CoV infection, wound-healing macrophages produce IL-8 and low amounts of MCP1 to recruit neutrophils and blood monocytes, whereas the presence

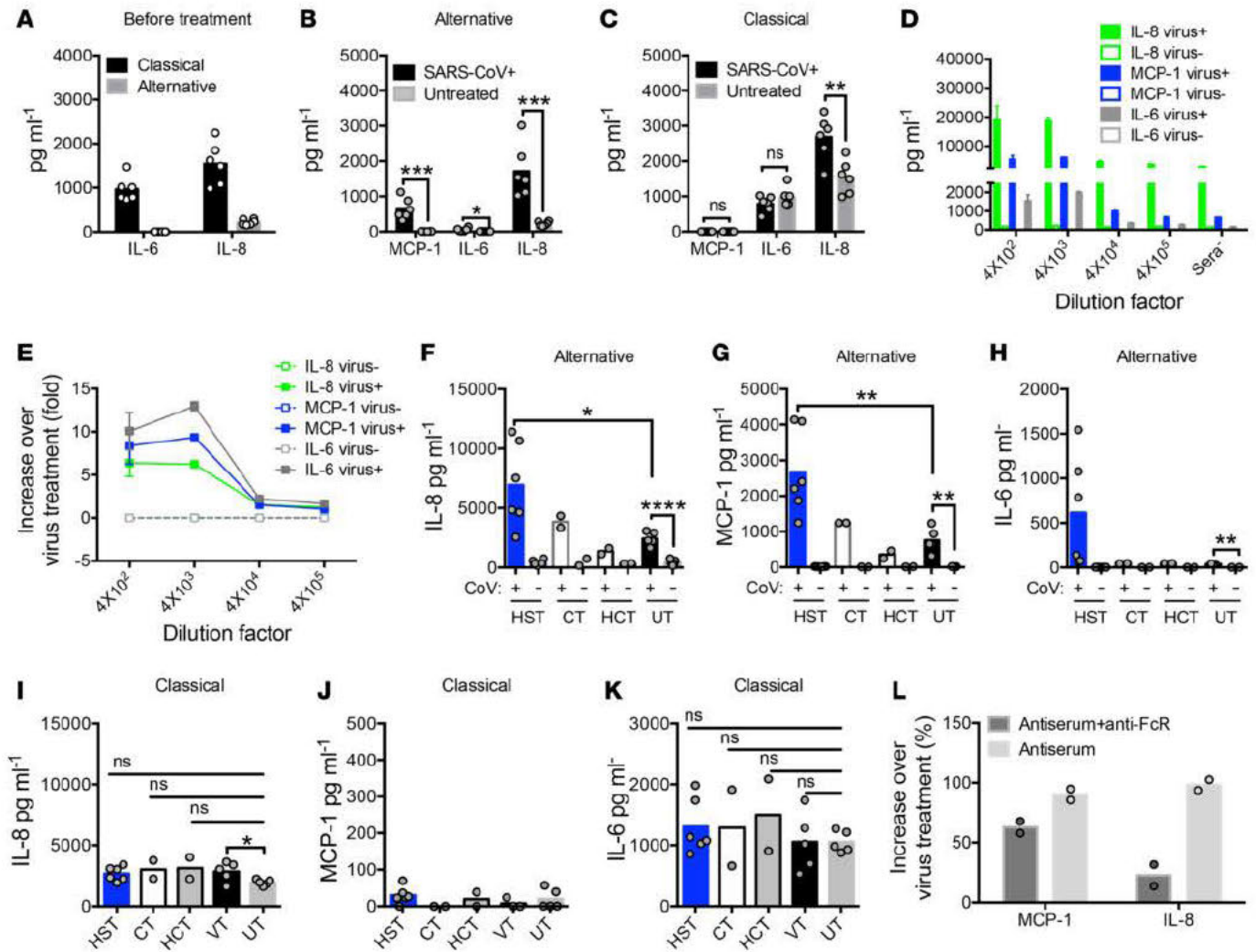


Figure 6. S-IgG significantly amplified proinflammatory cytokine production by SARS-CoV-treated alternatively activated macrophages. In vitro-polarized alternatively activated macrophages were either left unstimulated or were incubated with SARS-CoV pseudovirus alone or cocultured with SARS-CoV pseudovirus and diluted sera from the high-dose S-IgG group ($n = 6$) or C-IgG group ($n = 2$) collected at 2 dpi or from healthy macaques ($n = 2$) for 20 hours. Secreted cytokine and chemokine levels were measured in the culture supernatant and are shown in data represented as a column graph (A–D and F–K) and fold or percentage over supernatants from macrophages treated with virus alone (E and L). A shows the levels of IL-8 and IL-6 in the supernatant of classically activated and alternatively activated MDM before treatment. B and C show that SARS-CoV treatment induced MCP1, IL-8, and very low levels of IL-6 production by alternatively activated MDM, as well as enhanced IL-8 production by classically activated MDM. D and E show that sera from S-IgG recipients caused dose-dependent increase in cytokine production from SARS-CoV-treated alternatively activated MDM. F–H show that virus treated alternatively activated MDM (VT), but not sera treated or untreated cells (UT), secreted proinflammatory cytokines IL-8 (F), MCP1 (G), and very low levels of IL-6 (H). Addition of sera (1:4,000 dilutions) from high-dose S-IgG (HST), but not C-IgG treated macaques (CT) or healthy controls (HCT), significantly amplified IL-8 (F), MCP1 (G), and IL-6 (H) production. I–K show that addition of sera (1:4,000 diluted) from high-dose S-IgG-treated (HST), C-IgG treated macaques (CT), or healthy controls (HCT) had no effect on IL-8 (I), MCP1 (J), and IL-6 (K) production by SARS-CoV-treated classically activated MDM. L shows that blockade of FcγR significantly reduced antiserum-enhanced IL-8 secretion and partially reduced MCP1 secretion. Data represent mean values or mean values \pm SEM of at least 3 independent experiments. Two-tailed unpaired Student's *t* test was used for statistical analysis. * $P < 0.05$; ** $P < 0.01$; *** $P < 0.001$; **** $P < 0.0001$.

of S-IgG can result in 5- to 10-fold increases in IL-8, MCP1, and IL-6 production by wound-healing macrophages, leading to significantly enhanced and persistent monocytes infiltration and tissue injury. Critically, in the presence of Fcγ receptor (FcγR) blocking antibody, IL-8 was significantly reduced when cells were treated with SARS-CoV pseudovirus and sera from high-dose S-IgG-treated macaques (diluted 1:4,000), indicating that anti-SARS-CoV antibody modifies wound-healing response partially through FcγRs (Figure 6L). Therefore, we conclude that S-IgG directly modifies functional response of alternatively activated macrophages during acute infection, thus skewing wound-healing response, leading to hypercytokinemia, aggressive inflammation and severe lung injury.

Deceased SARS patients displayed higher levels of serum NAb, accumulated proinflammatory, macrophages infiltration, and absence of wound-healing macrophages in the lungs. To examine the role of S-IgG in promoting ALI in a clinical setting, we investigated antibody responses during the early stage of infection in 2 groups of deceased patients or individuals recovered from SARS and characterized the heterogeneity of monocytes/macrophages in the lungs of 3 deceased SARS patients. H&E staining of lung specimens derived from 3 deceased SARS patients revealed severe ALI (Figure 7A). Consistent with the macaque findings, IHC analysis revealed significant infiltration of CD163⁺ monocytes/macrophages into the lungs of patients, with little TGF- β expression and loss of the wound-healing marker CD206⁺, indicating predominantly proinflammatory macrophage activation and reduced inflammatory-resolving response (Figure 7B). Moreover, significantly higher levels of anti-S NAb were detected in the sera of deceased patients ($n = 6$) during acute infection compared with recovered patients ($n = 8$) (Figure 7C). These results, therefore, are consistent with findings in experimental macaques.

Antisera from deceased SARS patients skewed wound-healing response during SARS-CoV infection partially through the Fc γ R. To examine whether human anti-SARS-CoV antibody modifies wound-healing response during SARS-CoV infection, we treated in vitro-polarized alternatively activated MDM with SARS-CoV pseudovirus for 20 hours in the presence of sera collected from SARS patients during acute infection. Macrophages treated with SARS-CoV pseudovirus or sera alone were included as controls. We then examined the protein levels of cytokines/chemokines in the cell culture supernatant. Consistent with findings in macaques, administration of sera from a deceased SARS patient (D1; Supplemental Table 5) into SARS-CoV-treated alternatively activated MDM caused a dose-dependent increase in the production of cytokines, leading to a 2- to 3-fold increase in MCP1 and IL-8 after 20 hours (Figure 8, A and B). This enhancement, however, was not observed in cells treated with sera alone (Figure 8, A–D). Administration of sera from recovered patients ($n = 8$; Supplemental Table 5) had no effect on cytokine production except 1 sample (Figure 8, C and D). These differences may be explained, at least in part, by their lower NAb titers, although it is also possible that sera from recovered patients contain different antibody populations. Consistently, the only serum sample — R2, which enhanced chemokine production — has a relatively higher NAb titer among the samples tested (Supplemental Table 5). Moreover, statistical analysis shows that IL-8 production strongly correlates with NAb titer of sera from deceased patients (Figure 8E). Furthermore, IL-8 production was significantly reduced when cells were treated with SARS-CoV pseudovirus and sera from deceased SARS patient (diluted 1:4,000) in the presence of Fc γ R blocking antibody, indicating that anti-SARS-CoV antibody modifies wound-healing response in humans partially through Fc γ Rs (Figure 8F).

Discussion

Here, we present evidence of a detrimental role of anti-S-IgG in ALI during SARS-CoV infection. Respiratory CoVs infection poses a unique challenge to the immune system: not only must the virus be rapidly eliminated, but lung inflammation must also be controlled to prevent acute respiratory failure (33). In the present study, we show that, despite markedly reducing virus titers, anti-S-IgG caused lung injury during the early stages of infection by abrogating a wound-healing macrophage response and TGF- β production, while promoting proinflammatory cytokine IL-8 and MCP1 production and inflammatory macrophage accumulation. To our knowledge, our data demonstrate a previously unrecognized mechanism underlying virus-mediated ALI and suggest that modulation of the anti-S antibody response or blockage of Fc γ receptors during acute infection might be needed for effective treatment for respiratory CoV infection.

Many studies have demonstrated the role of NAb induced by the S glycoproteins in protecting viral replication in susceptible hosts, including mice, ferrets, hamsters, and macaques (24, 34, 35). However, the effect of S-specific immunity in protecting against pulmonary immunopathology has been controversial. In some cases, vaccination-induced immunity assists the viral clearance and protects mice or ferrets against lethal challenge (36–39), whereas in many other situations, multiple vaccine platforms appear to induce increased eosinophilic proinflammatory pulmonary response upon challenge (18, 23, 40). These differences may be explained, in part, by the characteristics of the vaccine being studied, the infectious dose, and the viral strain employed, as well as by the type or quality of immune response elicited. Recent studies suggest that CD8⁺ T cell response plays a crucial role in viral clearance and protection of mice against eosinophilic immunopathology and lethal SARS-CoV infection, whereas immunopathology predominantly reflects an inadequate vaccine-induced Th1 response (20–23).

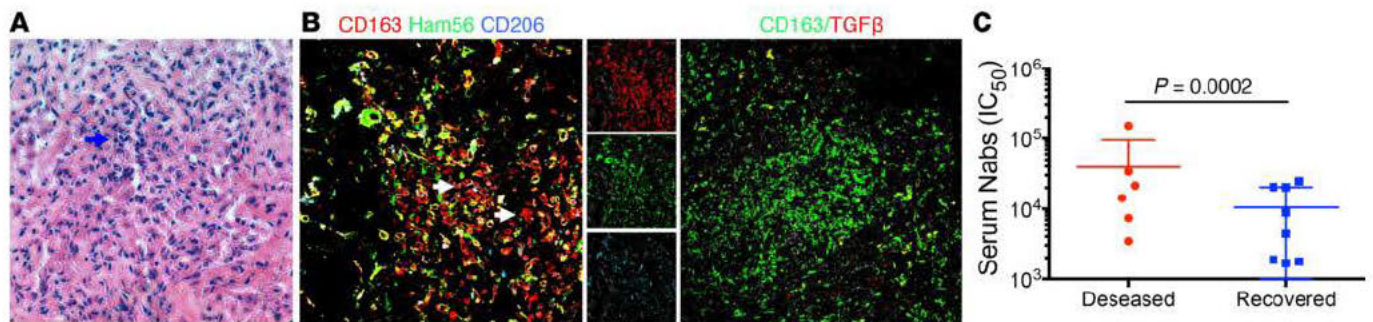


Figure 7. NAb response and phenotype analysis of accumulating monocytes/macrophages in the lungs in deceased SARS patients. (A) Pathology changes of the lung tissue. Sections from deceased SARS patients were stained with H&E. **A** is representative of 3 patients (original magnification, 100 \times), showing symptom of acute DAD with massive cell infiltration in alveolar cavities (blue arrow). (B) Massive accumulation of IMM and absence of wound-healing macrophage response in the lungs of deceased patients. These sections were triple-immunostained with antibodies for CD206 (cyan), HAM56 (FITC), and CD163 (TRITC) or double-immunostained with TGF- β (TRITC) and CD163 (FITC) (original magnification, 200 \times). The right panel in the left image shows single colors from the left image (200 \times). These representative images show accumulation of IMM (CD163 $^{+}$ CD68 $^{+}$ CD206 $^{-}$ HAM56 $^{+}$, white arrows) and the absence of wound-healing response, indicated by loss of the signal for CD206 (cyan, B1) and TGF- β (TRITC, B2) in the lungs. (C) Serum-neutralizing activity against SARS-CoV. Sera collected from deceased (red, $n = 6$) or recovered (blue, $n = 8$) SARS patients at the early stage of infection were tested for the capacity to neutralize SARS-CoV pseudotype virus. Two-tailed unpaired Student's *t* test was used for statistical analysis.

In fact, a protective effect against pulmonary immunopathology mediated by full length S protein-based vaccine in SARS-CoV-infected nonhuman primate models has not been described, to our knowledge. Although several vaccine candidates protected macaques against viral replication in the lungs, pulmonary immunopathology was not evaluated in these studies (24, 41, 42). By contrast, it was shown that SARS-CoV-specific immune memory induced by prior infection enhanced lung inflammation following homologous challenge in African green monkeys (17). Similarly, **augmentation of disease by vaccination has also been described in studies of atypical measles and dengue hemorrhagic fever, as well as several respiratory diseases, including respiratory syncytial virus (RSV) and pandemic influenza (16, 43).** In the study of RSV vaccine conducted in 1966 and 1967, 80% of RSV vaccinees needed hospitalization, whereas only 5% of RSV-infected children in the control vaccine group required admission, although the underlying mechanisms remain incompletely understood. Using Chinese rhesus macaques, we show that an ADS-MVA-based vaccine protected macaques against viral replication but significantly enhanced acute DAD at both 7 and 35 dpi compared with the control ADC-MVA group, suggesting that S-specific but not MVA-specific immunity promotes ALI (Figure 1). **Until now, it remains unknown if SARS vaccine candidates with a focus on the receptor-binding domain (RBD) of S protein can avoid the induction of ALI in nonhuman primates.** These vaccines have been shown to induce highly potent NAb responses and elicit long-term protective immunity in immunized small animals (38).

SARS-CoV infection of Chinese macaques is often characterized by the rapid control of viral replication with mild lung lesions in most macaques (25). The mechanisms underlying why Chinese macaques do not often develop ALI, as observed in most SARS patients, are largely unknown. Our data suggest that these effects, in part, reflect the rapid control of viral replication in the lungs, which peaked between 24 and 48 hours after inoculation (hpi) and diminished within 7 days, thus creating an interval between lung inflammation and high titer antibody production in most macaques. Indeed, although SARS-CoV infection resulted in significant infiltration of macrophages in the lungs, the number of macrophages was rapidly reduced following virus clearance at 3 dpi (Figure 5). At 7 dpi, inflammation appeared to be mostly resolved (Figure 5). By contrast, control of virus replication is less efficient in SARS patients, and the peak in viral load coincides with the first appearance of an antibody response, approximately 10 days after the onset of symptoms (6).

The low rate of ALI and interval between lung inflammation resolution and antibody production, however, makes Chinese macaques an ideal animal model for the present study. Using vaccination and passive immunization, we conditioned anti-S antibody titers in macaques during the early stage of infection when ALI was not typically observed. We found that prior administration of anti-S-IgG led to massive accumulation of monocytes/macrophages in the lungs within 2 dpi. This result is consistent with previous reports, in which mice given the SARS vaccine exhibited an immunopathologic lung reaction after the subsequent challenge with SARS-CoV (18, 19). Moreover, in SARS patients, clinical course and outcome are more favorable in children younger than 12 years of age compared with adolescents and adults (44), indicating that prior alternative CoV infection might

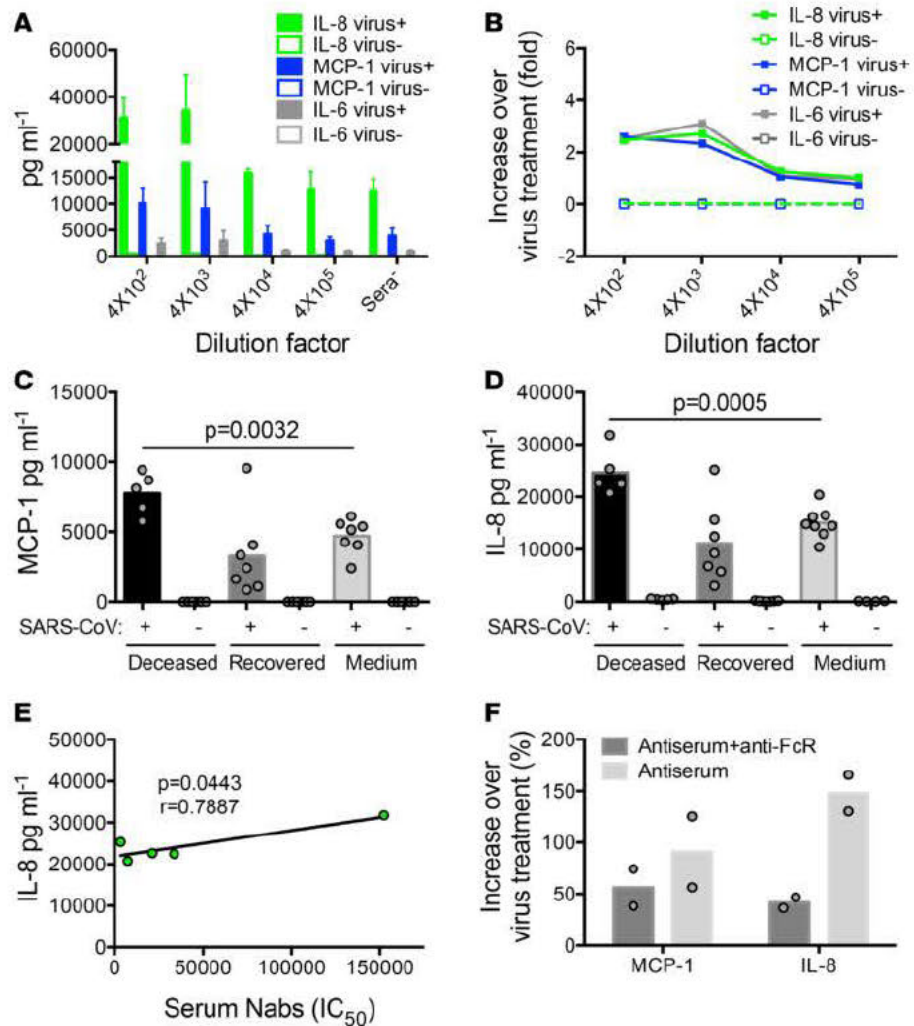


Figure 8. Sera from deceased SARS patients skewed wound-healing macrophage response partially through $Fc\gamma R$. In vitro-polarized alternatively activated MDM were either left unstimulated or were incubated with SARS-CoV pseudovirus alone or cocultured with SARS-CoV pseudovirus and 1–400,000 serials diluted or 1/4,000 diluted sera from deceased ($n = 5$) or recovered SARS patients ($n = 7$) for 20 hours. Cells treated with sera from patients alone served as controls. Secreted cytokine and chemokine levels were measured in the culture supernatant and are shown in data represented as a column graph (**A**, **C**, and **D**) and fold or percentage over supernatants from macrophages treated with virus alone (**B** and **F**). **A** and **B** show that addition of sera from deceased patient (D1) dose-dependently enhanced production of IL-8, IL-6, and MCP1 by SARS-CoV-treated alternatively activated MDM. **C** and **D** show significantly enhanced IL-8 and MCP1 production by alternatively activated macrophages treated with sera from deceased SARS patients and virus compared with cells treated with virus alone. Sera treatment alone did not induce IL-8 or MCP1 production. (**E**) Correlation of IL-8 production with NAb titers of sera of deceased patients. Solid lines denote the relationship between histopathology scores and serum neutralizing activity. (**F**) Blockade of human $Fc\gamma R$ significantly reduced antiserum-enhanced IL-8 secretion and partially reduced MCP1 secretion. In vitro-polarized alternatively activated human monocyte-derived macrophages were cocultured with SARS-CoV pseudovirus and 1–4,000 diluted sera from deceased patient (D1) with or without $Fc\gamma R$ blocking antibody for 20 hours. Secreted cytokine and chemokine levels were measured in the culture supernatant and are shown in data represented as increase over supernatants from macrophages treated with virus alone. Data represent mean values or mean values \pm SEM of at least 3 independent experiments. Two-tailed unpaired Student's t test and Spearman's rank correlation test were used for statistical analysis.

play a role in driving enhanced pulmonary inflammation. A recent study reported that pathogenic immune complexes promoted lung injury during the 2009 H1N1 pandemic (16). It remains unknown whether immune complexes may also play a role in driving ALI during SARS-CoV infection.

Detailed analyses of macrophage heterogeneity at different stages of infection and in lungs with severe injury or mild lesion revealed distinct roles for proinflammatory and wound-healing macrophages in SARS disease progression. We observed that the early transition of macrophage responses from proinflammatory

to wound healing with increased TGF- β expression is associated with inflammation resolution and mild lung injury. By contrast, abrogated wound healing by S-IgG resulted in decreased TGF- β production and prolonged classical macrophage activation, and it promoted severe lung injury. Our findings are primarily based on imaging of formalin-fixed tissues of infected macaques, which may have technical limitations. A detailed flow cytometric analysis would be helpful to further characterize macrophage subpopulations in infected lungs. Unfortunately, we were not allowed to obtain any live cells, including macrophages, for analysis by flow cytometry outside the BSL-3 laboratory in China, which is in line with “WHO biosafety guidelines for handling of SARS specimens” (https://www.who.int/csr/sars/biosafety2003_04_25/en/). Having said this, TGF- β is mainly derived from wound-healing macrophages but not from classically activated macrophages. Therefore, by staining both TGF- β and CD206 (another biomarker of wound-healing macrophages), we believe that the finding of reduction of this type of macrophages in the S-IgG-treated lungs is convincing.

Patients who received convalescent plasma from recovered SARS patients had shorter hospital stays and lower mortality rates without evident adverse effects (45–47). These results might reflect a different quality of antibodies in recovered patients from deceased patients during early infection. Indeed, we previously observed that deceased patients had significantly higher NABs with a very low level of anti-N antibodies in serum during the early stage of infection (14). In contrast, recovered patients had more rapid anti-N antibody and slower NAb development (14). Consistently, serum from deceased patients — but not SARS survivors during early stages of infection — enhanced IL-6, IL-8, and MCP1 production by wound-healing macrophages (Figure 8). We previously identified epitopes in S protein that elicited NABs and antibodies that enhanced SARS-CoV infection (48, 49). Further studies that will attempt to identify antibodies and epitopes that mediate prevention or enhancement of ALI might be needed for future vaccine design and immunotherapy.

Lastly, blockade of Fc γ Rs reduced proinflammatory cytokine production, suggesting a potential role of Fc γ Rs for the postulated reprogramming of alternatively activated macrophage. Fc γ Rs are functionally divided into activating and inhibitory receptors. Activating Fc γ Rs, such as Fc γ RI, Fc γ RIIA, and Fc γ RIII, triggers production of proinflammatory chemokines and cytokines through an immunoreceptor tyrosine-based activation motif (ITAM) in their intracytoplasmic domain and SRC family kinases and spleen tyrosine kinase (SYK), whereas the inhibitory Fc γ R, Fc γ RIIB, has an immunoreceptor tyrosine-based inhibition motif (ITIM) in its intracytoplasmic domain and counteracts the signals that are mediated by activating Fc γ Rs. Based on literature and our experiments, human monocyte-derived wound-healing macrophages express higher levels of CD16 (Fc γ RIII) and CD32A (Fc γ RIIA) (50). Therefore, it is likely that S-IgG promoted proinflammatory cytokine production through Fc γ RI and/or Fc γ RIIA. S-IgG did not affect classically activated macrophage function *in vitro*. This difference can be possibly explained by the high baseline level of proinflammatory cytokines before infection and the downregulated expression of Fc γ R on classically activated MDM by SARS-CoV treatment.

Methods

Immunization of animals. We vaccinated Chinese rhesus macaques as previously described (51). Briefly, 16 Chinese rhesus monkeys were immunized twice on days 0 and 28. Eight of these animals received ADS-MVA, whereas the other 8 animals received ADC-MVA. ADS-MVA and ADC-MVA vectors encoding SARS-CoV S protein or HCV E1E2 were constructed and produced as previously described (51). The dose for both immunizations was 5×10^8 TCID₅₀. The vaccine strain SARS-CoV HKU39849 (AY278491) shares 100% sequence homology of the S gene with the challenge strain SARS-CoV_{PUMC} (AY350750).

Animals, tissues, and SARS-CoV infection. SARS-CoV-infected animals and control animals were all adult female Chinese rhesus macaques. A total of 42 Chinese rhesus macaques were challenged *i.n.* with a live pathogenic SARS-CoV (PUM, TCID₅₀ = 50) as previously described (25). An additional 3 uninfected macaques were inoculated with PBS as negative controls. Animals were subjected to daily measurement of anal temperature, routine blood assays, and chest radiography. Animals were euthanized at 2, 3, 7, 21, and 35 days after inoculation (Figure 1, Figure 2, and Figure 6). All animals were humanely euthanized with an *i.v.* overdose of pentobarbital and were immediately necropsied. Lung tissues (left and right cranial, middle and caudal lobes, and right accessory lobe) were collected and fixed in 10% neutral-buffered formalin, embedded in paraffin, and sectioned at 5 μ m.

Passive transfer of IgG. SARS-CoV S protein-immune serum was generated by vaccination with ADS-MVA vectors. IgG was purified from pooled sera by protein G affinity chromatography to >95% purity. IgG was depyrogenated, concentrated to 20–30 mg protein ml⁻¹, and administered *i.v.* Recipients received 200 mg or 5 mg of purified IgG per kg body weight at 48 hours before the viral challenge.

Neutralization. A neutralization assay was established to determine the humoral immune responses generated by the vaccine as previously described (51). The neutralizing activity of heat-inactivated animal sera was determined using a pseudotype viral entry assay. The pseudotype virus was generated through cotransfection of 293T cells with 2 plasmids, pcDNA-Sopt9 and pNL4-3Luc_Env_Vpr_, carrying the optimized S gene and a human immunodeficiency virus type 1 backbone, respectively. The serially diluted serum samples were incubated with equal amounts of pseudotype virus at 37°C for 1 hour. The serum-virus mixtures were subsequently added into preseeded HEK 293T-ACE2 cells. After 56 hours, infected cells were lysed to measure luciferase activity.

Nested RT-PCR and isolation of SARS-CoV. Pharyngeal swab samples were collected from infected monkeys on the first day after inoculation and subsequently tested for SARS-CoV using nested RT-PCR as previously described (25). Briefly, RNA was isolated using TRIZOL (Invitrogen). RT-PCR was performed in a 50 µl reaction volume with outer primer pair (5'-GCTGCATTGGTTTGTATATCGTTA-TGC-3') and (5'-ATACAGAATACAT-AGATTGCTGTATCC-3'), inner primer pair (5'-TCACTTGCTTC-CGTTGAGGTAGC-CAGCGTGGT-GGTCATACAA-3') and (5'-GGTTTCGGATGTTACAGC-GTCTCCCGG-CAGAAAGCTGTAAGCT-3'). All PCR products were verified by nucleotide sequencing. SARS-CoV was isolated as previously described. Briefly, pharyngeal swab samples from the infected macaques were inoculated onto Vero-E6 cells and cultured in DMEM (Thermo Fisher Scientific). Both cytopathic effect (CPE) and immunofluorescence assay (IFA) (incubation with 1:10 dilution of SARS patient serum) were used to determine the infection status of the animals.

Double and triple immunofluorescence staining on paraffin sections. The samples were deparaffinized and rehydrated. After blocking with normal goat serum for 30 minutes at room temperature, a rabbit anti-SARS-CoV nucleocapsid antibody (ss-006-0100, eNZYME) was applied at 4°C overnight, followed by an Alexa Fluor 448 conjugated goat anti-rabbit IgG antibody for 1 hour at room temperature. Additional immunofluorescence staining was subsequently performed by overnight incubation with primary antibodies, followed by the detection of signals using appropriate fluorescent secondary antibodies (MilliporeSigma) for 1 hour at room temperature.

Primary antibodies for immunofluorescence staining. The following primary antibodies were used in this study: SARS-CoV NP (ss-006-0100, eNZYME); MAC387 (clone MAC387, AbD, Serotec); CD68 (clone KPI, DAKO; ab125047, Abcam); CD163 (clone EDHu1, AbD and ab183476, Abcam); HAM56 (clone HAM56, DAKO); CD206 (HPA004114, MilliporeSigma); TGF-β (sc-146, Santa Cruz Biotechnology Inc.); IL-6 (sc-1265, Santa Cruz Biotechnology Inc.); AE1/AE3 (clone AE1/AE3, DAKO).

ISH studies. ISH was developed for the detection of SARS-CoV. DNA fragments of N and S proteins from the SARS-CoV strain from Hong Kong (AY278491) were used as templates to generate RNA probes. The probes were labeled with digoxigenin (GENEWIZ Inc.). After deparaffinization and rehydration, the sections were treated with microwave heating in an 800 W domestic microwave oven (NN-ST556M, Panasonic) at medium power for 10 minutes in 0.01 M sodium citrate buffer. Hybridization was performed at high stringency with 150 ng/ml of denatured probe at 45°C for 16 hours in 50 µl of hybridization mix (50% formamide, 10% dextran sulfate in 2× saline sodium citrate [SSC]) in a moist chamber. Excess probe was removed by washing twice in 2× SSC for 20 minutes at 45°C, followed by 2 washes in 1× SSC and 0.1× SSC for 20 minutes at 45°C. Immunological detection was conducted using the DIG Nuclear Acid Detection Kit (Roche Diagnostics) according to the manufacturer's instructions. Briefly, after incubation with 1% blocking reagent for 30 minutes, the sections were incubated with sheep anti-digoxigenin alkaline phosphatase conjugate (11093274910, Roche Diagnostics) diluted at 1: 500 for 2 hours at room temperature. After 3 separate washes with washing buffer (0.1 M maleic acid, 0.15 M NaCl [pH 7.5], 0.3% Tween 20), the signal was developed using 200 µl of a HNPP/Fast Red TR mix (1758888, Roche Diagnostics) in the dark for 45 minutes. The sections were counterstained with DAPI. Tissue sections incubated with sense RNA probe were used as a negative control.

Confocal microscopy. Confocal microscopy was performed using a Carl Zeiss LSM 700 confocal microscope equipped with 4 lasers (Zeiss). ZEN (Zeiss) was used to assign colors to the 4 channels collected: Alexa Fluor 568 and HNPP/Fast Red, which fluoresces when exposed to a 568-nm wavelength laser and appears red; Alexa Fluor 488 (Molecular Probes), which appears green; Alexa Fluor 647 (Molecular Probes), which appears cyan; and the differential interference contrast (DIC) image, which is in gray scale. The 4 channels were simultaneously collected. To differentiate between individual cells, Hoechst 33258 (nuclear marker; Molecular Probes) was used at 1 µg/ml and incubated for 5 minutes, followed by rinsing with water. The colocalization of antigens was demonstrated by the addition of colors as indicated in the figure legend.

Monocyte isolation, differentiation, and polarization of macrophages. Monocytes were purified from peripheral blood mononuclear cells obtained from blood buffy coats (provided by Red Cross, Hong Kong, China) or monkey peripheral blood, as we previously described (52). Monkey peripheral blood was obtained in heparinized vacutainer collection tubes from healthy female rhesus monkeys. To generate M1 macrophages, monocytes were differentiated in RPMI 1640 medium (Thermo Fisher Scientific) supplemented with GM-CSF (400 IU/ml), 2 mM glutamine, 10% decompartmented FCS, 100 IU/ml penicillin, and 100 µg/ml streptomycin (Thermo Fisher Scientific) for 4 days, followed by exposure to fresh medium supplemented with 5% FCS and containing GM-CSF and LPS (100 ng/ml) + IFN-γ (20 ng/ml) for an additional 72 hours. To generate M2 macrophages, monocytes were differentiated in RPMI 1640 medium (Thermo Fisher Scientific) supplemented with M-CSF (50 ng/ml), 2 mM glutamine, 10% decompartmented FCS, 100 IU/ml penicillin, and 100 µg/ml streptomycin for 4 days, followed by exposure to fresh medium supplemented with 5% FCS and containing M-CSF (50 ng/ml) + IL-4 (20 ng/ml) for an additional 72 hours.

Quantification of cytokine levels. A panel of 13 cytokines, including IL-1β, IFN-α, IFN-γ, TNF-α, MCP1, IL-6, IL-8, IL-10, IL-12p70, IL-17A, IL-18, IL-23, and IL-33 in monkey sera and in culture medium were quantified using multiplexing laser bead technology (BioLegend). To assess the cytokine production of macrophages, in vitro-polarized cells were washed 3 times with PBS and were subsequently activated with SARS-CoV pseudotype virus in RPMI 1640 medium (Thermo Fisher Scientific) with or without administration of highly diluted and heat-inactivated (56°C) sera from macaques or SARS patients. FcγR-specific mouse monoclonal antibody (5 µg, clone 3G8, anti-hCD16, 16016682; clone FL18.26, anti-hCD32, 16032981; and clone 10.1, anti-hCD64, 16064981 [BD Pharmingen]) was used for blockade of human FcγR. The supernatant of these cultures was recovered after 20 hours of stimulation, and the cytokine levels were measured and analyzed.

Statistics. All statistical analyses were performed using the 2-tailed Student's *t* test. *P* values less than 0.05 were considered statistically significant. Data are presented as the mean values ± SEM of at least 3 independent experiments unless otherwise indicated.

Study approval. The experiment was conducted in a Biosafety Level 3 animal facility. Handling and experimental procedures, including injections, blood collection, virus challenge, and sacrificing were approved and performed according to the animal welfare committee on the Use of Live Animals in Teaching and Research of Institute of Laboratory Animal Science, Beijing, China. All study subjects gave informed consent, and procedures were reviewed and approved by the University of Hong Kong Research Ethics Committee.

Author contributions

ZC, LL, and QW designed the study. LL and QW analyzed the data. LL, ZC, KYY, SP, and AL contributed to drafting the manuscript. ZC is the principal investigator, with overall responsibility for the design of the study. QW and CQ coordinated the autopsy organization and collection of autopsy materials of Chinese macaques. QW was involved in the development and performance of the RT-PCR assay. LL, HT, TW, and KWC performed the neutralization assay. LL, XA, and AL were involved in the development of the H&E, SARS-CoV IHC, and ISH assays. HW performed the ISH assay and the IHC staining of NP and calculation of the mean fluorescence intensity in the lungs. LL, HK, and KN performed the H&E and double- or triple-IHC staining. JF and HT performed culture of monocyte-derived macrophages. QL, HT, JP, and ZT performed analysis of cytokine production in cell culture supernatant and monkey sera. KHC and KYY coordinated the collection of sera and tissue sample from SARS patients. All authors were involved in the correlative interpretation of the pathological and molecular data.

Acknowledgments

This work was financially supported by grants from the U.S. NIH RO1HL080211 and Hong Kong Research Grants Council TRS T11-706/18-N to ZC, the TNPRC (base grant RR00164), RO1060699 to SP, HMRF16150662, and the University Development Fund/Li Ka Shing Faculty of Medicine Matching Fund of the University of Hong Kong to its AIDS Institute and Hong Kong RGV. The authors would like to thank D.D. Ho and K. Liu for support and scientific advice, and Wenjie Yu for assistance of S-IgG and C-IgG purification.

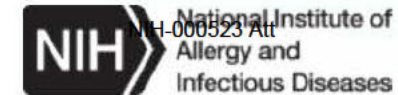
Address correspondence to: Zhiwei Chen or Li Liu, AIDS Institute and Department of Microbiology, State Key Laboratory of Emerging Infectious Disease, Li Ka Shing Faculty of Medicine, The University of Hong Kong, 21 Sassoon Road, Pokfulam, Hong Kong S.A.R., China. Phone: 852.28199831; Email: zchenai@hku.hk (ZC). Phone: 852.39179094; Email: liuli71@hku.hk (LL).

1. Drosten C, et al. Identification of a novel coronavirus in patients with severe acute respiratory syndrome. *N Engl J Med*. 2003;348(20):1967–1976.
2. Ksiazek TG, et al. A novel coronavirus associated with severe acute respiratory syndrome. *N Engl J Med*. 2003;348(20):1953–1966.
3. Hwang DM, Chamberlain DW, Poutanen SM, Low DE, Asa SL, Butany J. Pulmonary pathology of severe acute respiratory syndrome in Toronto. *Mod Pathol*. 2005;18(1):1–10.
4. Peiris JS, Guan Y. Confronting SARS: a view from Hong Kong. *Philos Trans R Soc Lond, B, Biol Sci*. 2004;359(1447):1075–1079.
5. Nicholls J, Dong XP, Jiang G, Peiris M. SARS: clinical virology and pathogenesis. *Respirology*. 2003;8 Suppl:S6–S8.
6. Peiris JS, et al. Clinical progression and viral load in a community outbreak of coronavirus-associated SARS pneumonia: a prospective study. *Lancet*. 2003;361(9371):1767–1772.
7. Ware LB, Matthay MA. The acute respiratory distress syndrome. *N Engl J Med*. 2000;342(18):1334–1349.
8. Herold S, Mayer K, Lohmeyer J. Acute lung injury: how macrophages orchestrate resolution of inflammation and tissue repair. *Front Immunol*. 2011;2:65.
9. Murray PJ, Wynn TA. Protective and pathogenic functions of macrophage subsets. *Nat Rev Immunol*. 2011;11(11):723–737.
10. Mosser DM, Edwards JP. Exploring the full spectrum of macrophage activation. *Nat Rev Immunol*. 2008;8(12):958–969.
11. Wynn TA, Vannella KM. Macrophages in Tissue Repair, Regeneration, and Fibrosis. *Immunity*. 2016;44(3):450–462.
12. Perlman S, Dandekar AA. Immunopathogenesis of coronavirus infections: implications for SARS. *Nat Rev Immunol*. 2005;5(12):917–927.
13. Channappanavar R, et al. Dysregulated Type I Interferon and Inflammatory Monocyte-Macrophage Responses Cause Lethal Pneumonia in SARS-CoV-Infected Mice. *Cell Host Microbe*. 2016;19(2):181–193.
14. Zhang L, et al. Antibody responses against SARS coronavirus are correlated with disease outcome of infected individuals. *J Med Virol*. 2006;78(1):1–8.
15. To KK, et al. High titer and avidity of nonneutralizing antibodies against influenza vaccine antigen are associated with severe influenza. *Clin Vaccine Immunol*. 2012;19(7):1012–1018.
16. Monsalvo AC, et al. Severe pandemic 2009 H1N1 influenza disease due to pathogenic immune complexes. *Nat Med*. 2011;17(2):195–199.
17. Clay C, et al. Primary severe acute respiratory syndrome coronavirus infection limits replication but not lung inflammation upon homologous rechallenge. *J Virol*. 2012;86(8):4234–4244.
18. Bolles M, et al. A double-inactivated severe acute respiratory syndrome coronavirus vaccine provides incomplete protection in mice and induces increased eosinophilic proinflammatory pulmonary response upon challenge. *J Virol*. 2011;85(23):12201–12215.
19. Tseng CT, et al. Immunization with SARS coronavirus vaccines leads to pulmonary immunopathology on challenge with the SARS virus. *PLoS ONE*. 2012;7(4):e35421.
20. Zhao J, et al. Airway Memory CD4(+) T Cells Mediate Protective Immunity against Emerging Respiratory Coronaviruses. *Immunity*. 2016;44(6):1379–1391.
21. Channappanavar R, Fett C, Zhao J, Meyerholz DK, Perlman S. Virus-specific memory CD8 T cells provide substantial protection from lethal severe acute respiratory syndrome coronavirus infection. *J Virol*. 2014;88(19):11034–11044.
22. Zhao J, Zhao J, Perlman S. T cell responses are required for protection from clinical disease and for virus clearance in severe acute respiratory syndrome coronavirus-infected mice. *J Virol*. 2010;84(18):9318–9325.
23. Honda-Okubo Y, Barnard D, Ong CH, Peng BH, Tseng CT, Petrovsky N. Severe acute respiratory syndrome-associated coronavirus vaccines formulated with delta inulin adjuvants provide enhanced protection while ameliorating lung eosinophilic immunopathology. *J Virol*. 2015;89(6):2995–3007.
24. Chen Z, et al. Recombinant modified vaccinia virus Ankara expressing the spike glycoprotein of severe acute respiratory syndrome coronavirus induces protective neutralizing antibodies primarily targeting the receptor binding region. *J Virol*. 2005;79(5):2678–2688.
25. Liu L, et al. Spatiotemporal interplay of severe acute respiratory syndrome coronavirus and respiratory mucosal cells drives viral dissemination in rhesus macaques. *Mucosal Immunol*. 2016;9(4):1089–1101.
26. Li BJ, et al. Using siRNA in prophylactic and therapeutic regimens against SARS coronavirus in Rhesus macaque. *Nat Med*. 2005;11(9):944–951.
27. Qin C, et al. An animal model of SARS produced by infection of *Macaca mulatta* with SARS coronavirus. *J Pathol*. 2005;206(3):251–259.
28. Soulas C, et al. Recently infiltrating MAC387(+) monocytes/macrophages a third macrophage population involved in SIV and HIV encephalitic lesion formation. *Am J Pathol*. 2011;178(5):2121–2135.
29. Cai Y, Sugimoto C, Arainga M, Alvarez X, Didier ES, Kuroda MJ. In vivo characterization of alveolar and interstitial lung macrophages in rhesus macaques: implications for understanding lung disease in humans. *J Immunol*. 2014;192(6):2821–2829.
30. Murray PJ, et al. Macrophage activation and polarization: nomenclature and experimental guidelines. *Immunity*. 2014;41(1):14–20.
31. Imai Y, et al. Identification of oxidative stress and Toll-like receptor 4 signaling as a key pathway of acute lung injury. *Cell*. 2008;133(2):235–249.
32. Atreya R, et al. Blockade of interleukin 6 trans signaling suppresses T-cell resistance against apoptosis in chronic intestinal inflammation: evidence in crohn disease and experimental colitis in vivo. *Nat Med*. 2000;6(5):583–588.
33. Braciale TJ, Sun J, Kim TS. Regulating the adaptive immune response to respiratory virus infection. *Nat Rev Immunol*. 2012;12(4):295–305.

34. Subbarao K, et al. Prior infection and passive transfer of neutralizing antibody prevent replication of severe acute respiratory syndrome coronavirus in the respiratory tract of mice. *J Virol*. 2004;78(7):3572–3577.
35. Yang ZY, et al. A DNA vaccine induces SARS coronavirus neutralization and protective immunity in mice. *Nature*. 2004;428(6982):561–564.
36. Du L, et al. Priming with rAAV encoding RBD of SARS-CoV S protein and boosting with RBD-specific peptides for T cell epitopes elevated humoral and cellular immune responses against SARS-CoV infection. *Vaccine*. 2008;26(13):1644–1651.
37. Du L, et al. Intranasal vaccination of recombinant adeno-associated virus encoding receptor-binding domain of severe acute respiratory syndrome coronavirus (SARS-CoV) spike protein induces strong mucosal immune responses and provides long-term protection against SARS-CoV infection. *J Immunol*. 2008;180(2):948–956.
38. Du L, et al. Receptor-binding domain of SARS-CoV spike protein induces long-term protective immunity in an animal model. *Vaccine*. 2007;25(15):2832–2838.
39. Fett C, DeDiego ML, Regla-Nava JA, Enjuanes L, Perlman S. Complete protection against severe acute respiratory syndrome coronavirus-mediated lethal respiratory disease in aged mice by immunization with a mouse-adapted virus lacking E protein. *J Virol*. 2013;87(12):6551–6559.
40. Iwata-Yoshikawa N, et al. Effects of Toll-like receptor stimulation on eosinophilic infiltration in lungs of BALB/c mice immunized with UV-inactivated severe acute respiratory syndrome-related coronavirus vaccine. *J Virol*. 2014;88(15):8597–8614.
41. Qin E, et al. Immunogenicity and protective efficacy in monkeys of purified inactivated Vero-cell SARS vaccine. *Vaccine*. 2006;24(7):1028–1034.
42. Zhou J, et al. Immunogenicity, safety, and protective efficacy of an inactivated SARS-associated coronavirus vaccine in rhesus monkeys. *Vaccine*. 2005;23(24):3202–3209.
43. Openshaw PJ, Tregoning JS. Immune responses and disease enhancement during respiratory syncytial virus infection. *Clin Microbiol Rev*. 2005;18(3):541–555.
44. Stockman LJ, et al. Severe acute respiratory syndrome in children. *Pediatr Infect Dis J*. 2007;26(1):68–74.
45. Mair-Jenkins J, et al. The effectiveness of convalescent plasma and hyperimmune immunoglobulin for the treatment of severe acute respiratory infections of viral etiology: a systematic review and exploratory meta-analysis. *J Infect Dis*. 2015;211(1):80–90.
46. Cheng Y, et al. Use of convalescent plasma therapy in SARS patients in Hong Kong. *Eur J Clin Microbiol Infect Dis*. 2005;24(1):44–46.
47. Soo YO, et al. Retrospective comparison of convalescent plasma with continuing high-dose methylprednisolone treatment in SARS patients. *Clin Microbiol Infect*. 2004;10(7):676–678.
48. Wang Q, et al. Immunodominant SARS Coronavirus Epitopes in Humans Elicited both Enhancing and Neutralizing Effects on Infection in Non-human Primates. *ACS Infect Dis*. 2016;2(5):361–376.
49. Yi CE, Ba L, Zhang L, Ho DD, Chen Z. Single amino acid substitutions in the severe acute respiratory syndrome coronavirus spike glycoprotein determine viral entry and immunogenicity of a major neutralizing domain. *J Virol*. 2005;79(18):11638–11646.
50. Pahl JH, et al. Macrophages inhibit human osteosarcoma cell growth after activation with the bacterial cell wall derivative liposomal muramyl tripeptide in combination with interferon- γ . *J Exp Clin Cancer Res*. 2014;33:27.
51. Kieran J, et al. The relative efficacy of boceprevir and telaprevir in the treatment of hepatitis C virus genotype 1. *Clin Infect Dis*. 2013;56(2):228–235.
52. Cheng L, et al. Monoclonal antibodies specific to human Δ 42PD1: A novel immunoregulator potentially involved in HIV-1 and tumor pathogenesis. *MAbs*. 2015;7(3):620–629.



Dale and Betty Bumpers
VACCINE RESEARCH CENTER
National Institute of Allergy and Infectious Diseases
National Institutes of Health
Department of Health and Human Services



“Advances” in Enhanced Disease Models for RSV Vaccines

WHO Consultation on RSV Vaccine Development Geneva, Switzerland April 26, 2016

NIH006410

**Barney S. Graham, MD,
PhDVaccine Research
CenterNIAID, NIH**

Papers reporting FI-RSV vaccine-enhanced disease (Am J Epidemiol 1969) NIH-000523 Att

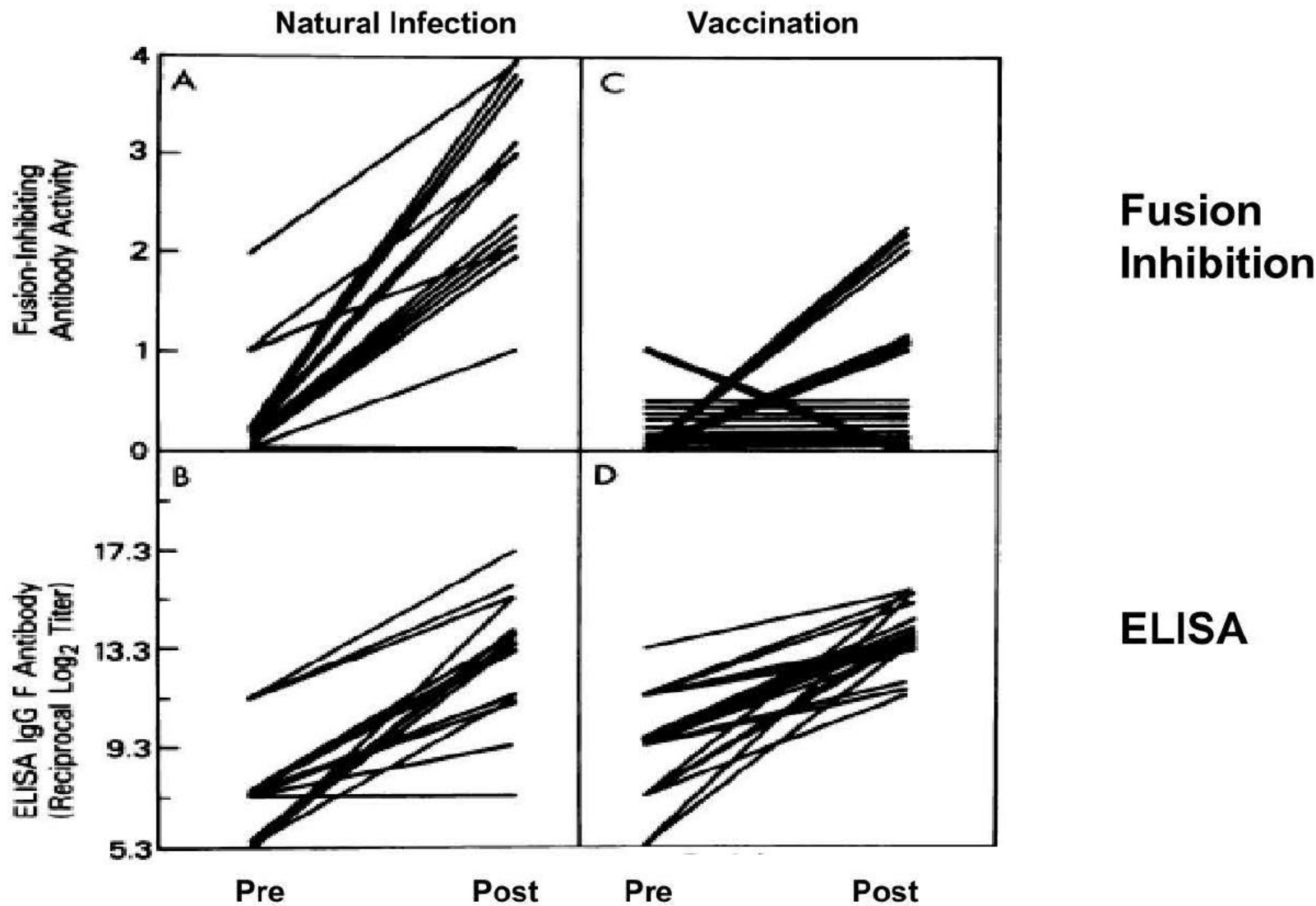
- Chin et al. (0,1 schedule; 4 mo. – 10 year; 43 <1 yr.) Eosinophilia CF response <6 mo (36%), 6-18 mo (55%), 2-9 yrs. (84%) Higher rate and severity of illness in vaccinees (?higher virus load) Fulginiti et al. (0,1,2 schedule; 6 mo.-7 yrs.) 7/51 (13.7%) vaccinees vs. 1/65 (1.5%) TPV recipients hospitalized Of 19 with >4X CF responses only 9 had NT responses Kapikian et al. (0,1,2 schedule; 5-65 mo. of age; only 2 <1yr.) 9/13 vaccinees with pneumonia vs. 4/47 nonvaccinated (5 & 0 hosp.) Relatively high CF antibody and NT response, and no eosinophilia Kim et al. (0,1,4 schedule 2-7 mo. of age) Peribronchial monocytic infiltrate with excess of eosinophils Relatively high CF antibody response in vaccinees High lymphoproliferation index in vaccinees

FI-RSV Vaccine-Enhanced Disease

Vaccine	n*	Infected (%)	Hospitalized (%)**	Deaths***
FI-RSV	31	20 (65)	16 (80)	
2FI-PIV-1	40	21 (53)	1 (5)	0

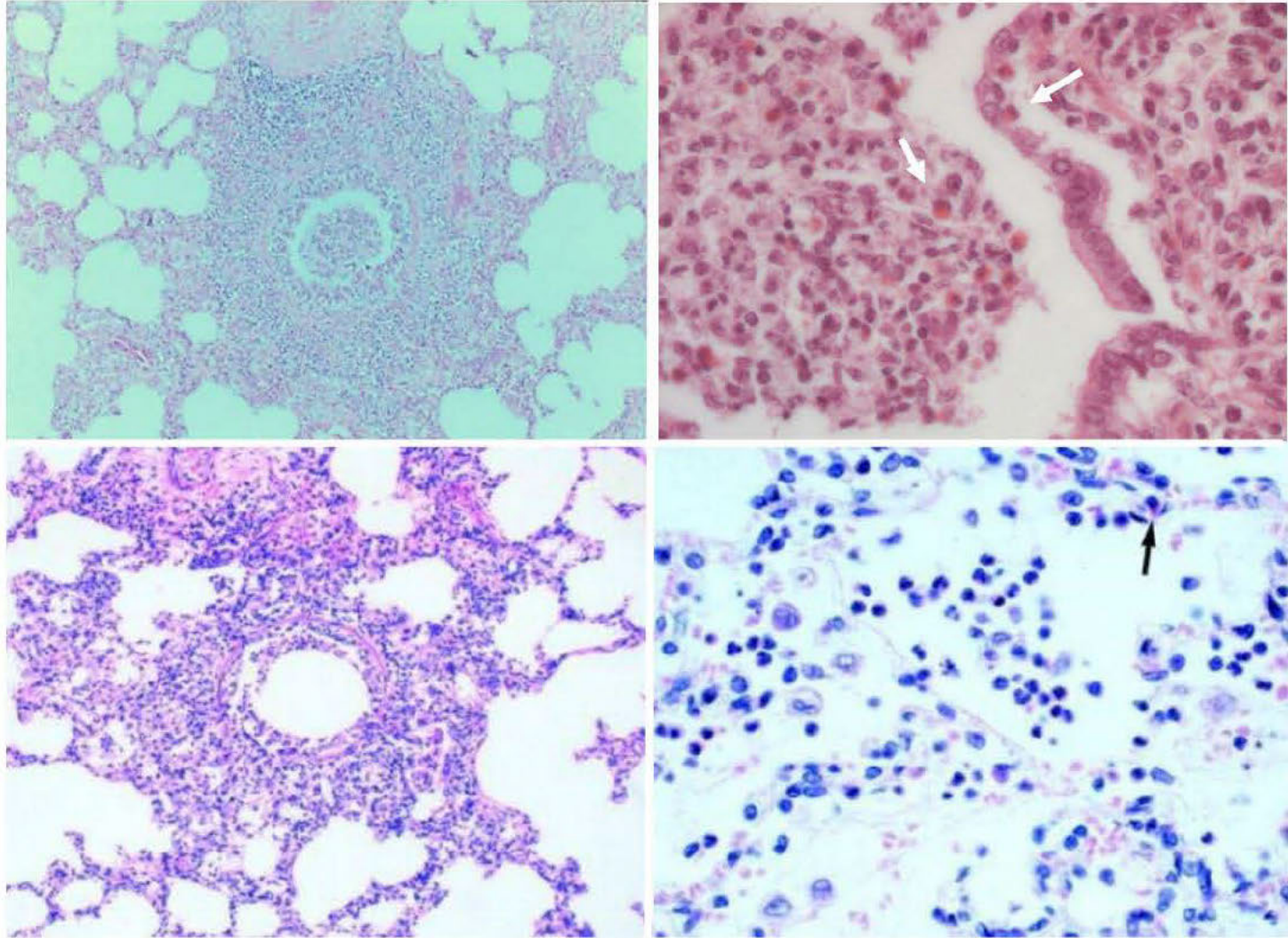
* 1 injection (n=2); 2 injections (n=8); 3 injections (n=21) ** In unpublished 1962/3 trial - 21/54 infected; 10/21 hospitalized*** 14 and 16 mo. of age; 3 injections starting at 2 and 5 mo. of age. Both had bacterial pneumonia complicating RSV

FI-RSV Immunization Results in a Discordance Between Functional and Binding Antibody



NIH006413

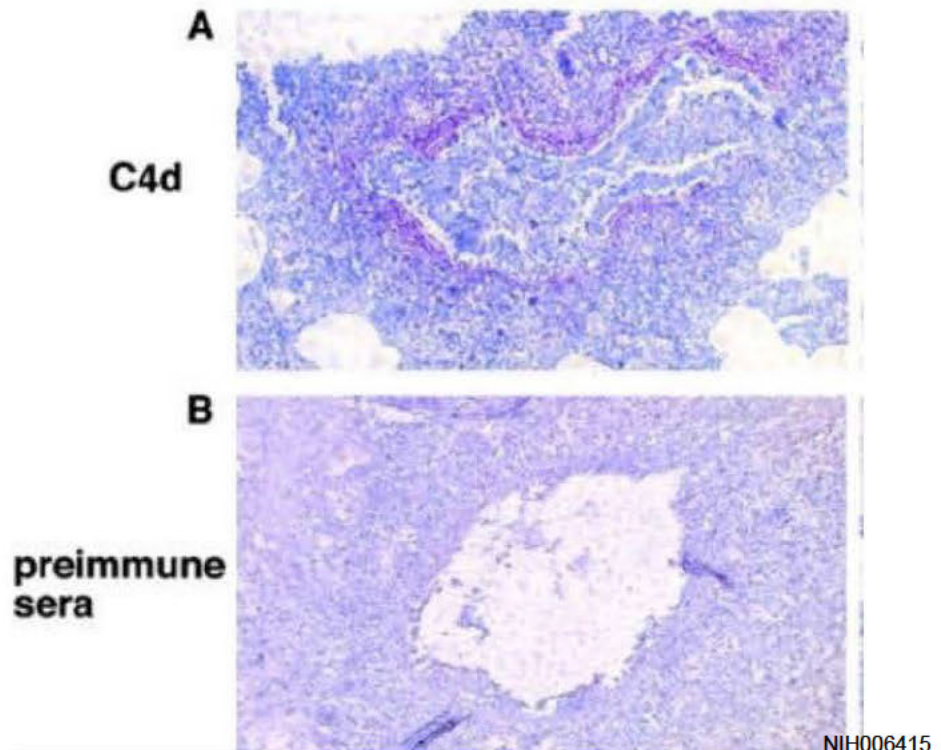
Histopathology in FI-RSV Vaccine-Enhanced Disease



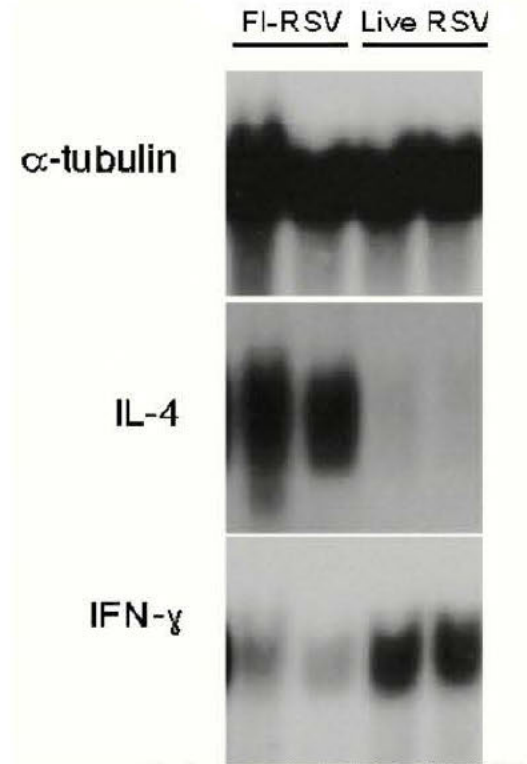
Immune Response Patterns Associated with FI-RSV Vaccine-Enhanced Illness

Antibodies with poor NT activity
↓ Immune complex deposition

CD4+ Th2-biased response ↓
Allergic inflammation



Polack et al. J Exp Med 2002; 196:859

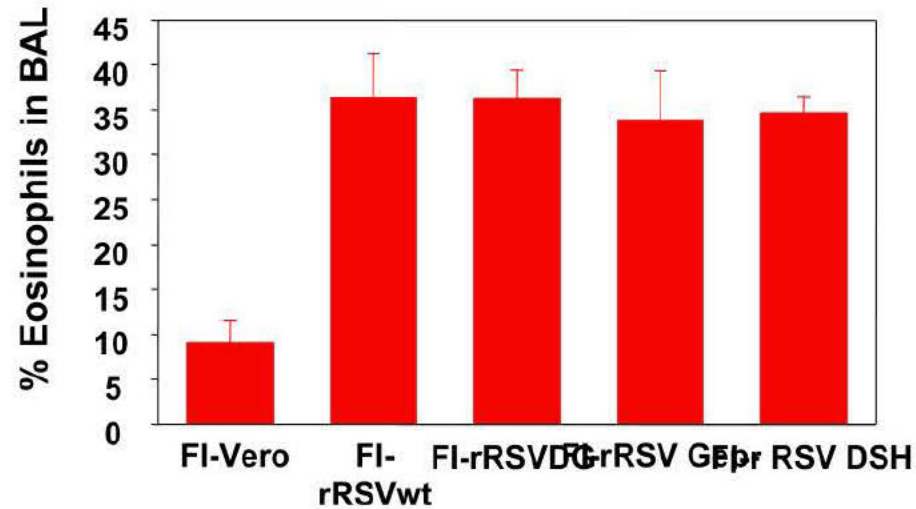


Graham et al. JI 1993;151:2032

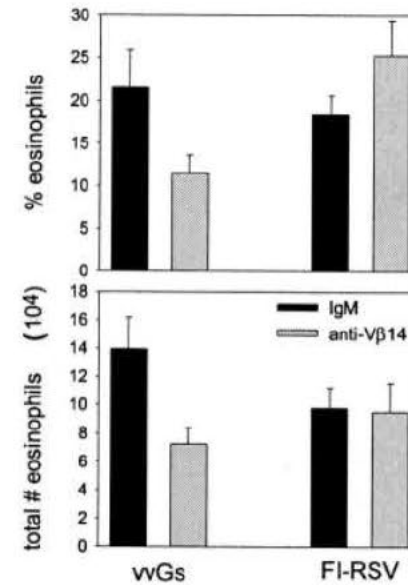
Animal Models of RSV

- Rodents
Mice
immunocompromised
Pneumovirus of mice
Cotton rats
Guinea pigs
Large animal
Bovine
Ovine
Nonhuman primates
Chimpanzees
African Green monkeys
Baboons
Other
Ferret
Chinchilla

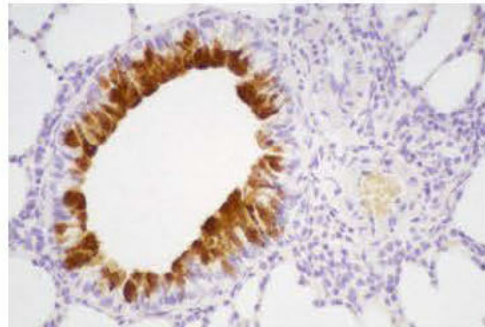
Determinants of FI-RSV Vaccine Enhanced Illness in BALB/c Mice



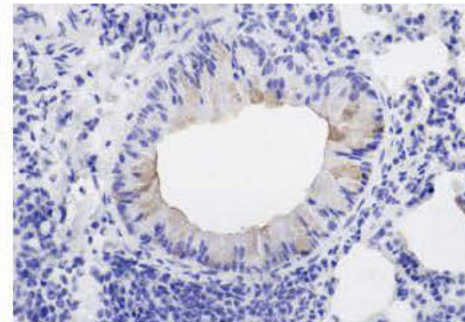
Johnson & Graham et al. J Virol 2004; 78:6024



Johnson et al. J Virol 2004; 78:8753

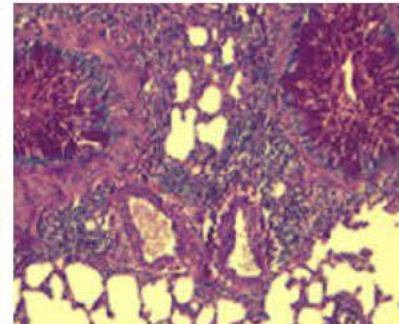


Gob-5

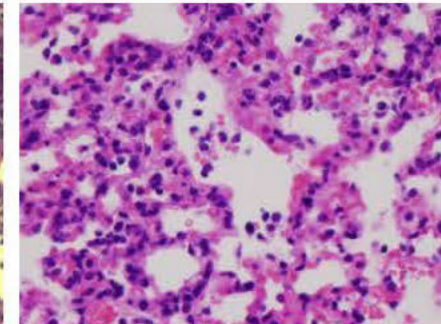


Muc5ac

NIH006417



Mucus by PAS



Alveolitis

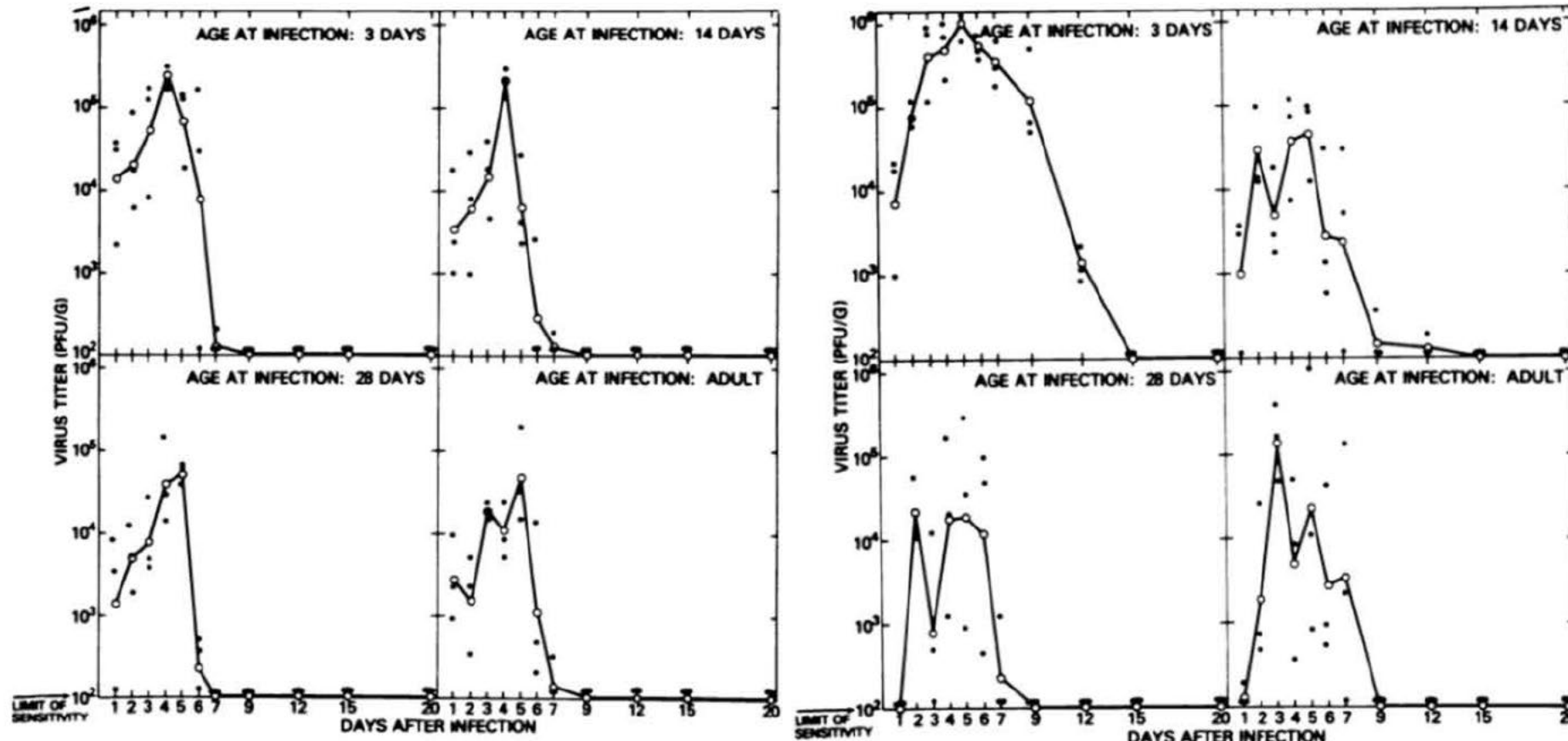
Potential Advantages of Cotton Rats Over Mice

- 3d old cotton rats >1 log₁₀ pfu more replication in nose than adults with delayed viral clearance
More prominent neutrophil infiltrate
Slightly more permissive than mice, particularly neonates

RSV Replication in Cotton Rat Lung and Nose

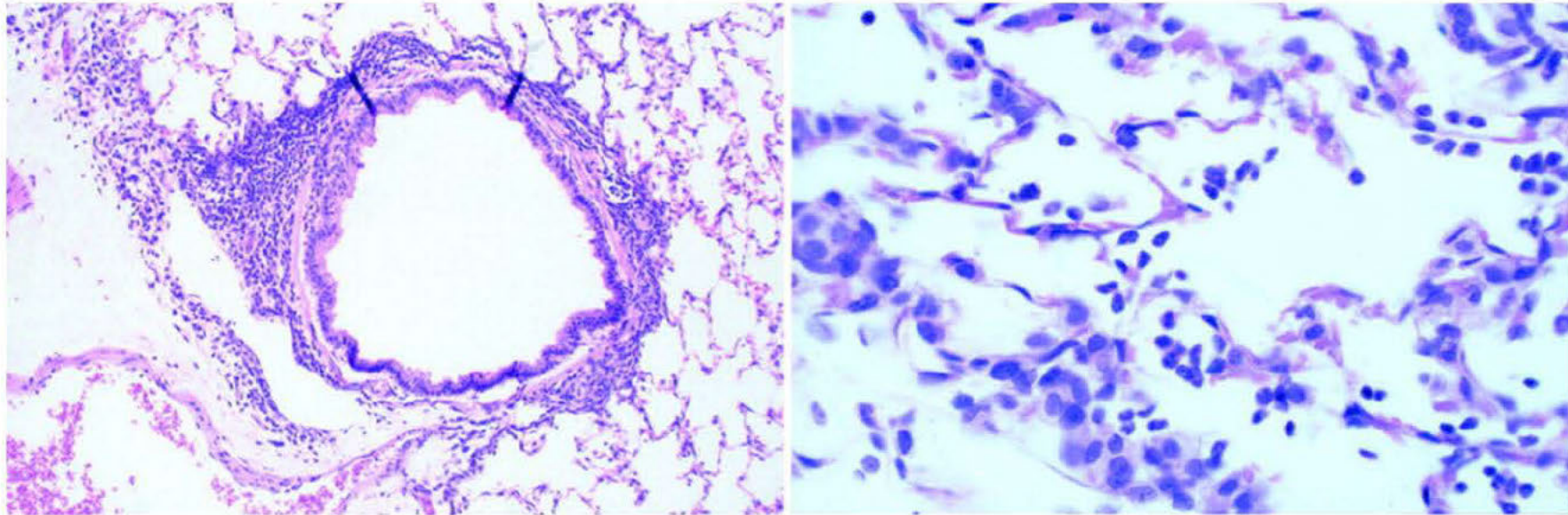
Lung

Nose



NIH006419

FI-RSV Enhanced Disease Endpoint in Cotton Rats



Prince GA, et al. *J Virol* 1986; 57:721

Mice

- Semi-permissiveRelatively high body temperatureType I IFN not inhibited by NS1/2Large inoculum directly to lungBALB/c model characteristics based largely on two unusual T cells – a V β 13.2 M282-90 CD8 and a V β 14 G184-198 CD4

Cotton Rats

- Semi-permissiveLarge inoculum directly to lungDoes not exhibit illnessLimited immunological assessment based on inbred strains and reagentsDifficult to distinguish neutrophils from eosinophils

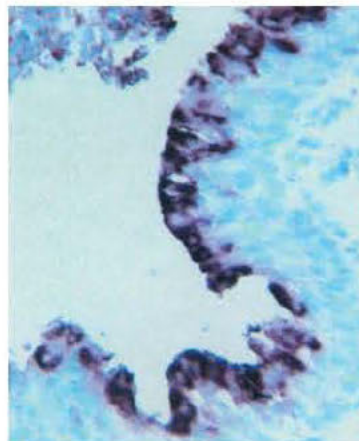
Caveats – 1) cannot assess histopathology in absence of viral replication, 2) cannot reinfect after primary infection

Bovine Model of bRSV

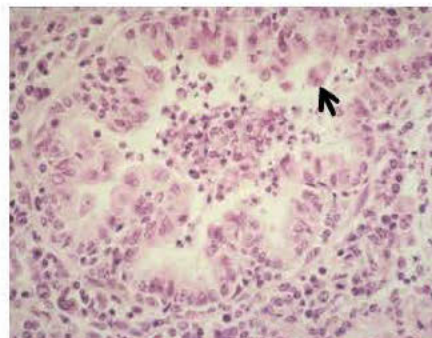
Lung
consolidation



Infection of
bronchiolar epithelium



Bronchiolitis



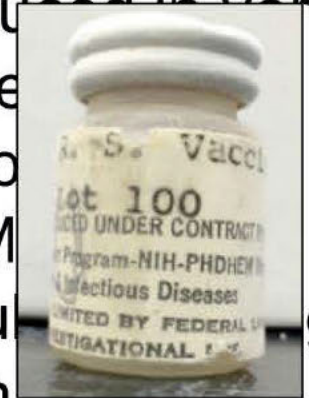
Alveolitis



Caveats – 1) bRSV is not hRSV, 2) generally small group sizes in each experiment, 3) Uses large inoculum into lower airway, 4) limited immunological reagents

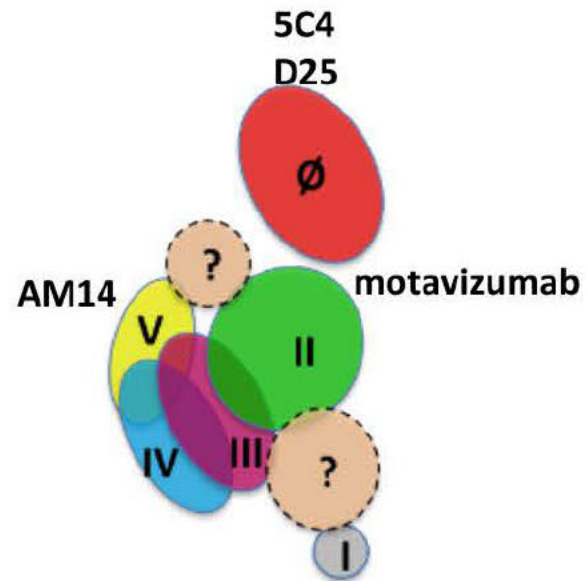
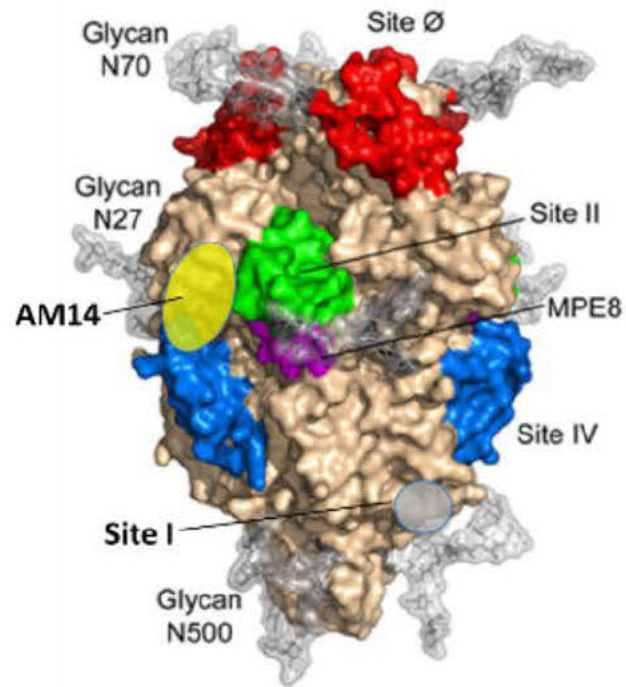
Pfizer Lot 100 FI-RSV

- Bernett strain of RSV isolated in primary human embryonic kidney from throat swab at NIH, May 1961 and passaged X3
Passaged X10 and produced in monkey kidney cells
3 early (day 4) and 11 late (day 7) sublot harvested
combined
Clarified by Millipore SM filtration
72 hours at 36°C with force
1/4000 wt/vol
50,000 rpm pellet and 25-fold concentration in EMEM
salt solution
Alum precipitation (4 mg/ml) (?aluminum potassium sulfate)
at 4°C with polymyxin, neomycin, streptomycin, and benzethonium
preservatives
IM delivery on a 0,1 or 0,1,2 or 0,1,4 month schedule
Control was Parainfluenza I then trivalent Para 1,2,3

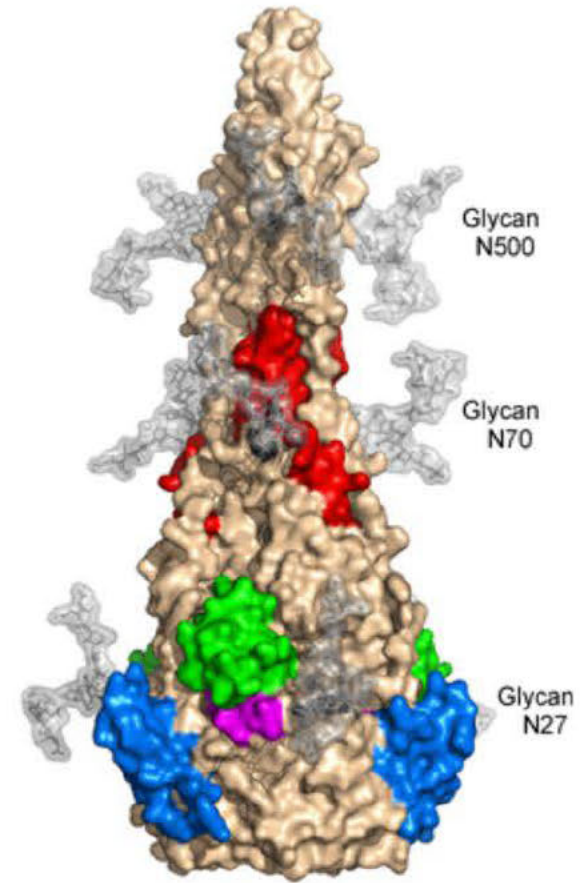


Neutralizing Epitopes on RSV F

Pre-F5 defined
epitopes 3 more being
mapped

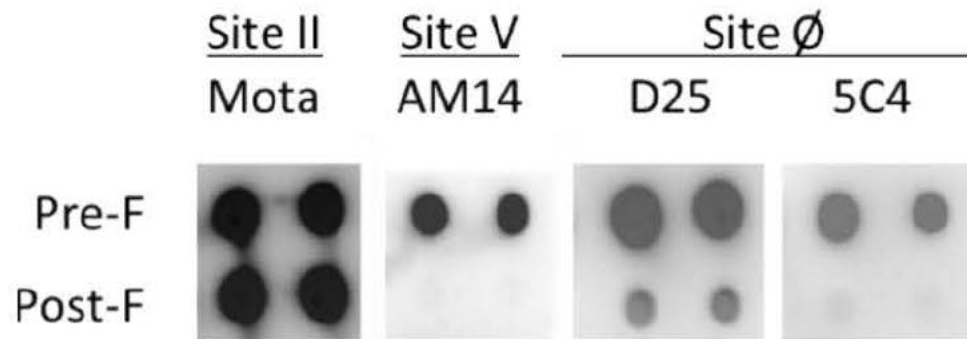
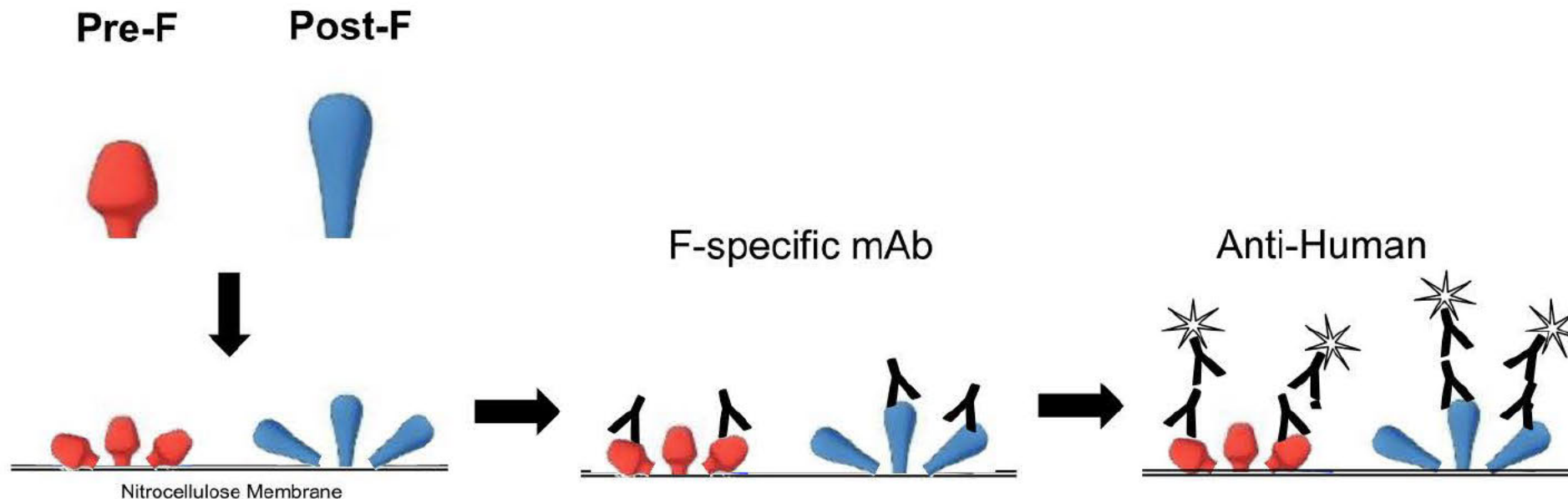


NIH006424



Post-F2 shared
epitopes

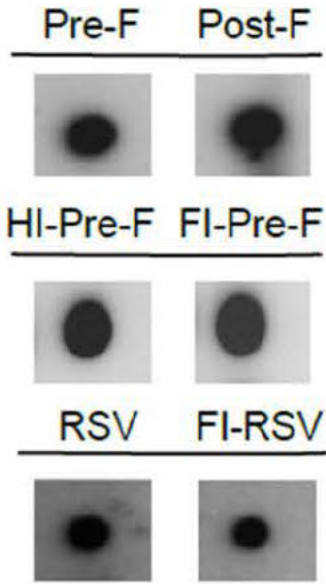
Dot Blot for Antigenicity



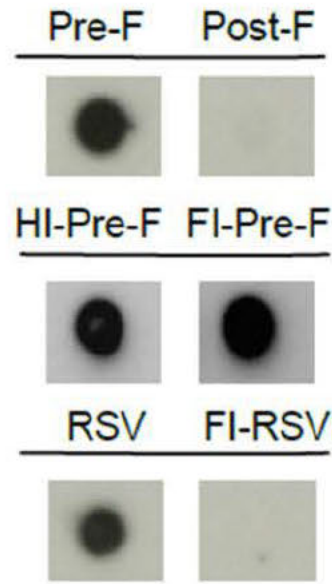
Antigenicity of RSV F Proteins and Virus Particles

NIH-000523 Att

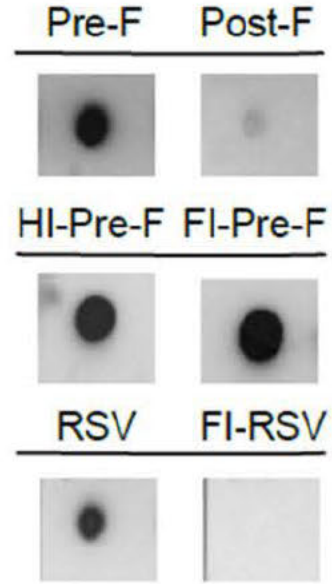
Motavizumab



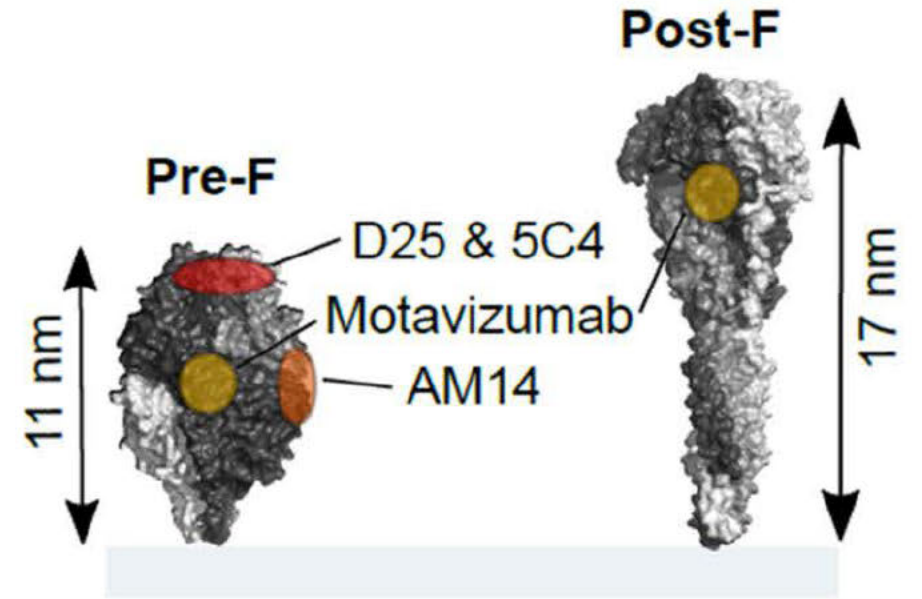
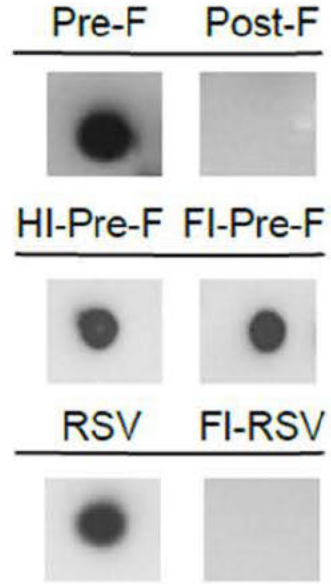
AM14



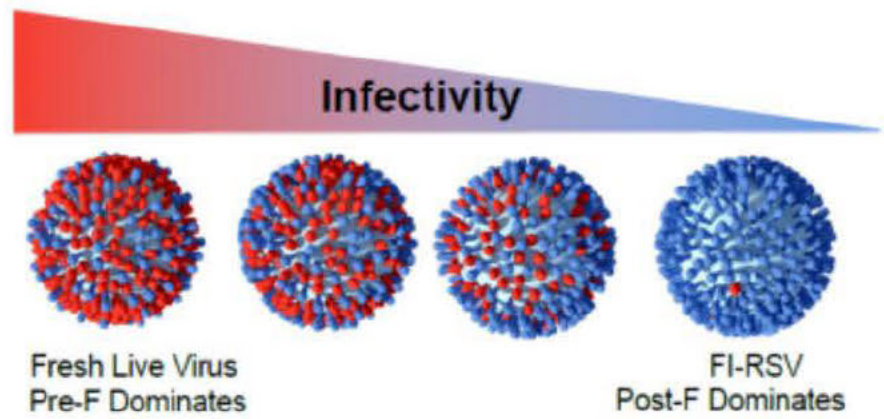
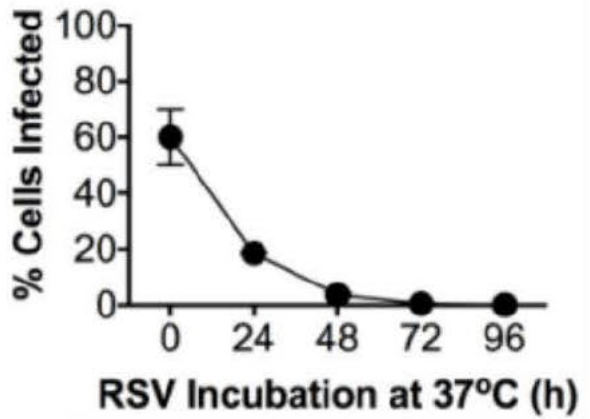
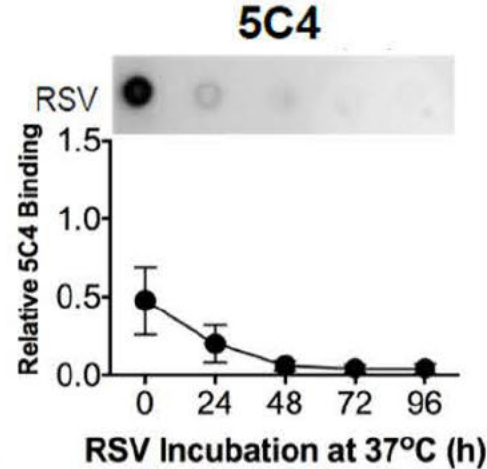
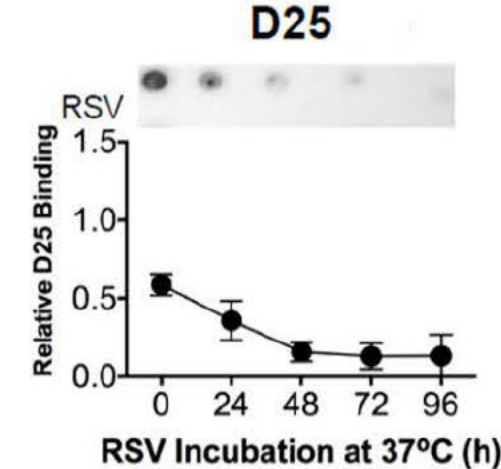
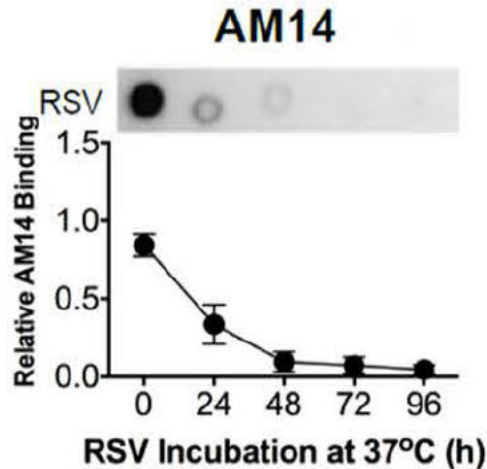
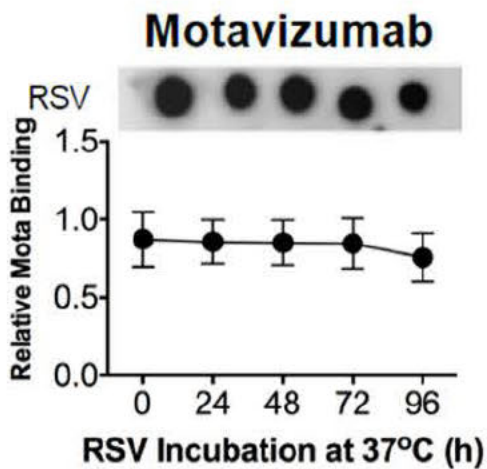
D25



5C4



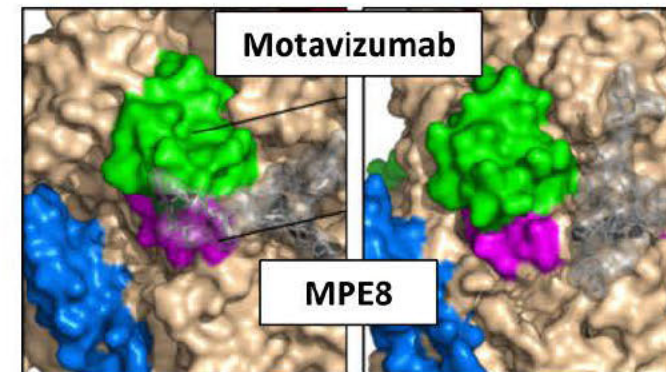
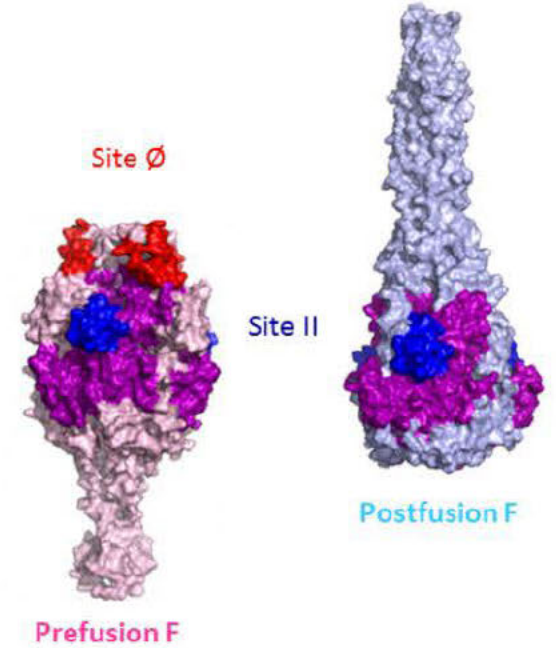
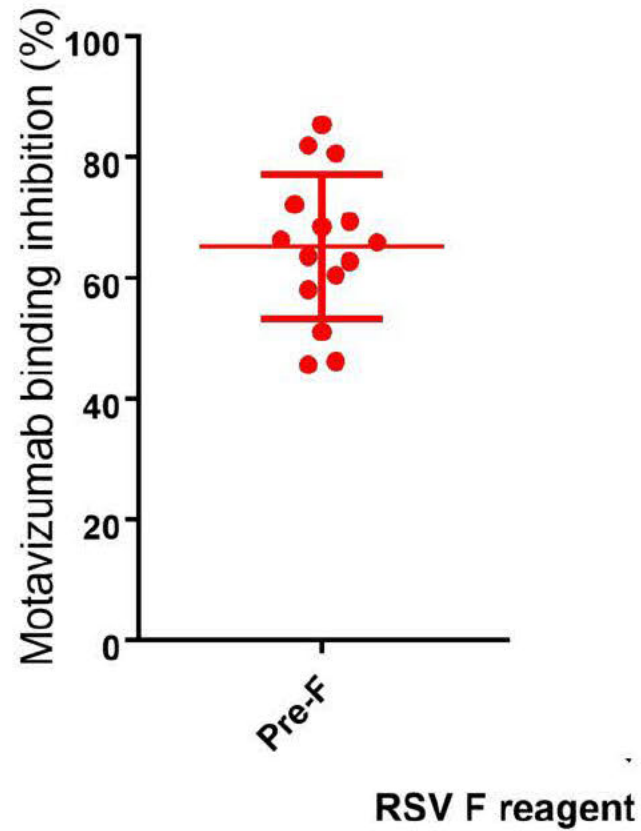
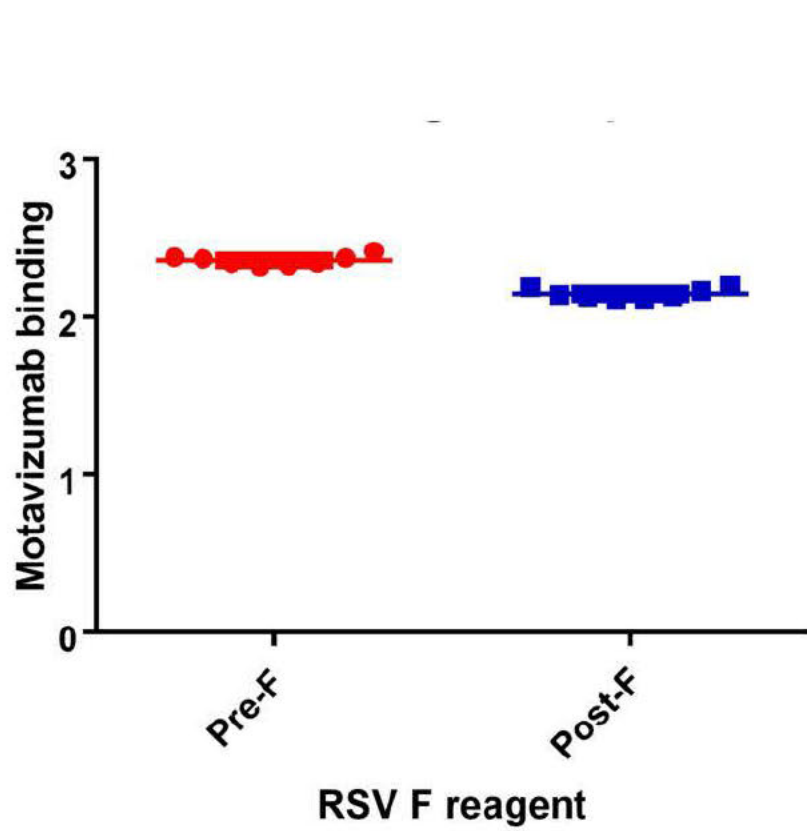
Pre-F Rapidly Flips to Post-F on RSV at 37°C in 0.025% Formaldehyde



Conclusions

- FI-RSV caused enhanced illness in children <24 mo. old Antibody response had high ratio of binding to functional antibody and resulted in immune complex deposition and complement activation Animal models and human pathology suggest a Th2-biased immune response was associated with enhanced disease Most NT-sensitive epitopes are on pre-F conformation FI-RSV did not present pre-F epitopes

Motavizumab Binding and Serum Competition



VRC Viral Pathogenesis Laboratory

NIH-000523 Att

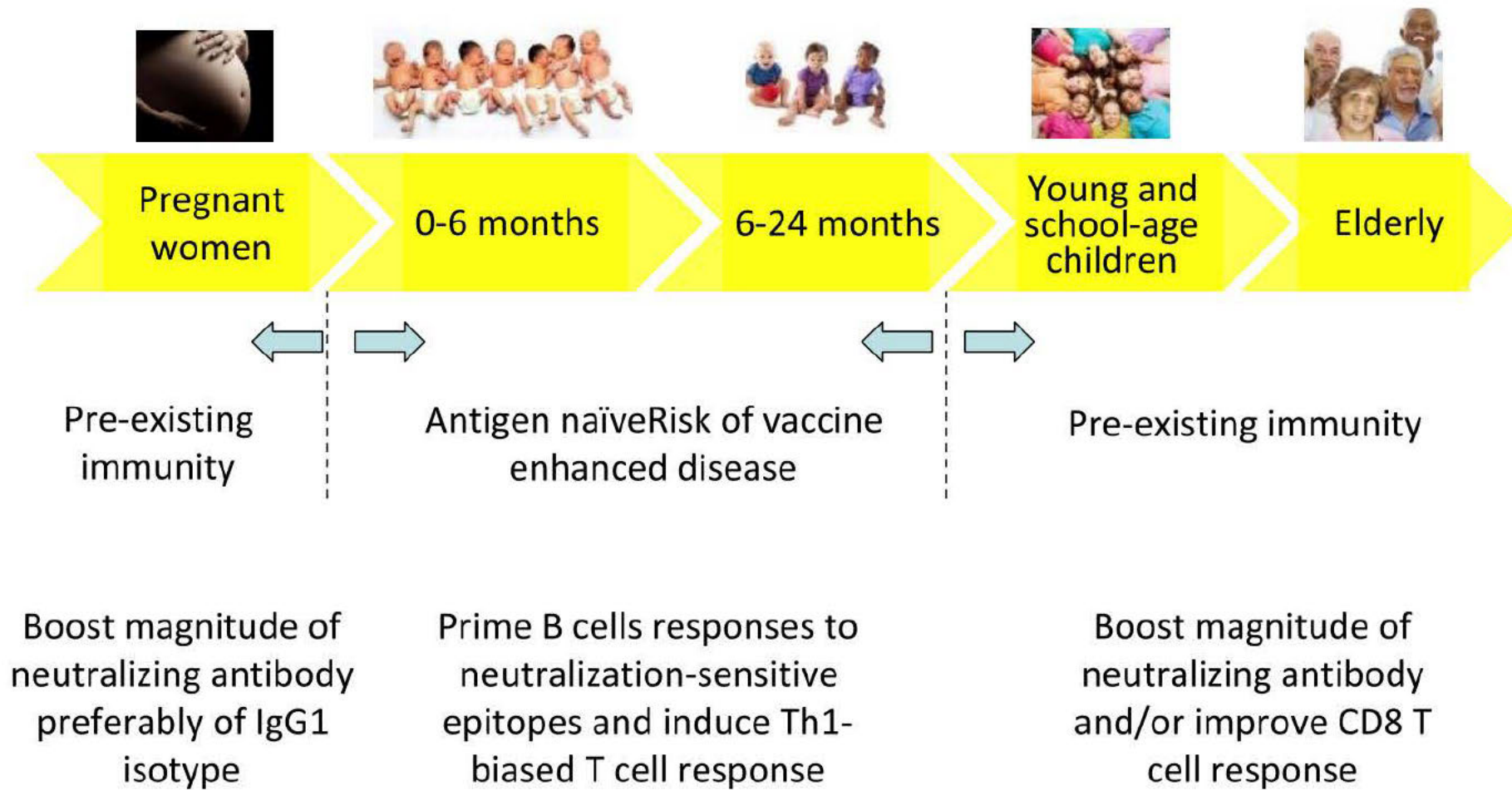


**Top row: Man Chen, Tracy Ruckwardt, Joan Ngwuta, April Killikelly, Kaitlyn Morabito, Jie Liu
Truck bed: Michelle Crank, Kizzmekia Corbett, Rebecca Gillespie
Standing: Azad Kumar, Syed Moin, Masaru Kanekiyo, Monique Young**

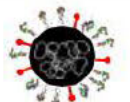



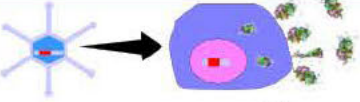
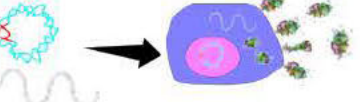
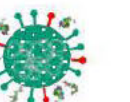

NIH006430

December 2015

Immunogenicity Goals for RSV Vaccines

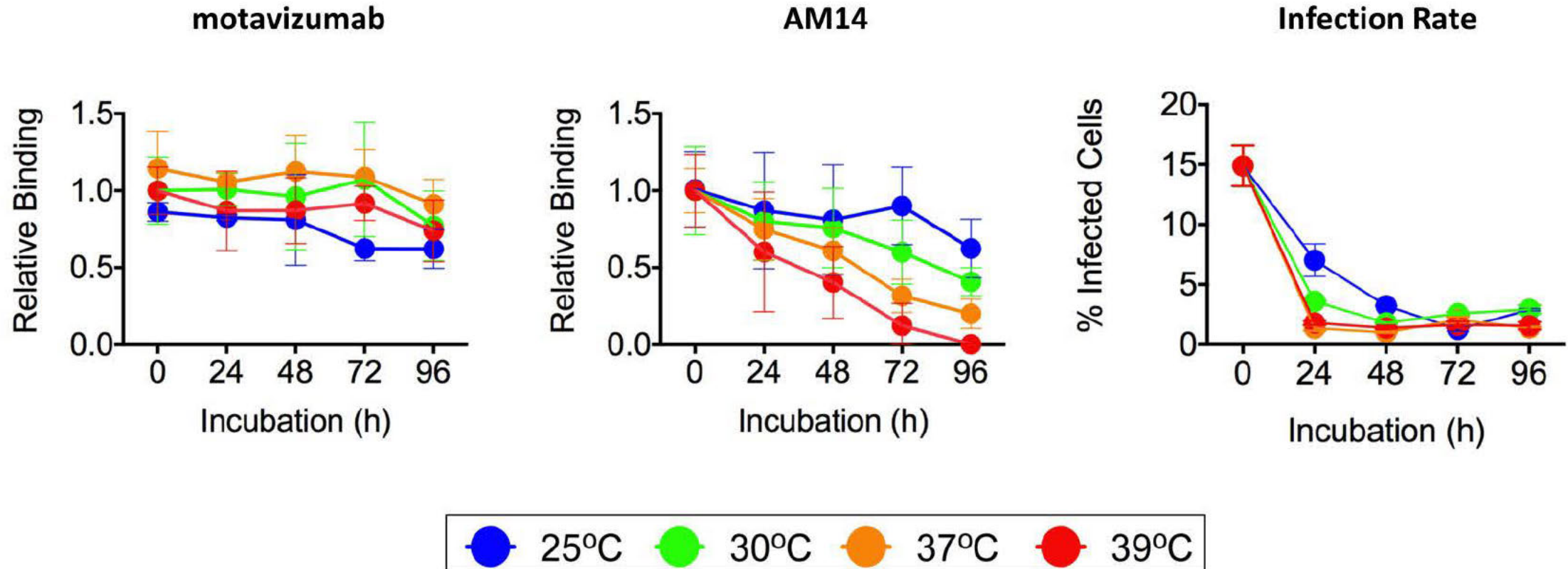


Biological Profile of Candidate RSV Vaccines

		Neutralizing epitopes	MHC pathway	CD8 T cell induction	IL-4	Delivery route	Immune modulation	Replication competence
Whole-inactivated virus		-	II	-	++	IM	+/-	-
Post-fusion F or G subunit		+/-	II	-	+/-	IM	-/+	-
VLPs or virosomes		+	II +/- I	+/-	-/+	IM	-/+	-
Pre-fusion F subunit		+++	II	-	+/-	IM	-	-
Vectors		++	I & II	++	-	IM or nasal	-	- or +
Naked DNA or RNA		++	I & II	+	-	IM	-	-
Recombinant or chimeric viruses		++	I & II	+	-	nasal	+/-	+
WT or attenuated virus		++	I & II	+	-	nasal or IM	+	+

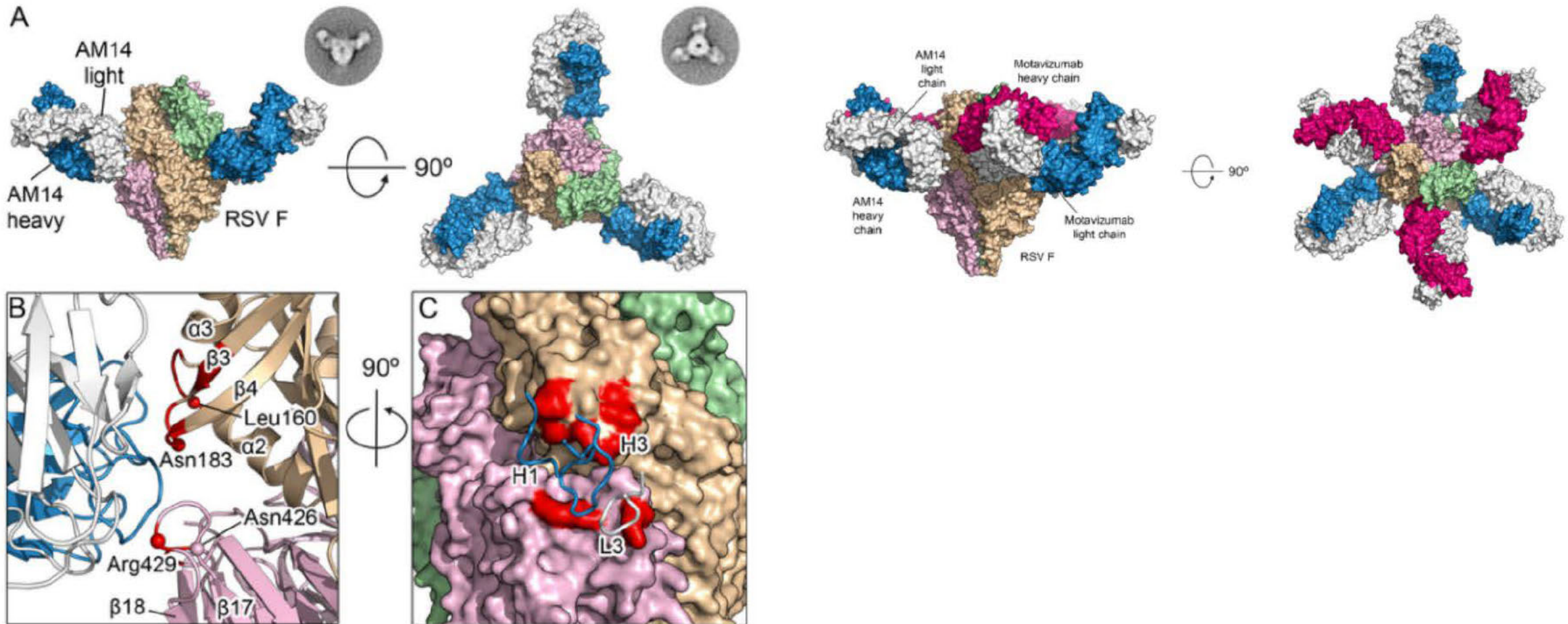
Effect of Temperature on Antigenicity and Infectivity

NIH006433 Att



AM14 is a Quaternary Pre-F and Trimer-Specific Human mAb

NIH-000523 Att



Gilman et al. ^{NIH006434} PLoS Pathog. 2015 Jul 10;11(7):e1005035.

FI-RSV Vaccine-Induced Antibody

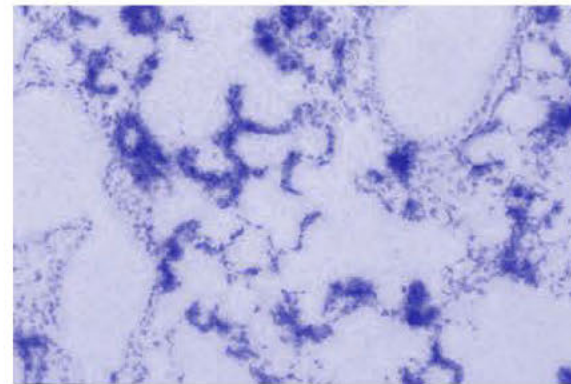
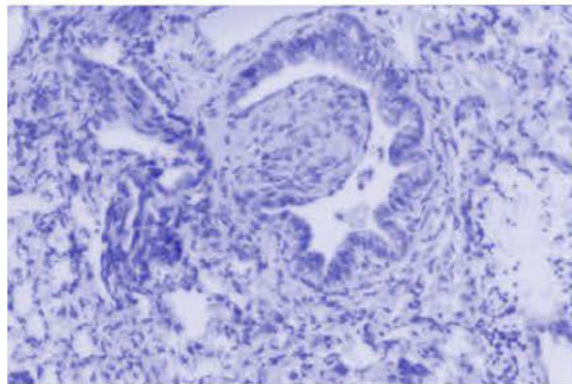
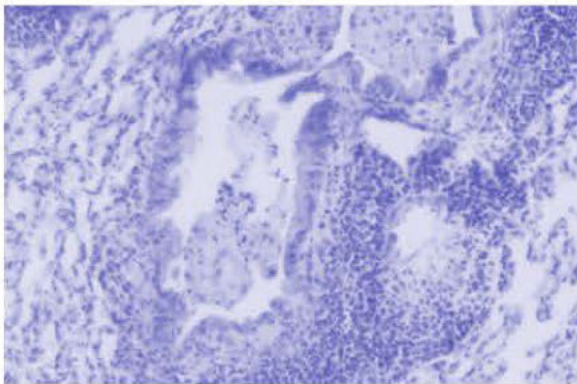
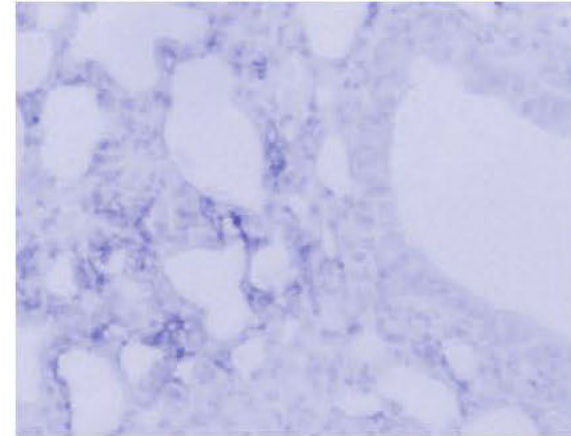
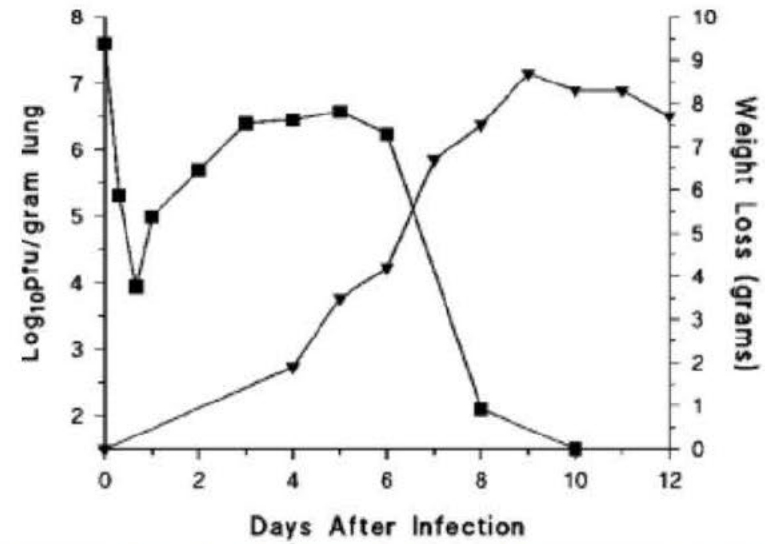
	N	% 4-fold rise	Mean fold rise	Post RSV mean fold rise
NT with C'	23	43	2.6	21 (12 of 16)
CF	23	91	30	165 (15 of 16)*

Binding antibody was induced out of proportion to neutralizing antibody

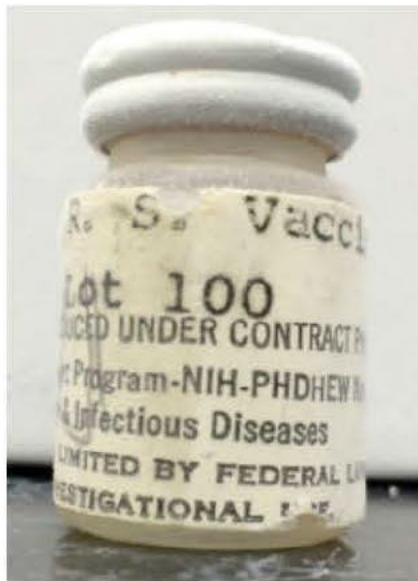
History of FI-RSV Vaccine Enhanced Disease in Clinical Trials

<1966 – Live and inactivated RSV given parenterally without benefit, but no reported harm 1966-7 – 4 independent studies using Pfizer lot 100 formalin-inactivated RSV did not protect and caused enhanced disease>1967 - Live RSV IM, live-attenuated RSV IN given without harm

Murine Model of RSV



Vaccine-Enhanced Disease



What was the antigenic content of the Lot 100 FI-RSV vaccine used in the 1960's?

Immunological Lessons from Respiratory Syncytial Virus Vaccine Development

Tracy J. Ruckwardt,¹ Kaitlyn M. Morabito,¹ and Barney S. Graham^{1,*}

¹Vaccine Research Center, National Institute of Allergy and Infectious Diseases, National Institutes of Health, Bethesda, MD 20892, USA

*Correspondence: bgraham@nih.gov

<https://doi.org/10.1016/j.immuni.2019.08.007>

Respiratory syncytial virus (RSV) has eluded active vaccination efforts for more than five decades and continues to cause substantial morbidity and mortality in infants, the immunocompromised, and older adults. Although newer approaches of passive antibody-mediated protection show promise, vaccines aimed at eliciting fusion protein (F)-targeting antibodies have repeatedly failed to meet pre-established, modest-efficacy goals. Newer candidates, including protein-based vaccines, live-attenuated viruses, and gene-based delivery platforms, incorporate structurally defined and stabilized versions of the prefusion form of the F glycoprotein and are advancing rapidly into critical efficacy studies in susceptible target populations. This review discusses the storied history of RSV vaccine development, immunological lessons learned along the way, and critical findings about protein structure that remodeled our understanding of protective immunity to this important pathogen.

Introduction

Respiratory syncytial virus (RSV) was discovered in 1956 as chimpanzee coryza agent (Blount et al., 1956) and associated with the clinical syndrome of bronchiolitis in 1957 (Chanock and Finberg, 1957). Bronchiolitis may have been first described in western literature in 1826 (Parrish, 1826), and the pathology and clinical features of bronchiolitis were reported in 1939 and 1941, respectively (Adams, 1941, 1948; Goodpasture et al., 1939). RSV bronchiolitis was associated with childhood asthma in 1959 and is the leading cause of hospitalization in young infants (Beem et al., 1960; Hall et al., 2013; Wittig and Glaser, 1959). It is ubiquitous and present in all geographic locations and climates throughout the world (Shi et al., 2017, 2019). RSV and metapneumovirus together account for nearly half of all medically attended respiratory infections in children less than one year of age (Lozano et al., 2012), and a large case-controlled study on the etiology of pneumonia implicated RSV as the cause of approximately 31% of pneumonia cases in African and Asian children, the greatest etiological fraction of all pathogens (Pneumonia Etiology Research for Child Health [PERCH] Study Group, 2019). RSV causes annual seasonal outbreaks which occur primarily in winter months in temperate climates but year-round in tropical climates (Hall et al., 2013). Virtually all children are infected by their second year of life, and about 2%–3% will require hospitalization during primary infection, with the peak age of severe disease being 1–3 months of age. Reinfection occurs throughout life, and severe disease with hospitalization is not uncommon through age 5 (Hall et al., 1986). Infection is usually restricted to the upper respiratory tract in older children and adults, with relatively mild illness until compromised by old age or immunodeficiency. In the frail elderly, infection rates are about 5%–10% per year, with about a 0.1% incidence of severe disease requiring hospitalization, similar to rates of influenza (Falsey et al., 2005).

RSV infection and bronchiolitis in infants is characterized by tachypnea and wheezing with chest wall indrawing as a sign of distress. These clinical findings reflect viral tropism that includes

the differentiated, polarized, ciliated bronchiolar epithelium and type I alveolar pneumocytes (Figures 1A and 1B). Lower respiratory tract infection (LRTI) with hypoxemia is common during primary infection because of infection and inflammation in the alveolus and small airways. Small infants, especially those born prematurely or with bronchopulmonary dysplasia or congenital heart disease, are particularly susceptible to severe disease. This is due in part to airway obstruction from sloughed epithelium, inflammatory cell debris, fibrin, and mucus. In young infants, in whom the lung and airways are still developing, damaged epithelium and inflammation may have lasting effects on lung function and be manifested as childhood wheezing or early onset of chronic obstructive pulmonary disease (COPD) in adults (Berry et al., 2016; Taussig et al., 2003). LRTI by RSV may also be complicated by high right-heart pressures because of inflammation around small vessels in the airway. This could explain why congenital heart disease is a risk factor for severe RSV disease and why morbidity in the elderly is usually expressed as an exacerbation of underlying cardiopulmonary disease.

Until 2016, RSV was taxonomically classified within a subfamily of *Paramyxoviridae* but is now a member of the newly established *Pneumoviridae* family. This change was based on the distinct phylogeny of the polymerase (L) and the presence of a conserved M2 gene involved in various aspects of transcription regulation and virus morphology (Kiss et al., 2014; Rima et al., 2017). RSV shares many general characteristics of paramyxoviruses as a negative-sense, single-stranded RNA-enveloped virus with a cytoplasmic replication cycle. RSV is distinct from human metapneumovirus by the presence of additional nonstructural genes, NS1 and NS2, at the 3' end of its negative-sense RNA genome (Figure 1C). These proteins are entirely devoted to interfering with the induction and effector functions of type I interferons (Bitko et al., 2007; Spann et al., 2004, 2005; Swedan et al., 2009). This feature of RSV has profound effects on innate susceptibility to infection and reinfection and influences the induction and maintenance of adaptive immunity.



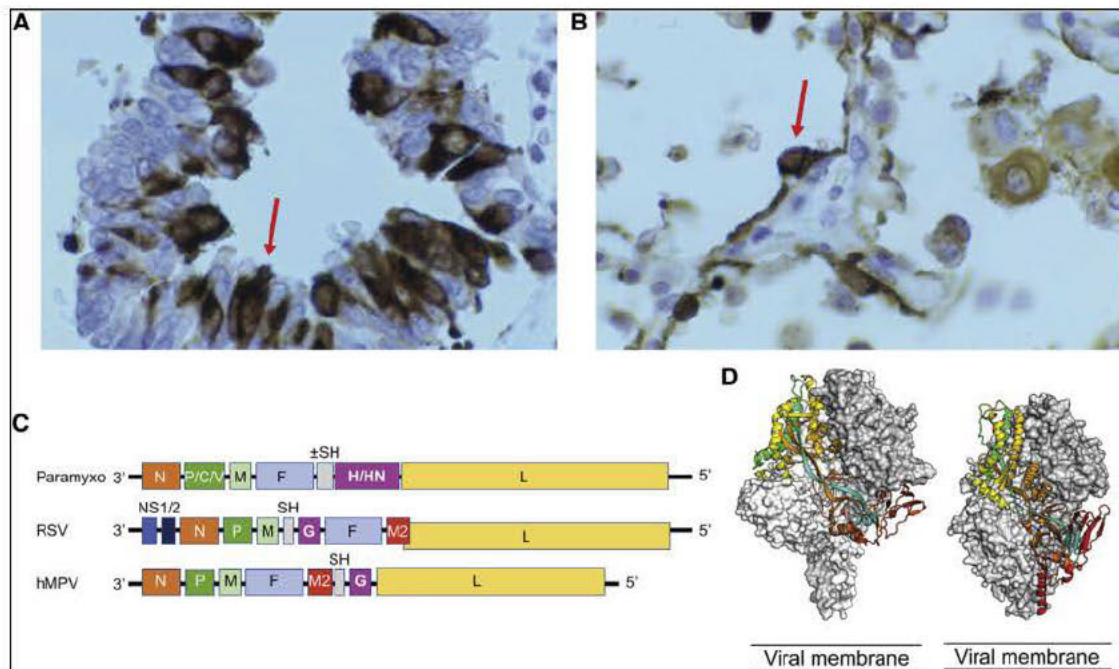


Figure 1. Features of RSV Pathogenesis, Genome Organization, and Prefusion F Structure

(A and B) Red arrows indicate RSV-infected (A) ciliated bronchiolar epithelial cells and (B) type I pneumocytes following immunohistochemistry of the lung of an infected infant.

(C) The genome of RSV is uniquely configured compared with that of human metapneumovirus (hMPV) and members of the paramyxovirus family.

(D) RSV pre-F displayed on the right has a distinct shape from the F protein of human parainfluenza virus 5 (PIV5), shown on the left.

RSV Surface Proteins Are Key Antibody Targets

RSV displays three viral proteins on its surface: SH, F, and G (Figure 2). SH is a pentameric ion channel similar to the M2 protein encoded by influenza virus (Gan et al., 2012), which can be a target for antibodies with Fc-mediated effector functions (Schepens et al., 2014). The G glycoprotein is a putative attachment protein and is a transmembrane protein anchored at the N terminus analogous to proteins with hemagglutination (H) and neuraminidase (HN) properties on other paramyxoviruses. RSV G also has an alternative initiation codon in the transmembrane domain and therefore exists in both a membrane-anchored and a secreted form (Roberts et al., 1994). G has highly variable mucin domains at both ends of the molecule with high proline content and extensive O-linked glycosylation that surround a central conserved domain. The membrane-anchored version of RSV G could be a target for neutralizing antibodies that bind epitopes in the central conserved domain around the cysteine-noose structure (Jones et al., 2018; Plotnicky-Gilquin et al., 1999). The heparin binding domains and the O-linked glycan domains can bind C-type lectins, endowing the secreted form of G with immunomodulatory functions (Chirkova et al., 2013; Feldman et al., 1999; Johnson et al., 2012). G-specific antibodies that block G binding to airway epithelial cells or antigen-presenting cells could potentially reduce disease severity, as they do in animal models (Boyoglu-Barnum et al., 2014; Chirkova et al., 2015; Choi et al., 2012; Zhang et al., 2010).

The RSV F protein, which mediates fusion of the virus with the host cell membrane, has two major conformational states: prefusion and postfusion. The metastable prefusion F protein (pre-F) undergoes a conformational change to mediate membrane

fusion and form a stable postfusion F structure (post-F). Antibodies to F are directed at several domains designated antigenic sites. Antigenic sites I–IV are shared between pre-F and post-F, but sites Ø and V are displayed exclusively on the pre-F conformation (Figure 3). Even among the shared sites, not all antibodies bind equally to both conformations (Gilman et al., 2016; Phung et al., 2019). This is particularly notable for site III and site I, which are more pronounced on pre-F and post-F, respectively (Goodwin et al., 2018). Although RSV F is comparable to paramyxovirus F proteins in its organization, the prefusion conformations have different shapes and domain structures (Figure 1D). Unlike the G protein, there is relatively little glycosylation on F and only three glycans (amino acids 27, 70, and 500) in the mature cleaved trimer. F is relatively conserved, and even between the two subtypes A and B, there are only ~25 amino acid differences in the 498 residues of the F ectodomain. Unlike the antigenic drift demonstrated in influenza and other RNA viruses, the variation in F is more of a toggling of the amino acid differences between subtypes A and B. Most of these are conservative changes, and there is no significant immunodominance pattern recognizing one domain over another. Conformational instability of F may be a feature that helps RSV avoid neutralization. As virus is shed from infected cells, F tends to spontaneously flip into the post-F conformation, which is 16 nm tall compared with the 11-nm-tall pre-F conformation. This limits the amount of functional pre-F on the viral surface but may also make pre-F less accessible to neutralizing antibodies.

In contrast to F, the G protein exhibits significant sequence variation in its mucin domains, and RSV subtyping by genotype is typically based on G sequences. Although antibodies against

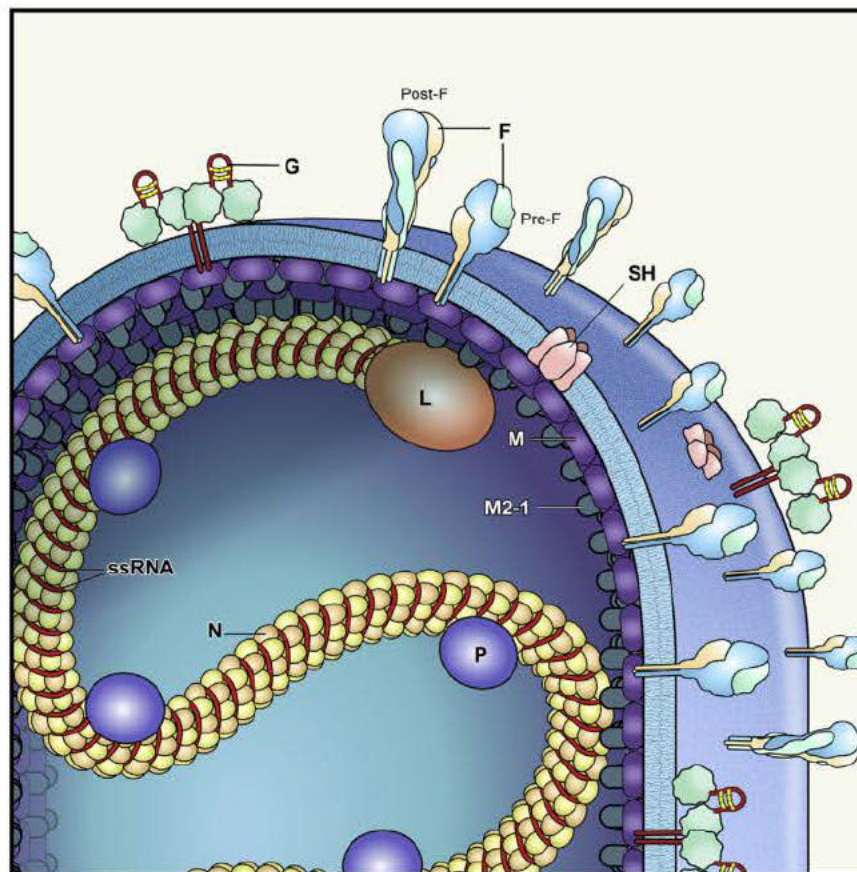


Figure 2. Respiratory Syncytial Virus Particle

RSV virions bud from infected cells as filamentous particles exhibiting a well-organized scaffold of M and M2-1 proteins, which house the single-stranded RNA (ssRNA)-containing ribonucleocapsid. After RSV buds from the cell, the matrix layer becomes fragmented, and the particles become pleomorphic and eventually round. Passive antibody transfer and vaccination strategies have largely focused on the three surface glycoproteins: F, G, and SH. F present on the surface of viral filaments is usually in the active pre-F conformation. As virions are shed from infected cells, the metastable F flips spontaneously into the post-F conformation over time, and spontaneous rearrangement is accelerated by high temperatures. G is a type 2 membrane protein and is disordered with mucin-like O-linked glycan domains on each end (green) surrounding a conserved cysteine-noose structure centrally (yellow). While F and G are targets of neutralizing antibody, SH, a pentameric ion channel, can be a target for antibodies with Fc-mediated effector functions.

were observed in histological examination of the lung following lethal cases of RSV, suggesting a protective role for CD8⁺ T cells (Johnson et al., 2007; Welliver et al., 2007). Children with T cell deficits experience prolonged viral shedding, which can resolve following bone marrow transplantation and engraftment of CD8⁺ T cells (El Saleeby et al., 2004). Following

either F or G are capable of blocking infection, F is often considered to be a more attractive target for intervention because of its multiple highly neutralization-sensitive epitopes and relative conservation between A and B subtype isolates. In RSV-experienced individuals, studies have shown a positive correlation of RSV-specific serum IgG and/or nasal IgA with protection from infection and/or severe disease (Chu et al., 2014; Falsey, 2007; Glezen et al., 1981; Habibi et al., 2015; Luchsinger et al., 2012; Piedra et al., 2003). In RSV-naïve infants, lower susceptibility to disease has been shown among infants who receive higher levels of antenatally transferred neutralizing antibody from their mothers (Glezen et al., 1981; Stensballe et al., 2009). Given the clear protective role of antibody, including the success of passive immunoprophylaxis with F-specific monoclonal antibodies, the elicitation of neutralizing antibodies is the primary goal of most active vaccination approaches.

T Cell Responses to RSV

CD8⁺ T cells are important for the clearance of RSV-infected lung epithelial cells, yet the contribution of RSV-specific T cells to protection is less clear. Animal models of RSV infection have demonstrated that T cells are capable of mediating both beneficial and deleterious effects, but they have not been shown to directly mediate immunopathology in human infection (Heidema et al., 2007; Lukens et al., 2010). In fact, in infants hospitalized after primary RSV infection, the CD8⁺ T cell response correlates with recovery from disease, and relatively few CD8⁺ T cells

allogeneic bone marrow or lung transplantation, individuals are particularly susceptible to fatal disease, likely because they lack CD8⁺ T cells capable of clearing infection from the lung (Ghosh et al., 2000; Kim et al., 2014; Neemann and Freifeld, 2015). The establishment of lung-resident RSV-specific T cells, in particular, may facilitate viral clearance and mitigate disease during the numerous reinfections with RSV throughout life as evidenced by human challenge studies (Jozwik et al., 2015). The elicitation of CD8⁺ T cells and T helper 1 (Th1)-type CD4⁺ responses to support both adaptive T and B cell responses is not the primary goal of active vaccination but would likely promote viral clearance and provide a second line of defense against severe disease. Given the differences in risk factors associated with severe disease between infants and the elderly, the optimal balance of T cell and antibody responses may be age dependent. Although this review is focused largely on the antibody response, the role of RSV-specific CD4⁺ and CD8⁺ T cells in both protection and disease has been reviewed elsewhere (Christiaansen et al., 2014; Schmidt and Varga, 2018).

Specific Challenges with RSV Vaccine Target Populations

RSV vaccines aimed at protecting infants are currently under development for pediatric or maternal administration, and products aimed at boosting pre-existing adaptive immune responses to sufficiently protect the elderly are also undergoing clinical testing. Each of these target populations has unique challenges

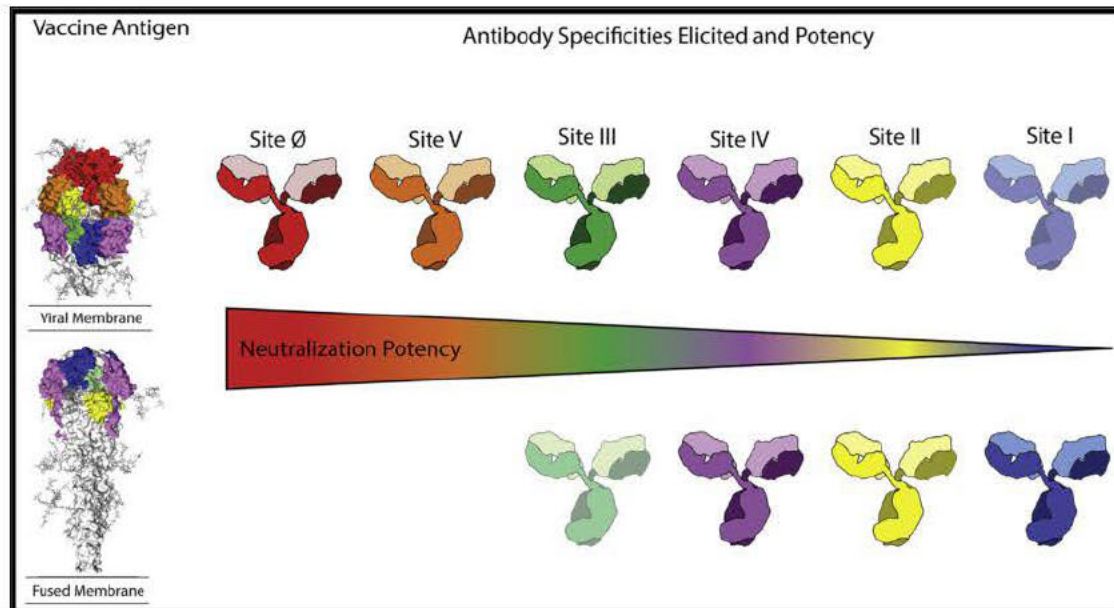


Figure 3. Antigenic Site-Specific Antibodies Elicited by Pre-F or Post-F Antigens

Pre-F elicits antibodies to all the antigenic sites that have been identified on the F protein. While post-F elicits antibodies to antigenic sites I, II, III, and IV, which can sometimes recognize shared surfaces on the pre-F structure, it does not display sites Ø and V, which have been shown to elicit antibodies with high neutralizing activity. Antibodies targeting site I show preference for post-F and tend to have low neutralizing activity, while those that target site III show preference for pre-F and have relatively potent neutralizing activity.

and considerations, and it is likely that distinct products tailored toward inducing the most favorable immune profile for each target population will be needed to achieve licensure.

RSV has the greatest impact during early life, particularly in the first year of life, during which malaria is the only single pathogen that accounts for higher global mortality (Lozano et al., 2012). Infant susceptibility has both physical and immunological underpinnings. Airway maturation and alveolarization are incomplete at birth and can take months to years following parturition (Schittny, 2017). Infants have narrow airways that are more easily occluded by inflammatory infiltrates (Johnson et al., 2007). Early-life deficiencies in both innate and adaptive immunity thought to contribute to RSV disease are well documented (Lambert et al., 2014; Ruckwardt et al., 2016). Interestingly, despite reduced levels of B cell class-switching and somatic hypermutation, infants are able to generate potent site III-specific antibodies with little to no somatic hypermutation (Goodwin et al., 2018). Infants have an inherent Th2 bias that impairs their ability to elicit optimal CD8⁺ and helper T cell responses. Immunity is further impaired by viral subversion of type I interferon responses and immune modulation by the secretory form of the G protein. Immune responses to RSV exhibit a lack of durability and protective memory despite relatively limited genetic variability of the virus (Hall et al., 1991). The lack of immunological prowess during the primary exposure in early life may leave a suboptimal imprint on the adaptive immune response. The goal of direct immunization in RSV-naïve infants would be to elicit highly neutralizing antibodies, supportive T helper responses, and sufficient CD8⁺ T cells to clear viral infection and diminish shedding. Preventing Th2-biased immunity or the elicitation of poorly neutralizing antibodies will be paramount to ensuring vaccine safety and elimi-

nating the threat of vaccine-enhanced disease, as discussed below. Given the insufficiencies of the natural immune response, significantly altering the parameters surrounding the initial exposure to viral antigens may be required to elicit long-lasting RSV-specific memory.

In addition to the physical and immunological challenges of infants, maternally transferred antibodies have been found to suppress the induction of RSV-specific immunity, particularly in the first few months of life (Murphy et al., 1986; Shinoff et al., 2008). This leaves a window of susceptibility within the first few months of life, as maternal antibody waning precedes the ability of infants to fully harness the power of the germinal center response and affect somatic hypermutation toward the generation of higher avidity antibodies. The extension of protection through maternally transferred antibodies is the goal of vaccines aimed at immunizing pregnant women. This approach has historical precedence, and maternal immunization has been effective in mitigating both maternal and infant influenza and pertussis-mediated respiratory consequences (Munoz and Jamieson, 2019). The major immunological challenge of maternal vaccination for RSV is to boost neutralizing antibody safely, because cellular immunity is not conferred to the infant. Pregnancy naturally evokes a period of immunological suppression to prevent potentially adverse responses to the developing fetus. Nonetheless, an immunogenic vaccine delivered in the late second or early third trimester could enhance vertical transfer of polyclonal anti-RSV antibodies that could prevent disease during the highly vulnerable first six months of life (Munoz, 2015).

Many of the greatest challenges for maternal vaccination strategies are practical rather than biological. Successful implementation of maternal vaccination programs will require

an infrastructure that supports antenatal care and immunization services for pregnant women in low- to middle-income countries, which bear the greatest burden of RSV disease (Krishnaswamy et al., 2019; Shi et al., 2017). Education and vaccine acceptance will be as critical as timing of vaccination during pregnancy and in relation to the regional seasonality of RSV. In addition to these obstacles, other endemic pathogens are known to alter the efficiency of antibody transfer from mother to child. Two notable examples of this are during HIV and malaria infection, in which impaired transport of RSV antibodies can result in cord-to-maternal titer ratios < 1.0 (Atwell et al., 2016; Jallow et al., 2018). Whether protection of infants through maternal or pediatric vaccine administration or passive delivery of monoclonal antibodies to neonates will be more effective is likely to vary geographically.

Finally, protection from RSV disease at the opposite end of the age spectrum presents its own unique set of challenges. These challenges are, in part, due to immunosenescence, a hallmark of immunity in older adults. Thymic involution and altered T cell function result in paltry support for B-cell- and antibody-mediated immunity. Although low serum antibody in the institutionalized elderly portends increased incidence of disease, many other factors contribute to susceptibility in the elderly (Walsh et al., 2004). Among them, COPD and functional disabilities factor heavily (Mehta et al., 2013). Boosting neutralizing antibodies and promoting anti-viral T cell effector responses that facilitate clearance are goals of RSV vaccines in the elderly, but achieving these goals may require the use of adjuvants or novel gene-based approaches. The outcome of several subunit vaccine trials in the elderly has been disappointing, and leveraging our knowledge of glycoprotein structure, as discussed below, will be a critical step toward eliciting protective immunity in adult populations.

Other important goals for vaccination are to prevent severe disease in young children, avoid hospitalization, and prevent infection in immunocompromised persons to avoid mortality. Although the burden of disease is lower in school-aged children, they have been implicated as a primary source of transmission to infants and the elderly (Munywoki et al., 2014). Vaccination of this population could prevent RSV infection of more vulnerable populations (Poletti et al., 2015). Other high-risk populations include the immunocompromised and transplant recipients, but these populations are not being targeted by active vaccination strategies.

Past and Present RSV Vaccine Strategies

In the subsequent sections, we will discuss the results of early attempts at RSV vaccination and lessons learned about RSV immunity in the process. The fledgling field began with a major misstep, a formalin-inactivated vaccine that caused enhanced respiratory disease (ERD) upon natural infection. This is the 50th anniversary of the publications describing the FI-RSV vaccine-associated ERD, and consequences of that event are still foremost considerations in the development of new vaccine approaches and immunological strategies. Although many of the initial vaccine attempts were not successful, each taught us an important lesson about protective immunity to RSV. The field has advanced cautiously, with critical findings about RSV virology and protein structure transforming live-attenuated and subunit vaccine approaches, and refining the selection of monoclonal antibodies used for pas-

sive prophylaxis. Past and present approaches are outlined in Figure 4, along with the anticipated or actual outcomes of these efforts. The field is rapidly changing, and a list of current candidate vaccines and antibodies is maintained by PATH at <https://vaccineresources.org/details.php?i=1562>.

Formalin-Inactivated RSV

Shortly after RSV was discovered, vaccine development efforts were initiated using the technology available at the time, namely live-attenuated or inactivated whole-virus vaccine approaches. Early efforts were complicated by difficulty growing the virus to high titer and maintaining viability. In pivotal studies in the 1960s, a whole inactivated virus vaccine was tested in infants in a small pilot study, then extended into four studies with different age cohorts and geographic locations (Chin et al., 1969; Fulginiti et al., 1969; Kapikian et al., 1969; Kim et al., 1969). The youngest cohort included infants who were immunized between two and seven months of age with up to three doses of FI-RSV between 1965 and 1966 (Kim et al., 1969). During the subsequent winter season, RSV infections occurred in 20 of the 31 infants who had received the “lot 100” FI-RSV vaccine in the study; 16 of the 20 required hospitalization, and two infants died from severe RSV disease (Kim et al., 1969). Comparing outcomes of different age cohorts suggested that the children who were youngest at the time of vaccination were most at risk for severe disease associated with FI-RSV vaccine, implying that the aberrant responses associated with immunopathology were induced by primary immunization in RSV antigen-naïve infants. Although children previously infected with RSV before exposure to FI-RSV were not protected from subsequent RSV infection, vaccine ERD was not as evident. Similarly, intramuscular vaccination of RSV-naïve infants with a low dose of live RSV was not sufficiently immunogenic to afford protection from infection but did not result in enhanced disease (Belshe et al., 1982). Therefore, establishing T cell memory with the right phenotype and B cell memory with the right specificity are key priorities for safe vaccines targeting young infants. Since then, studies based on serum and tissue from the clinical trials and supported by animal models have elucidated distinct immunological patterns associated with the FI-RSV ERD syndrome, one involving T cells and the other involving antibodies.

Children vaccinated with FI-RSV had evidence of robust CD4⁺ T cell proliferation, and tissue sections demonstrated the presence of eosinophils in addition to neutrophils, lymphocytes, and mononuclear cell infiltrates after RSV infection (Kim et al., 1976). Similarly, animal studies in mice, nonhuman primates, and cattle have shown that priming with FI-RSV followed by airway challenge with live virus results in a Th2-biased T cell response with eosinophilia and excess mucus production (De Swart et al., 2002; Graham et al., 1993b; Kalina et al., 2005). This is consistent with findings that a family history of atopy and a variety of Th2-related cytokine and receptor genetic polymorphisms are risk factors for severe RSV disease (Choi et al., 2002; Gentile et al., 2003; Hoebee et al., 2003; Puthothu et al., 2006; Trefny et al., 2000). Therefore, induction of responses that involve IL-4, IL-5, IL-9, and IL-13 should be avoided when vaccinating antigen-naïve infants. Because neonates tend to be naturally Th2 biased, the method of antigen delivery is particularly important in this age group. Live-attenuated virus vaccines have been shown to be safe in antigen-naïve infants, and in

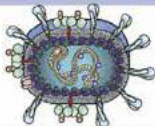



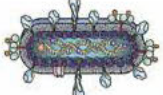













	Vaccine Platform	Target population	Immunogenicity and Potential or Actual** Clinical Outcomes
FI-RSV			Disproportionate increase in binding antibody with poor neutralization capacity. ERD following natural infection resulting in severe illness and two deaths
F-specific mAb			No induction of adaptive immunity. Transferred antibody provides passive protection from severe illness.
Live-attenuated and Chimeric			Induction of mucosal antibody and T cell responses. Prevention of severe upper and lower respiratory tract disease, and potential for sterilizing immunity.
Nucleic Acid			Induction of both antibody and T cell responses and prevention of upper and lower respiratory tract disease.
Vector-based			Induction of both antibody and T cell responses and prevention of upper and lower respiratory tract disease.
Post-F Subunit*			Increase in antibodies to moderately neutralization-sensitive sites. Failure to meet primary efficacy objectives in several clinical trials.
Stabilized Pre-F Subunit*			Increase in antibodies to highly neutralization-sensitive sites and improved serum neutralizing potency.
G Subunit			Increase in antibodies that neutralize virus by binding central conserved domain or block immunomodulatory effects.
SH Subunit			Induction of SH-binding antibodies that mediate ADCC.

Figure 4. RSV Vaccine Approaches

Several vaccine approaches are being pursued for pediatric, maternal, and elderly target populations. Ongoing clinical trials use lessons learned from early attempts involving FI-RSV and from passive prophylaxis studies. The primary goal is the elicitation of potentially neutralizing antibody, which may be aided by appropriately targeted T cell responses in infants and the elderly. *Numerous VLP and nanoparticle approaches incorporate either pre-F or post-F with the goal of enhancing immune responses through multimerization. **Actual outcomes from the FI-RSV vaccine and large-scale clinical efficacy studies are shown in bold.

animal models, priming with live virus or gene-based vectors that induced CD8⁺ and Th1 CD4⁺ T cells prevented subsequent Th2-biased responses from FI-RSV. Although there is still some controversy about the role of Th2-biased CD4⁺ T cell responses and the fidelity of animal models in understanding FI-RSV-associated ERD, the association of allergic inflammation with severe RSV disease in the pathogenesis of natural infection suggests that primary vaccination of neonates should avoid these responses.

Although FI-RSV was made from whole virus, the antigenic content was never documented. The vaccine was prepared by growing RSV in Vero cells, concentration by centrifugation, inactivation with 0.025% formalin, and formulation with aluminum salts. Given that the virus was inactivated and washed prior to formulation, the secreted form of G would have been removed leaving only the membrane-anchored form, and the quantity

and composition of G in the lot 100 FI-RSV vaccine used in children have not been demonstrated. Although early experiments in murine models suggested that G might play a role in the Th2-biased CD4⁺ T cell response (Hancock et al., 1996; Johnson and Graham, 1999; Johnson et al., 1998; Openshaw et al., 1992), subsequent studies showed that G was not required for vaccine-associated ERD in mice (Johnson et al., 2004a). Instead, an MHC class II epitope in G that is recognized by a Vβ14⁺ CD4⁺ T cell, which is inherently biased toward IL-4 production, caused the increased eosinophilia after prior immunization with G (Johnson et al., 2004b). It is also important to note that these and other studies of enhanced disease in semi-permissive animal models of infection should be interpreted with caution, as appropriate controls to determine the role of viral replication and possible contaminants should be included (Piedra et al., 1993; Shaw et al., 2013). It is unclear how well these findings can be

extrapolated to ERD in human infants. The allergic inflammation associated with prior FI-RSV priming in animals cannot be attributable to a specific RSV epitope or antigen but is rather a more general phenomenon related to obligate MHC class II antigen presentation followed by airway challenge. In mice, the presence of RSV-specific CD8⁺ T cells during vaccination regulates the differentiation of CD4⁺ T cells, resulting in a dominant Th1 CD4⁺ T cell response (Srikiatkachorn and Braciale, 1997). As noted, live RSV given nasally or parenterally does not cause ERD, suggesting that the aberrant T cell responses associated with FI-RSV immunization are related to antigen presentation in general and not antigen specific.

Serology from children immunized with FI-RSV showed that substantial binding antibody responses could be measured by complement fixation or ELISA, but neutralizing or fusion-inhibiting activity was weak (Kim et al., 1969; Murphy et al., 1986; Murphy and Walsh, 1988). This was associated with immunohistochemical evidence in tissue of immune complex deposition and complement fixation (Delgado and Polack, 2004; Polack et al., 2002). Therefore, future vaccines should avoid inducing an antibody with poor functional activity, which may lead to high viral loads, immune complex formation, and immunopathology. In contrast to T-cell-mediated allergic inflammation, there is evidence that the poorly functional antibody responses associated with FI-RSV-associated ERD is related to antigenicity of the vaccine, specifically the conformational state of the F glycoprotein. The untriggered, metastable pre-F trimer spontaneously flips to post-F as virion filaments bud from infected cells (Ke et al., 2018). This process is accelerated when the matrix layer becomes fragmented and the virus assumes a polymorphic shape and eventually becomes round. The pace of F rearranging into the nonfunctional post-F conformation increases with increasing temperature, and this process results in a non-infectious virion. Heating virus to 37°C for more than 24 h inactivates virtually all virions in a liquid suspension and drives the unidirectional rearrangement of all F into the postfusion state (Killikelly et al., 2016). Therefore, FI-RSV-induced antibody responses to the post-F molecule that had binding activity but low neutralization potency and a propensity to form immune complexes, a profile which should be avoided.

The failure of the FI-RSV vaccine to protect infants and, further, that it caused vaccine-enhanced illness in RSV-naive infants has shaped the field of RSV vaccines. The FI-RSV vaccine studies serve as a cautionary tale and highlight important immune responses to avoid in the antigen-naive population (Th2-biased CD4⁺ T cell responses and binding antibodies with low neutralization potency) and have taught us about the impact of immunological priming on subsequent natural infection. Furthermore, research using animal models for RSV vaccines and infection studies demonstrates the utility and caveats of using semi-permissive animal models to study a virus distinctly specialized for infecting humans.

Live-Attenuated and Gene-Based Vaccination

Clinical trials using live-attenuated RSV delivered intranasally began shortly after the tragic failure of formalin-inactivated virus. The rationale for this approach is based on the tenet that limited viral replication in the respiratory tract and intracellular processing and presentation of viral antigens would both promote naturally balanced B and T cell responses and avoid the circum-

stances that led to vaccine-enhanced disease. This approach is well suited to antigen-naive infants. It offers needle-free delivery and the opportunity to generate responses directly in the respiratory mucosa, where immune suppression mediated by maternally transferred IgG is limited. Because RSV buds from the apical surface of epithelial cells, the F and G glycoproteins on the surface of *de novo* viral particles preserve their native glycosylation patterns and conformational integrity, including the retention of the pre-F-exclusive immunogenic antigenic sites. Stimulation of T and B cell responses in induced lymphoid tissue in the lung and lung-draining lymph nodes also has the potential to promote tissue-resident responses and offer a more robust barrier to progression of infection from the upper to the lower airway.

Evaluation of live-attenuated vaccines began with biologically derived attenuated viral strains. Viruses altered by cold-passage (cp) or mutagenesis techniques were laboriously derived and tested. One of these, cp-52, had a natural deletion of the G and SH proteins (Karron et al., 1997). These vaccines were replaced by a newer generation of mutant viruses rescued using reverse genetics, which allowed for precise manipulation and incorporation of mutations known to improve genetic stability and progressively attenuate viral replication (Karron et al., 2013). Despite this major advance, recombinant live-attenuated vaccines have met similar clinical stumbling blocks as their biologically derived predecessors: inability to strike a viable balance between attenuation and immunogenicity. Over nearly four decades of testing, multiple live-attenuated candidates have advanced through sequential testing in seropositive adults and children before progressing into seronegative children over the age of six months and finally into younger seronegative cohorts (Karron et al., 2013). Minimal shedding in seropositive adults and children is needed to ensure sufficient attenuation, but attenuated viruses need to replicate and provide the innate stimuli required to be immunogenic in RSV-naive infants or children. Conversely, insufficient attenuation has led to the induction of symptoms of respiratory tract infection in young infants. Despite these limitations, there has been no evidence of enhanced disease resulting from live-attenuated vaccines, even in very young infants unlike FI-RSV.

The newest generation of recombinant live-attenuated vaccines has capitalized on knowledge of RSV virology. Understanding how the M2-2 protein regulates the switch from transcription of genes to replication of the genome informed one approach, and the importance of NS2 inhibiting type I interferon induction and effector mechanisms to evade innate immunity has informed other approaches. In conjunction with stabilizing mutations that eliminate the risk of viral reversion, deletion of the regulatory M2-2 protein has been used to uncouple viral transcription and replication, favoring transcription and higher antigen expression (McFarland et al., 2018). Other mutations, such as deletion of the immune evasion gene NS2, are also being combined with stabilizing mutations to fine-tune immunogenicity (Luongo et al., 2013). The expression of NS1 and NS2 virulence genes can also be diminished by codon deoptimization (Meng et al., 2014). Each set of mutations must be empirically tested, and the *in vivo* response can be complicated by age- and host-dependent susceptibility factors. It is unknown if these strategies can alter the context of vaccine antigen presentation

enough to shift the paradigm of natural infection toward the generation of more durable adaptive responses, as these vaccines still possess some of the immunomodulatory features of wild-type RSV. Ultimately, immune responses superior to natural infection will be needed to confer protective and durable immunity. Some new live-attenuated virus vaccine approaches are utilizing F proteins that are less likely to flip from pre-F to post-F to improve thermostability (Rostad et al., 2018; Stobart et al., 2016). Expression of stabilized pre-F in the context of parainfluenza vectors are being explored in preclinical studies, and other live-attenuated platforms are being used to deliver RSV antigens in the context of vectors like Sendai virus, further disassociating them from the immunomodulatory context of natural infection and capitalizing on the increased potency of pre-F specific neutralizing antibodies (Jones et al., 2012; Liang et al., 2017; Liu et al., 2017; Russell and Hurwitz, 2016).

DNA- and RNA-based vaccine approaches also offer the induction of both B- and T-cell-mediated adaptive immunity and are currently in preclinical testing, while several vector-based candidates have advanced to phase I and phase II clinical trials. MVA and adenovirus vector delivery of RSV vaccine antigens provide innate stimuli and high-level gene expression that could boost the elicitation of CD8⁺ T cells and Th1 CD4⁺ T cells balanced with potently neutralizing antibodies, particularly when used to deliver pre-F. These approaches are moving forward for pediatric target groups, capitalizing on immunological lessons learned from live-attenuated vaccines about promoting safe immune responses in antigen-naïve infants. Overcoming the barrier of maternal antibody, balancing attenuation with immunogenicity, and surpassing the shortcomings of immunity to natural infection remain significant challenges for infant vaccination. In the elderly, gene-based approaches will need to overcome the restrictions of live-attenuated vaccines and provide a substantial boost to pre-existing antibody and T cell responses.

Subunit and Nanoparticle Vaccination

Not far behind live-attenuated modalities, the 1990s marked several attempts to actively vaccinate small cohorts of healthy antigen-experienced children or the elderly with F subunit vaccines. Purified fusion proteins, Lederle-Praxis products PFP-1 and PFP-2, commonly elicited a more than 4-fold boost in ELISA-binding antibody in these small studies (Belshe et al., 1993; Falsey and Walsh, 1996, 1997; Paradiso et al., 1994; Tristram et al., 1993). Similar boosts in neutralizing antibody were less frequent, and the vaccines uniformly demonstrated an inability to protect from respiratory infection with modest protection from symptoms. Larger studies with purified F followed in the 2000s. Due to the metastable properties of pre-F, these F protein products without stabilizing mutations manufactured by Sanofi, Novartis, GlaxoSmithKline, MedImmune, and Novavax have similar antigenic, morphological, and physical properties to the post-F protein. The furthest progressed, sf9 insect cell-produced Novavax nanoparticle was not effective in preventing medically attended RSV LRTI in a large phase III study in older adults (<https://ir.novavax.com/news-releases/news-release-details/novavax-announces-topline-rsv-f-vaccine-data-two-clinical-trials>). A second large phase III study testing the product for maternal immunization failed to meet its primary efficacy endpoint for protection of infants up to 90 days of age ([https://ir.novavax.com/news-releases/news-release-details/novavax-announces-topline-results-phase-](https://ir.novavax.com/news-releases/news-release-details/novavax-announces-topline-results-phase-3-preparetm-trial)

[3-preparetm-trial](https://ir.novavax.com/news-releases/news-release-details/novavax-announces-topline-results-phase-3-preparetm-trial)). In phase II, a Sanofi product containing post-F, G, and M induced a 4-fold increase in neutralizing activity in fewer than half of vaccinees at 1 month post-vaccination and did not progress into phase III trials. MEDI7510, an adjuvanted purified post-F subunit manufactured by MedImmune, failed to protect elderly recipients in a phase II study and has similarly been terminated (Falloon et al., 2017). Because of the presence of antigenic site II on both pre-F and post-F, post-F vaccines elicit antibodies that compete with palivizumab in vaccinated subjects. Measuring palivizumab-competing antibody (PCA) is considered by some to be a surrogate for functional antibody responses because of the clinical efficacy of palivizumab. However, most antibodies that compete with palivizumab binding do not have the level of neutralizing activity conferred by palivizumab, and the usefulness of this metric has not been established. Because of the close proximity of antigenic sites, antibodies to adjacent sites can contribute to these readouts and confound interpretation of PCA data (Phung et al., 2019). The late-phase failures of these three vaccines highlight our lack of ability to predict protective immunity to RSV and to elicit appropriately targeted adaptive immune responses.

All of the above vaccine development efforts were initiated prior to solving the RSV pre-F structure in 2013. Defining the atomic level structure in its pre-triggered, prefusion conformation resulted in the discovery of new highly neutralization-sensitive antigenic sites (Ø and V) exclusive to the apex of pre-F and allowed mapping the epitopes of other neutralizing monoclonal antibodies (mAbs) such as MPE8 (site III) (Corti et al., 2013; McLellan et al., 2013b; Mousa et al., 2017). It was subsequently demonstrated that most RSV neutralizing activity in human serum and the most potent neutralizing mAbs target pre-F-exclusive surfaces (Gilman et al., 2016; Goodwin et al., 2018; Magro et al., 2012; Ngwuta et al., 2015). Building upon this discovery, mutations were introduced to stabilize the prefusion conformation for use as an immunogen, which was named DS-Cav1 (McLellan et al., 2013a). The immunogenicity of pre-F for neutralizing activity in nonhuman primates was 80 times greater than that for post-F, and in a phase I clinical trial, immunization of healthy adults with 150 µg of DS-Cav1 boosted neutralizing activity on average 12- to 15-fold above baseline (Crank et al., 2019). This is in striking contrast to the 2- to 5-fold increases in neutralization typically seen with post-F subunit vaccines. In line with the potent induction of neutralizing antibody, the DS-Cav1 subunit vaccine demonstrated clear proof of the elicitation of responses to pre-F exclusive antigenic sites (Crank et al., 2019). Further refinements and approaches for stabilizing pre-F have quickly advanced into phase I and II testing by GlaxoSmithKline, Janssen, and Pfizer. Larger clinical studies of pre-F candidate vaccines will be needed to determine the efficacy of this approach on the basis of induction of potent neutralizing activity. Stabilizing RSV F in the prefusion conformation has also improved the immunogenicity for neutralizing activity in chimeric viruses (Liang et al., 2015, 2017), virus-like particles (McGinnes Cullen et al., 2015), and live-attenuated virus vaccines (Rostad et al., 2018) and when displayed on self-assembling nanoparticles (Marcandalli et al., 2019).

Although vaccine development for RSV has primarily focused on the F proteins, subunit vaccines including G and SH are also in development (Figure 4). As noted above, most of RSV's diversity occurs in the G protein, which is highly glycosylated. Neutralizing antibodies to the G primarily target the cysteine noose

because large glycan regions shield the other protein domains (Figure 2). An early candidate G subunit vaccine was found to be modestly immunogenic in humans and elicited a greater than 2-fold increase in neutralizing antibodies in 33%–70% of vaccinees in the 100 and 300 μ g dose groups (Power et al., 2001). Another G subunit vaccine is currently in clinical evaluation by Beijing Advaccine Biotechnology. SH protein present on the viral envelope is another potential antibody target. In animal models, SH does not elicit neutralizing antibodies, but rather, protection is mediated by binding antibodies through FC-mediated mechanisms (Schepens et al., 2014). Immunovaccine is evaluating a vaccine that displays the ectodomain of the SH protein formulated with DepoVax or alum (Langley et al., 2018). It is unclear whether G- or SH-based vaccine strategies will be efficacious alone, but these studies demonstrate that there are other potential target antigens beyond F that may contribute to the efficacy of RSV vaccines. Although immunological studies have taught us that the presentation of structurally stabilized F protein can be optimized to elicit a favorable antibody profile, there is much to learn about the contribution and optimization of immunity to other viral determinants.

The postfusion and structurally undefined F subunit vaccines associated with modest increases in neutralizing antibody titers have failed to achieve efficacy endpoints in large phase III clinical trials, teaching us that a larger increase in neutralizing activity will be needed to impede RSV disease. The definition of the pre-F structure, along with demonstrations that preserving the structure of pre-F during vaccination leads to substantially higher neutralizing activity in preclinical, and now clinical studies, have been transformative. These findings provide hope that next-generation protein and nanoparticle vaccines based on the preservation of pre-F will perform better in clinical evaluation. Efficacy studies to validate the idea that the improvement in neutralizing titers will translate to protection from disease are the next crucial step.

Passive Monoclonal Antibody

Development of mAbs for prevention of RSV has advanced more rapidly and successfully than vaccines and has been instrumental in informing RSV vaccine development efforts. The initial proof of concept came from the development of passively administered polyclonal RSV immune globulin (RSV-IGIV or RespiGam) to protect premature infants from severe RSV disease (Groothuis et al., 1993). This was based in part on the early findings that the level of neutralizing activity transferred to infants was inversely correlated with severity of RSV disease (Glezen et al., 1981). Studies in animal models also suggested that passively administered polyclonal serum could prevent LRTI, reducing lung pathology and illness (Graham et al., 1993a, 1995; Prince et al., 1985). Because bronchopulmonary dysplasia and prematurity were the major risk factors for severe disease, and prematurity limited the amount of maternally transferred antibody, it was reasoned that supplying neutralizing activity would be a safe way of preventing RSV infection. RSV-IGIV successfully prevented severe RSV disease in premature infants and children with bronchopulmonary dysplasia (the PREVENT Study Group, 1997; Groothuis et al., 1995). Subsequently, murine neutralizing monoclonal antibodies were discovered and mapped to one of two major antigenic sites (II and IV) on post-F, which was the only protein reagent available at the time. The site II mAb 1129 was humanized and later became palivizumab (Beeler and van Wyke Coelingh, 1989; Johnson et al.,

1997). Palivizumab was evaluated in a series of clinical trials and shown to effectively reduce RSV disease severity and was licensed for use in 1998 (the IMPact-RSV Study Group, 1998). Clinically, it is given as immunoprophylaxis to premature infants monthly during the period of risk based on regional RSV seasonality. The success of palivizumab has been an important factor in how the current generation of maternal RSV vaccines have been designed. The goal is to achieve sufficient levels of F-specific neutralizing antibody in pregnant women, so children will acquire passive immunity sufficient to protect them through at least 6 months of age and cover the time when airways and the immune system are still actively evolving. A second-generation mAb, motavizumab, which was engineered for higher potency than its parental palivizumab, was also highly effective (O'Brien et al., 2015) but did not achieve licensure.

Since the licensure of palivizumab, mAbs to alternative antigenic sites on F have also been evaluated. MedImmune developed a mAb originally named MEDI8897 and generically nirsevimab, which is a derivative of the D25 antibody used to obtain the pre-F structure (Kwakkenbos et al., 2010; McLellan et al., 2013b). It has been engineered to increase potency and extend antibody half-life (Domachowske et al., 2018; Zhu et al., 2017). In a phase IIb efficacy trial, nirsevimab was recently reported to have achieved the primary endpoint of reduction of medically attended LRTIs and secondary endpoint of reduction of LRTI hospitalizations and was granted prime eligibility status by the European Medicines Agency and breakthrough status by the US Food and Drug Administration (FDA). This mAb recognizes site \emptyset on the apex of the pre-F molecule and was nearly 100 times more potent than palivizumab before engineering. The increased potency and extension of antibody half-life through engineering the Fc domain to contain amino acids that increase neonatal Fc receptor (FcRn)-mediated recycling allow it to be given as a single dose at birth for protection through an entire RSV season.

Other attempts at development of mAbs have been less successful. A site IV-specific mAb, RSHZ19, was developed in the 1990s but failed to meet its primary objectives and was discontinued (Johnson et al., 1999). Although the reason for the failure is not known, RSHZ19 had a lower affinity and faster off rate than palivizumab and was tested at a relatively low dose in the clinical trial. A more promising site IV mAb with an extended half-life YTE modification (MK-1654) is in early phase clinical development (Aliprantis et al., 2018). REGN2222, or suptavumab, a potent mAb specific targeting site V on pre-F, reportedly had substantial efficacy against subtype A, but no efficacy against RSV subtype B in a trial that failed to meet its endpoint (Mazur et al., 2018). This may be due to the inability to neutralize currently circulating subtype B viruses, which possess a mutation noted in the published patent to abrogate binding of this antibody (Gurnett-Bander et al., 2016). This failure illustrates viral escape as a major vulnerability for mAb prophylaxis. Recent RSV surveillance efforts have demonstrated that despite the high sequence conservation of the F protein, circulating isolates may contain mutations in one or more key antigenic site (Lu et al., 2019), which may significantly affect the efficacy of a single mAb. Further studies would be needed to determine the effect of these mutations on immune protection afforded by polyclonal responses induced by vaccination.

The site II mAb palivizumab has demonstrated considerable success, while other mAbs to sites IV and V have failed. However,

the success of nirsevimab, which targets site Ø, and the advancement of the MK-1654 site IV mAb provides evidence that protection is not a site-specific phenomenon and more likely related to neutralizing potency. Although potent neutralizing mAbs can be found to antigenic sites exclusive to pre-F or on the shared surfaces of pre-F and post-F, the pre-F exclusive sites evoke the greatest frequency of high-potency mAbs. In order for antibodies to neutralize, they must bind the native, functional pre-fusion conformation, and all known neutralizing sites on F are present on pre-F (Figure 3). Thus, it is logical that stabilized pre-F is a better immunogen than post-F, which only presents a fraction of the neutralization-sensitive surfaces present on pre-F. A major lesson learned from the development and clinical testing of RSV-specific mAbs is that designing immunogens that display multiple antigenic sites and induce polyclonal responses will help avoid escape and achieve cross-subtype immunity. Likewise, defining and preserving neutralization-sensitive sites on the immunogen will improve the potency of the neutralizing response and increase chances that a protective threshold of neutralization will be attained. Understanding the importance of F conformation and the importance of F-specific antibody neutralization for protection of infants has been transformative for RSV vaccine development.

Future Prospects for RSV Vaccines and Antibody-Mediated Prevention

A major focus of recent RSV vaccine development has been on the importance of conformation-dependent antigenicity of the RSV F glycoprotein and the potential for F-specific antibodies to provide protection against severe RSV disease. Other recent reviews cover the broader landscape of RSV vaccine development (Mazur et al., 2018; Villafana et al., 2017). Just as there are many mechanisms for RSV to cause illness depending on the size, genotype, and pre-existing conditions of the host, there are many ways to achieve effective immunity, and the type of immunity needed for each target population may be different. Induction of high serum-neutralizing activity by immunizing with a structurally defined immunogen may provide safe and effective protection for a large portion of RSV-mediated disease. However, induction of G-specific antibodies that contribute to neutralization and reduce RSV immunopathology may improve the outcome for some individuals. Elicitation of tissue-resident CD8⁺ T cells or SH-induced antibody that can provide Fc-associated cellular immunity may add another level of protection. Directly inducing mucosal responses through alternative delivery methods could reduce the duration of shedding and diminish transmission that would benefit not only the infected individual but the community at large. It will be important for ongoing and future clinical trials to measure immunological, clinical, and epidemiological endpoints to increase our understanding of protective immunity and correlates of protection and optimize vaccine approaches for each targeted high-risk group.

Concluding Remarks

During the next 5 years, there will be significant advances in the availability of options for protecting all the major target populations for RSV vaccines. Efficacy studies evaluating infants treated by passive immunoprophylaxis from maternal vaccination or delivery of new higher potency mAbs directly to the infant

should be completed. There will also be advances in immunizing antigen-naïve infants with live-attenuated viruses, chimeric viruses, or gene-based vectors. In addition, data should be available from studies using protein-based or gene-based approaches delivering pre-F trimers, proteins displayed on self-assembling nanoparticles, or virus-like particles. The field will continue to build upon the immunological discoveries derived from vaccine and mAb failures, and occasional successes, to advance RSV vaccine development. New challenges await vaccines that demonstrate efficacy, and efforts to educate pregnant women and mothers of young infants about the impact of RSV and promote vaccine acceptance may be essential components of vaccination programs. Support and infrastructure to deploy and administer vaccines in the developing world, where RSV exerts its largest toll, will also be critical. Despite these challenges, there is a good chance, as we approach the 70th anniversary of the discovery of RSV in 2026, that multiple options will be available to reduce the RSV disease burden.

ACKNOWLEDGMENTS

This work was supported by intramural funding from the National Institute of Allergy and Infectious Diseases.

DECLARATION OF INTERESTS

B.S.G. is an inventor on patents for the stabilization of the RSV F protein.

REFERENCES

- Adams, J.M. (1941). Primary virus pneumonitis with cytoplasmic inclusion bodies - Study of an epidemic involving thirty-two infants with nine deaths. *J. Am. Med. Assoc.* 116, 925–933.
- Adams, J.M. (1948). Primary virus pneumonitis in infants. *Pediatrics* 1, 398.
- Aliprantis, A., Wolford, D., Caro, L., Maas, B., Ma, H., Vora, K., Geng, D., Railkar, R., Lee, A., Sterling, L., and Lai, E. (2018). A randomized, double-blind, placebo-controlled trial to assess the safety and tolerability of a respiratory syncytial virus (RSV) neutralizing monoclonal antibody (MK-1654) in healthy subjects. *Open Forum Infect. Dis.* 5, S424–S425.
- Atwell, J.E., Thumar, B., Robinson, L.J., Tobby, R., Yambo, P., Ome-Kaius, M., Siba, P.M., Unger, H.W., Rogerson, S.J., King, C.L., and Karron, R.A. (2016). Impact of placental malaria and hypergammaglobulinemia on transplacental transfer of respiratory syncytial virus antibody in Papua New Guinea. *J. Infect. Dis.* 213, 423–431.
- Beeler, J.A., and van Wyke Coelingh, K. (1989). Neutralization epitopes of the F glycoprotein of respiratory syncytial virus: effect of mutation upon fusion function. *J. Virol.* 63, 2941–2950.
- Beem, M., Wright, F.H., Hamre, D., Egerer, R., and Oehme, M. (1960). Association of the chimpanzee coryza agent with acute respiratory disease in children. *N. Engl. J. Med.* 263, 523–530.
- Belshe, R.B., Anderson, E.L., and Walsh, E.E. (1993). Immunogenicity of purified F glycoprotein of respiratory syncytial virus: clinical and immune responses to subsequent natural infection in children. *J. Infect. Dis.* 168, 1024–1029.
- Belshe, R.B., Van Voris, L.P., and Mufson, M.A. (1982). Parenteral administration of live respiratory syncytial virus vaccine: results of a field trial. *J. Infect. Dis.* 145, 311–319.
- Berry, C.E., Billheimer, D., Jenkins, I.C., Lu, Z.J., Stern, D.A., Gerald, L.B., Carr, T.F., Guerra, S., Morgan, W.J., Wright, A.L., and Martinez, F.D. (2016). A distinct low lung function trajectory from childhood to the fourth decade of life. *Am. J. Respir. Crit. Care Med.* 194, 607–612.
- Bitko, V., Shulyayeva, O., Mazumder, B., Musiyenko, A., Ramaswamy, M., Look, D.C., and Barik, S. (2007). Nonstructural proteins of respiratory syncytial

- virus suppress premature apoptosis by an NF- κ B-dependent, interferon-independent mechanism and facilitate virus growth. *J. Virol.* 81, 1786–1795.
- Blount, R.E., Jr., Morris, J.A., and Savage, R.E. (1956). Recovery of cytopathogenic agent from chimpanzees with coryza. *Proc. Soc. Exp. Biol. Med.* 92, 544–549.
- Boyoglu-Barnum, S., Chirkova, T., Todd, S.O., Barnum, T.R., Gaston, K.A., Jorquera, P., Haynes, L.M., Tripp, R.A., Moore, M.L., and Anderson, L.J. (2014). Prophylaxis with a respiratory syncytial virus (RSV) anti-G protein monoclonal antibody shifts the adaptive immune response to RSV rA2-line19F infection from Th2 to Th1 in BALB/c mice. *J. Virol.* 88, 10569–10583.
- Chanock, R., and Finberg, L. (1957). Recovery from infants with respiratory illness of a virus related to chimpanzee coryza agent (CCA). II. Epidemiologic aspects of infection in infants and young children. *Am. J. Hyg.* 66, 291–300.
- Chin, J., Magoffin, R.L., Shearer, L.A., Schieble, J.H., and Lennette, E.H. (1969). Field evaluation of a respiratory syncytial virus vaccine and a trivalent parainfluenza virus vaccine in a pediatric population. *Am. J. Epidemiol.* 89, 449–463.
- Chirkova, T., Boyoglu-Barnum, S., Gaston, K.A., Malik, F.M., Trau, S.P., Oomens, A.G., and Anderson, L.J. (2013). Respiratory syncytial virus G protein CX3C motif impairs human airway epithelial and immune cell responses. *J. Virol.* 87, 13466–13479.
- Chirkova, T., Lin, S., Oomens, A.G., Gaston, K.A., Boyoglu-Barnum, S., Meng, J., Stobart, C.C., Cotton, C.U., Hartert, T.V., Moore, M.L., et al. (2015). CX3CR1 is an important surface molecule for respiratory syncytial virus infection in human airway epithelial cells. *J. Gen. Virol.* 96, 2543–2556.
- Choi, E.H., Lee, H.J., Yoo, T., and Chanock, S.J. (2002). A common haplotype of interleukin-4 gene IL4 is associated with severe respiratory syncytial virus disease in Korean children. *J. Infect. Dis.* 186, 1207–1211.
- Choi, Y., Mason, C.S., Jones, L.P., Crabtree, J., Jorquera, P.A., and Tripp, R.A. (2012). Antibodies to the central conserved region of respiratory syncytial virus (RSV) G protein block RSV G protein CX3C-CX3CR1 binding and cross-neutralize RSV A and B strains. *Viral Immunol.* 25, 193–203.
- Christiaansen, A.F., Knudson, C.J., Weiss, K.A., and Varga, S.M. (2014). The CD4 T cell response to respiratory syncytial virus infection. *Immunol. Res.* 59, 109–117.
- Chu, H.Y., Steinhoff, M.C., Magaret, A., Zaman, K., Roy, E., Langdon, G., Formica, M.A., Walsh, E.E., and Englund, J.A. (2014). Respiratory syncytial virus transplacental antibody transfer and kinetics in mother-infant pairs in Bangladesh. *J. Infect. Dis.* 210, 1582–1589.
- Corti, D., Bianchi, S., Vanzetta, F., Minola, A., Perez, L., Agatic, G., Guarino, B., Silacci, C., Marcandalli, J., Marsland, B.J., et al. (2013). Cross-neutralization of four paramyxoviruses by a human monoclonal antibody. *Nature* 507, 439–443.
- Crank, M.C., Ruckwardt, T.J., Chen, M., Morabito, K.M., Phung, E., Costner, P.J., Holman, L.A., Hickman, S.P., Berkowitz, N.M., Gordon, I.J., et al.; VRC 317 Study Team (2019). A proof of concept for structure-based vaccine design targeting RSV in humans. *Science* 365, 505–509.
- De Swart, R.L., Kuiken, T., Timmerman, H.H., van Amerongen, G., Van Den Hoogen, B.G., Vos, H.W., Neijens, H.J., Andeweg, A.C., and Osterhaus, A.D. (2002). Immunization of macaques with formalin-inactivated respiratory syncytial virus (RSV) induces interleukin-13-associated hypersensitivity to subsequent RSV infection. *J. Virol.* 76, 11561–11569.
- Delgado, M.F., and Polack, F.P. (2004). Involvement of antibody, complement and cellular immunity in the pathogenesis of enhanced respiratory syncytial virus disease. *Expert Rev. Vaccines* 3, 693–700.
- Domachowski, J.B., Khan, A.A., Esser, M.T., Jensen, K., Takas, T., Villafana, T., Dubovsky, F., and Griffin, M.P. (2018). Safety, tolerability and pharmacokinetics of MEDI8897, an extended half-life single-dose respiratory syncytial virus prefusion F-targeting monoclonal antibody administered as a single dose to healthy preterm infants. *Pediatr. Infect. Dis. J.* 37, 886–892.
- El Saleeby, C.M., Suzich, J., Conley, M.E., and DeVincenzo, J.P. (2004). Quantitative effects of palivizumab and donor-derived T cells on chronic respiratory syncytial virus infection, lung disease, and fusion glycoprotein amino acid sequences in a patient before and after bone marrow transplantation. *Clin. Infect. Dis.* 39, e17–e20.
- Falloon, J., Yu, J., Esser, M.T., Villafana, T., Yu, L., Dubovsky, F., Takas, T., Levin, M.J., and Falsey, A.R. (2017). An adjuvanted, postfusion F protein-based vaccine did not prevent respiratory syncytial virus illness in older adults. *J. Infect. Dis.* 216, 1362–1370.
- Falsey, A.R. (2007). Respiratory syncytial virus infection in adults. *Semin. Respir. Crit. Care Med.* 28, 171–181.
- Falsey, A.R., Hennessey, P.A., Formica, M.A., Cox, C., and Walsh, E.E. (2005). Respiratory syncytial virus infection in elderly and high-risk adults. *N. Engl. J. Med.* 352, 1749–1759.
- Falsey, A.R., and Walsh, E.E. (1996). Safety and immunogenicity of a respiratory syncytial virus subunit vaccine (PPF-2) in ambulatory adults over age 60. *Vaccine* 14, 1214–1218.
- Falsey, A.R., and Walsh, E.E. (1997). Safety and immunogenicity of a respiratory syncytial virus subunit vaccine (PPF-2) in the institutionalized elderly. *Vaccine* 15, 1130–1132.
- Feldman, S.A., Hendry, R.M., and Beeler, J.A. (1999). Identification of a linear heparin binding domain for human respiratory syncytial virus attachment glycoprotein G. *J. Virol.* 73, 6610–6617.
- Fulginiti, V.A., Eller, J.J., Sieber, O.F., Joyner, J.W., Minamitani, M., and Meiklejohn, G. (1969). Respiratory virus immunization. I. A field trial of two inactivated respiratory virus vaccines; an aqueous trivalent parainfluenza virus vaccine and an alum-precipitated respiratory syncytial virus vaccine. *Am. J. Epidemiol.* 89, 435–448.
- Gan, S.W., Tan, E., Lin, X., Yu, D., Wang, J., Tan, G.M., Vararattanavech, A., Yeo, C.Y., Soon, C.H., Soong, T.W., et al. (2012). The small hydrophobic protein of the human respiratory syncytial virus forms pentameric ion channels. *J. Biol. Chem.* 287, 24671–24689.
- Gentile, D.A., Doyle, W.J., Zeevi, A., Howe-Adams, J., Kapadia, S., Trecki, J., and Skoner, D.P. (2003). Cytokine gene polymorphisms moderate illness severity in infants with respiratory syncytial virus infection. *Hum. Immunol.* 64, 338–344.
- Ghosh, S., Champlin, R.E., Englund, J., Giralt, S.A., Rolston, K., Raad, I., Jacobson, K., Neumann, J., Ippoliti, C., Mallik, S., and Whimbey, E. (2000). Respiratory syncytial virus upper respiratory tract illnesses in adult blood and marrow transplant recipients: combination therapy with aerosolized ribavirin and intravenous immunoglobulin. *Bone Marrow Transplant.* 25, 751–755.
- Gilman, M.S., Castellanos, C.A., Chen, M., Ngwuta, J.O., Goodwin, E., Moin, S.M., Mas, V., Melerio, J.A., Wright, P.F., Graham, B.S., et al. (2016). Rapid profiling of RSV antibody repertoires from the memory B cells of naturally infected adult donors. *Sci. Immunol.* 7, eaaj1879.
- Glezen, W.P., Paredes, A., Allison, J.E., Taber, L.H., and Frank, A.L. (1981). Risk of respiratory syncytial virus infection for infants from low-income families in relationship to age, sex, ethnic group, and maternal antibody level. *J. Pediatr.* 98, 708–715.
- Goodpasture, E.W., Auerbach, S.H., Swanson, H.S., and Cotter, E.T. (1939). Virus pneumonia of infants secondary to epidemic infections. *Am. J. Dis. Child.* 57, 997–1011.
- Goodwin, E., Gilman, M.S.A., Wrapp, D., Chen, M., Ngwuta, J.O., Moin, S.M., Bai, P., Sivasubramanian, A., Connor, R.I., Wright, P.F., et al. (2018). Infants infected with respiratory syncytial virus generate potent neutralizing antibodies that lack somatic hypermutation. *Immunity* 48, 339–349.e5.
- Graham, B.S., Davis, T.H., Tang, Y.W., and Gruber, W.C. (1993a). Immunoprophylaxis and immunotherapy of respiratory syncytial virus-infected mice with respiratory syncytial virus-specific immune serum. *Pediatr. Res.* 34, 167–172.
- Graham, B.S., Henderson, G.S., Tang, Y.W., Lu, X., Neuzil, K.M., and Colley, D.G. (1993b). Priming immunization determines T helper cytokine mRNA expression patterns in lungs of mice challenged with respiratory syncytial virus. *J. Immunol.* 151, 2032–2040.
- Graham, B.S., Tang, Y.W., and Gruber, W.C. (1995). Topical immunoprophylaxis of respiratory syncytial virus (RSV)-challenged mice with RSV-specific immune globulin. *J. Infect. Dis.* 171, 1468–1474.
- Groothuis, J.R., Simoes, E.A., and Hemming, V.G.; Respiratory Syncytial Virus Immune Globulin Study Group (1995). Respiratory syncytial virus (RSV) infection in preterm infants and the protective effects of RSV immune globulin (RSVIG). *Pediatrics* 95, 463–467.
- Groothuis, J.R., Simoes, E.A., Levin, M.J., Hall, C.B., Long, C.E., Rodriguez, W.J., Arrobbio, J., Meissner, H.C., Fulton, D.R., Welliver, R.C., et al.; The

- Respiratory Syncytial Virus Immune Globulin Study Group (1993). Prophylactic administration of respiratory syncytial virus immune globulin to high-risk infants and young children. *N. Engl. J. Med.* **329**, 1524–1530.
- Gurnett-Bander, A., Perez-Caballero, D., Sivapalasingam, S., Duan, X., and MacDonald, D. (2016). Human antibodies to respiratory syncytial virus F protein and methods of use thereof. US patent, 10,125,188.
- Habibi, M.S., Jozwik, A., Makris, S., Dunning, J., Paras, A., DeVincenzo, J.P., de Haan, C.A., Wrammert, J., Openshaw, P.J., and Chiu, C.; Mechanisms of Severe Acute Influenza Consortium Investigators (2015). Impaired antibody-mediated protection and defective IgA B-cell memory in experimental infection of adults with respiratory syncytial virus. *Am. J. Respir. Crit. Care Med.* **191**, 1040–1049.
- Hall, C.B., Powell, K.R., MacDonald, N.E., Gala, C.L., Menegus, M.E., Suffin, S.C., and Cohen, H.J. (1986). Respiratory syncytial viral infection in children with compromised immune function. *N. Engl. J. Med.* **315**, 77–81.
- Hall, C.B., Simões, E.A., and Anderson, L.J. (2013). Clinical and epidemiologic features of respiratory syncytial virus. *Curr. Top. Microbiol. Immunol.* **372**, 39–57.
- Hall, C.B., Walsh, E.E., Long, C.E., and Schnabel, K.C. (1991). Immunity to and frequency of reinfection with respiratory syncytial virus. *J. Infect. Dis.* **163**, 693–698.
- Hancock, G.E., Speelman, D.J., Heers, K., Bortell, E., Smith, J., and Cosco, C. (1996). Generation of atypical pulmonary inflammatory responses in BALB/c mice after immunization with the native attachment (G) glycoprotein of respiratory syncytial virus. *J. Virol.* **70**, 7783–7791.
- Heidema, J., Lukens, M.V., van Maren, W.W., van Dijk, M.E., Otten, H.G., van Vught, A.J., van der Werff, D.B., van Gestel, S.J., Semple, M.G., Smyth, R.L., et al. (2007). CD8+ T cell responses in bronchoalveolar lavage fluid and peripheral blood mononuclear cells of infants with severe primary respiratory syncytial virus infections. *J. Immunol.* **179**, 8410–8417.
- Hoebee, B., Rietveld, E., Bont, L., Oosten, Mv., Hodemaekers, H.M., Nagelkerke, N.J., Neijens, H.J., Kimpen, J.L., and Kimman, T.G. (2003). Association of severe respiratory syncytial virus bronchiolitis with interleukin-4 and interleukin-4 receptor alpha polymorphisms. *J. Infect. Dis.* **187**, 2–11.
- The Impact-RSV Study Group (1998). Palivizumab, a humanized respiratory syncytial virus monoclonal antibody, reduces hospitalization from respiratory syncytial virus infection in high-risk infants. *Pediatrics* **102**, 531–537.
- Jallow, S., Agosti, Y., Kragadi, P., Vandecar, M., Cutland, C.L., Simoes, E.A.F., Nunes, M.C., Suchard, M.S., and Madhi, S.A. (2018). Impaired transplacental transfer of respiratory syncytial virus (RSV) neutralizing antibodies in HIV-infected compared to HIV-uninfected pregnant women. *Clin. Infect. Dis.* **69**, 151–154.
- Johnson, J.E., Gonzales, R.A., Olson, S.J., Wright, P.F., and Graham, B.S. (2007). The histopathology of fatal untreated human respiratory syncytial virus infection. *Mod. Pathol.* **20**, 108–119.
- Johnson, S., Griego, S.D., Pfarr, D.S., Doyle, M.L., Woods, R., Carlin, D., Prince, G.A., Koenig, S., Young, J.F., and Dillon, S.B. (1999). A direct comparison of the activities of two humanized respiratory syncytial virus monoclonal antibodies: MEDI-493 and RSH29. *J. Infect. Dis.* **180**, 35–40.
- Johnson, S., Oliver, C., Prince, G.A., Hemming, V.G., Pfarr, D.S., Wang, S.C., Dormitzer, M., O'Grady, J., Koenig, S., Tamura, J.K., et al. (1997). Development of a humanized monoclonal antibody (MEDI-493) with potent in vitro and in vivo activity against respiratory syncytial virus. *J. Infect. Dis.* **176**, 1215–1224.
- Johnson, T.R., and Graham, B.S. (1999). Secreted respiratory syncytial virus G glycoprotein induces interleukin-5 (IL-5), IL-13, and eosinophilia by an IL-4-independent mechanism. *J. Virol.* **73**, 8485–8495.
- Johnson, T.R., Johnson, J.E., Roberts, S.R., Wertz, G.W., Parker, R.A., and Graham, B.S. (1998). Priming with secreted glycoprotein G of respiratory syncytial virus (RSV) augments interleukin-5 production and tissue eosinophilia after RSV challenge. *J. Virol.* **72**, 2871–2880.
- Johnson, T.R., McLellan, J.S., and Graham, B.S. (2012). Respiratory syncytial virus glycoprotein G interacts with DC-SIGN and L-SIGN to activate ERK1 and ERK2. *J. Virol.* **86**, 1339–1347.
- Johnson, T.R., Teng, M.N., Collins, P.L., and Graham, B.S. (2004a). Respiratory syncytial virus (RSV) G glycoprotein is not necessary for vaccine-enhanced disease induced by immunization with formalin-inactivated RSV. *J. Virol.* **78**, 6024–6032.
- Johnson, T.R., Varga, S.M., Braciale, T.J., and Graham, B.S. (2004b). Vbeta14(+) T cells mediate the vaccine-enhanced disease induced by immunization with respiratory syncytial virus (RSV) G glycoprotein but not with formalin-inactivated RSV. *J. Virol.* **78**, 8753–8760.
- Jones, B.G., Sealy, R.E., Rudraraju, R., Traina-Dorge, V.L., Finneyfrock, B., Cook, A., Takimoto, T., Portner, A., and Hurwitz, J.L. (2012). Sendai virus-based RSV vaccine protects African green monkeys from RSV infection. *Vaccine* **30**, 959–968.
- Jones, H.G., Ritschel, T., Pascual, G., Brakenhoff, J.P.J., Keogh, E., Furmanova-Hollenstein, P., Lanckacker, E., Wadia, J.S., Gilman, M.S.A., Williamson, R.A., et al. (2018). Structural basis for recognition of the central conserved region of RSV G by neutralizing human antibodies. *PLoS Pathog.* **14**, e1006935.
- Jozwik, A., Habibi, M.S., Paras, A., Zhu, J., Guvenel, A., Dhariwal, J., Almond, M., Wong, E.H.C., Sykes, A., Maybeno, M., et al. (2015). RSV-specific airway resident memory CD8+ T cells and differential disease severity after experimental human infection. *Nat. Commun.* **6**, 10224.
- Kalina, W.V., Woolums, A.R., and Gershwin, L.J. (2005). Formalin-inactivated bovine RSV vaccine influences antibody levels in bronchoalveolar lavage fluid and disease outcome in experimentally infected calves. *Vaccine* **23**, 4625–4630.
- Kapikian, A.Z., Mitchell, R.H., Chanock, R.M., Shvedoff, R.A., and Stewart, C.E. (1969). An epidemiologic study of altered clinical reactivity to respiratory syncytial (RS) virus infection in children previously vaccinated with an inactivated RS virus vaccine. *Am. J. Epidemiol.* **89**, 405–421.
- Karron, R.A., Buchholz, U.J., and Collins, P.L. (2013). Live-attenuated respiratory syncytial virus vaccines. *Curr. Top. Microbiol. Immunol.* **372**, 259–284.
- Karron, R.A., Buonagurio, D.A., Georgiu, A.F., Whitehead, S.S., Adamus, J.E., Clements-Mann, M.L., Harris, D.O., Randolph, V.B., Udem, S.A., Murphy, B.R., and Sidhu, M.S. (1997). Respiratory syncytial virus (RSV) SH and G proteins are not essential for viral replication in vitro: clinical evaluation and molecular characterization of a cold-passaged, attenuated RSV subgroup B mutant. *Proc. Natl. Acad. Sci. U S A* **94**, 13961–13966.
- Ke, Z., Dillard, R.S., Chirkova, T., Leon, F., Stobart, C.C., Hampton, C.M., Strauss, J.D., Rajan, D., Rostad, C.A., Taylor, J.V., et al. (2018). The morphology and assembly of respiratory syncytial virus revealed by cryo-electron tomography. *Viruses* **10**, E446.
- Killikelly, A.M., Kanekiyo, M., and Graham, B.S. (2016). Pre-fusion F is absent on the surface of formalin-inactivated respiratory syncytial virus. *Sci. Rep.* **6**, 34108.
- Kim, H.W., Canchola, J.G., Brandt, C.D., Pyles, G., Chanock, R.M., Jensen, K., and Parrott, R.H. (1969). Respiratory syncytial virus disease in infants despite prior administration of antigenic inactivated vaccine. *Am. J. Epidemiol.* **89**, 422–434.
- Kim, H.W., Leikin, S.L., Arrobio, J., Brandt, C.D., Chanock, R.M., and Parrott, R.H. (1976). Cell-mediated immunity to respiratory syncytial virus induced by inactivated vaccine or by infection. *Pediatr. Res.* **10**, 75–78.
- Kim, Y.J., Guthrie, K.A., Waghmare, A., Walsh, E.E., Faisey, A.R., Kuypers, J., Cent, A., Englund, J.A., and Boeckh, M. (2014). Respiratory syncytial virus in hematopoietic cell transplant recipients: factors determining progression to lower respiratory tract disease. *J. Infect. Dis.* **209**, 1195–1204.
- Kiss, G., Holl, J.M., Williams, G.M., Alonas, E., Vanover, D., Lifland, A.W., Gudheti, M., Guerrero-Ferreira, R.C., Nair, V., Yi, H., et al. (2014). Structural analysis of respiratory syncytial virus reveals the position of M2-1 between the matrix protein and the ribonucleoprotein complex. *J. Virol.* **88**, 7602–7617.
- Krishnaswamy, S., Lambach, P., and Giles, M.L. (2019). Key considerations for successful implementation of maternal immunization programs in low and middle income countries. *Hum. Vaccin. Immunother.* **15**, 942–950.
- Kwakkenbos, M.J., Diehl, S.A., Yasuda, E., Bakker, A.Q., van Geelen, C.M., Lukens, M.V., van Bleek, G.M., Widjoatmodjo, M.N., Bogers, W.M., Mei, H., et al. (2010). Generation of stable monoclonal antibody-producing B cell receptor-positive human memory B cells by genetic programming. *Nat. Med.* **16**, 123–128.
- Lambert, L., Sagfors, A.M., Openshaw, P.J., and Culley, F.J. (2014). Immunity to RSV in Early-Life. *Front. Immunol.* **5**, 466.

- Langley, J.M., MacDonald, L.D., Weir, G.M., MacKinnon-Cameron, D., Ye, L., McNeil, S., Schepens, B., Saelens, X., Stanford, M.M., and Halperin, S.A. (2018). A respiratory syncytial virus vaccine based on the small hydrophobic protein ectodomain presented with a novel lipid-based formulation is highly immunogenic and safe in adults: a first-in-humans study. *J. Infect. Dis.* *218*, 378–387.
- Liang, B., Ngwuta, J.O., Surman, S., Kabatova, B., Liu, X., Lingemann, M., Liu, X., Yang, L., Herbert, R., Swerczek, J., et al. (2017). Improved prefusion stability, optimized codon usage, and augmented virion packaging enhance the immunogenicity of respiratory syncytial virus fusion protein in a vectored-vaccine candidate. *J. Virol.* *91*, e00189-17.
- Liang, B., Surman, S., Amaro-Carambot, E., Kabatova, B., Mackow, N., Lingemann, M., Yang, L., McLellan, J.S., Graham, B.S., Kwong, P.D., et al. (2015). Enhanced neutralizing antibody response induced by respiratory syncytial virus prefusion F protein expressed by a vaccine candidate. *J. Virol.* *89*, 9499–9510.
- Liu, X., Liang, B., Ngwuta, J., Liu, X., Surman, S., Lingemann, M., Kwong, P.D., Graham, B.S., Collins, P.L., and Munir, S. (2017). Attenuated human parainfluenza virus type 1 expressing the respiratory syncytial virus (RSV) fusion (F) glycoprotein from an added gene: effects of prefusion stabilization and packaging of RSV F. *J. Virol.* *91*, e01101-17.
- Lozano, R., Naghavi, M., Foreman, K., Lim, S., Shibuya, K., Aboyans, V., Abraham, J., Adair, T., Aggarwal, R., Ahn, S.Y., et al. (2012). Global and regional mortality from 235 causes of death for 20 age groups in 1990 and 2010: a systematic analysis for the Global Burden of Disease Study 2010. *Lancet* *380*, 2095–2128.
- Lu, B., Liu, H., Tabor, D.E., Tovchigrechko, A., Qi, Y., Ruzin, A., Esser, M.T., and Jin, H. (2019). Emergence of new antigenic epitopes in the glycoproteins of human respiratory syncytial virus collected from a US surveillance study, 2015–17. *Sci. Rep.* *9*, 3898.
- Luchsinger, V., Piedra, P.A., Ruiz, M., Zunino, E., Martínez, M.A., Machado, C., Fasce, R., Ulloa, M.T., Fink, M.C., Lara, P., and Avendaño, L.F. (2012). Role of neutralizing antibodies in adults with community-acquired pneumonia by respiratory syncytial virus. *Clin. Infect. Dis.* *54*, 905–912.
- Lukens, M.V., van de Pol, A.C., Coenjaerts, F.E., Jansen, N.J., Kamp, V.M., Kimpen, J.L., Rossen, J.W., Ulfman, L.H., Tacke, C.E., Viveen, M.C., et al. (2010). A systemic neutrophil response precedes robust CD8(+) T-cell activation during natural respiratory syncytial virus infection in infants. *J. Virol.* *84*, 2374–2383.
- Luongo, C., Winter, C.C., Collins, P.L., and Buchholz, U.J. (2013). Respiratory syncytial virus modified by deletions of the NS2 gene and amino acid S1313 of the L polymerase protein is a temperature-sensitive, live-attenuated vaccine candidate that is phenotypically stable at physiological temperature. *J. Virol.* *87*, 1985–1996.
- Magro, M., Mas, V., Chappell, K., Vázquez, M., Cano, O., Luque, D., Terrón, M.C., Melero, J.A., and Palomo, C. (2012). Neutralizing antibodies against the preactive form of respiratory syncytial virus fusion protein offer unique possibilities for clinical intervention. *Proc. Natl. Acad. Sci. U S A* *109*, 3089–3094.
- Marcandalli, J., Fiala, B., Ols, S., Perotti, M., de van der Schueren, W., Snijder, J., Hodge, E., Benhaim, M., Ravichandran, R., Carter, L., et al. (2019). Induction of potent neutralizing antibody responses by a designed protein nanoparticle vaccine for respiratory syncytial virus. *Cell* *176*, 1420–1431.e17.
- Mazur, N.I., Higgins, D., Nunes, M.C., Melero, J.A., Langedijk, A.C., Horsley, N., Buchholz, U.J., Openshaw, P.J., McLellan, J.S., Englund, J.A., et al.; Respiratory Syncytial Virus Network (ReSVINET) Foundation (2018). The respiratory syncytial virus vaccine landscape: lessons from the graveyard and promising candidates. *Lancet Infect. Dis.* *18*, e295–e311.
- McFarland, E.J., Karron, R.A., Muresan, P., Cunningham, C.K., Valentine, M.E., Perlowski, C., Thumar, B., Gnanashanmugam, D., Siberry, G.K., Schappell, E., et al.; International Maternal Pediatric Adolescent AIDS Clinical Trials (IMPAACT) 2000 Study Team (2018). Live-attenuated respiratory syncytial virus vaccine candidate with deletion of RNA synthesis regulatory protein M2-2 is highly immunogenic in children. *J. Infect. Dis.* *217*, 1347–1355.
- McGinnes Cullen, L., Schmidt, M.R., Kenward, S.A., Woodland, R.T., and Morrison, T.G. (2015). Murine immune responses to virus-like particle-associated pre- and postfusion forms of the respiratory syncytial virus F protein. *J. Virol.* *89*, 6835–6847.
- McLellan, J.S., Chen, M., Joyce, M.G., Sastry, M., Stewart-Jones, G.B., Yang, Y., Zhang, B., Chen, L., Srivatsan, S., Zheng, A., et al. (2013a). Structure-based design of a fusion glycoprotein vaccine for respiratory syncytial virus. *Science* *342*, 592–598.
- McLellan, J.S., Chen, M., Leung, S., Graepel, K.W., Du, X., Yang, Y., Zhou, T., Baxa, U., Yasuda, E., Beaumont, T., et al. (2013b). Structure of RSV fusion glycoprotein trimer bound to a prefusion-specific neutralizing antibody. *Science* *340*, 1113–1117.
- Mehta, J., Walsh, E.E., Mahadevia, P.J., and Falsey, A.R. (2013). Risk factors for respiratory syncytial virus illness among patients with chronic obstructive pulmonary disease. *COPD* *10*, 293–299.
- Meng, J., Lee, S., Hotard, A.L., and Moore, M.L. (2014). Refining the balance of attenuation and immunogenicity of respiratory syncytial virus by targeted codon deoptimization of virulence genes. *MBio* *5*, e01704–e01714.
- Mousa, J.J., Kose, N., Matta, P., Gilchuk, P., and Crowe, J.E., Jr. (2017). A novel pre-fusion conformation-specific neutralizing epitope on the respiratory syncytial virus fusion protein. *Nat. Microbiol.* *2*, 16271.
- Munoz, F.M. (2015). Respiratory syncytial virus in infants: is maternal vaccination a realistic strategy? *Curr. Opin. Infect. Dis.* *28*, 221–224.
- Munoz, F.M., and Jamieson, D.J. (2019). Maternal Immunization. *Obstet. Gynecol.* *133*, 739–753.
- Munywoki, P.K., Koeh, D.C., Agoti, C.N., Lewa, C., Cane, P.A., Medley, G.F., and Nokes, D.J. (2014). The source of respiratory syncytial virus infection in infants: a household cohort study in rural Kenya. *J. Infect. Dis.* *209*, 1685–1692.
- Murphy, B.R., Alling, D.W., Snyder, M.H., Walsh, E.E., Prince, G.A., Chanock, R.M., Hemming, V.G., Rodriguez, W.J., Kim, H.W., Graham, B.S., et al. (1986). Effect of age and preexisting antibody on serum antibody response of infants and children to the F and G glycoproteins during respiratory syncytial virus infection. *J. Clin. Microbiol.* *24*, 894–898.
- Murphy, B.R., and Walsh, E.E. (1988). Formalin-inactivated respiratory syncytial virus vaccine induces antibodies to the fusion glycoprotein that are deficient in fusion-inhibiting activity. *J. Clin. Microbiol.* *26*, 1595–1597.
- Neemann, K., and Freifeld, A. (2015). Respiratory syncytial virus in hematopoietic stem cell transplantation and solid-organ transplantation. *Curr. Infect. Dis. Rep.* *17*, 490.
- Ngwuta, J.O., Chen, M., Modjarrad, K., Joyce, M.G., Kanekiyo, M., Kumar, A., Yassine, H.M., Moin, S.M., Killikelly, A.M., Chuang, G.Y., et al. (2015). Prefusion F-specific antibodies determine the magnitude of RSV neutralizing activity in human sera. *Sci. Transl. Med.* *7*, 309ra162.
- O'Brien, K.L., Chandran, A., Weatherholtz, R., Jafri, H.S., Griffin, M.P., Bellamy, T., Millar, E.V., Jensen, K.M., Harris, B.S., Reid, R., et al.; Respiratory Syncytial Virus (RSV) Prevention study group (2015). Efficacy of motavizumab for the prevention of respiratory syncytial virus disease in healthy Native American infants: a phase 3 randomised double-blind placebo-controlled trial. *Lancet Infect. Dis.* *15*, 1398–1408.
- Openshaw, P.J., Clarke, S.L., and Record, F.M. (1992). Pulmonary eosinophilic response to respiratory syncytial virus infection in mice sensitized to the major surface glycoprotein G. *Int. Immunol.* *4*, 493–500.
- Paradiso, P.R., Hildreth, S.W., Hogerman, D.A., Speelman, D.J., Lewin, E.B., Oren, J., and Smith, D.H. (1994). Safety and immunogenicity of a subunit respiratory syncytial virus vaccine in children 24 to 48 months old. *Pediatr. Infect. Dis. J.* *13*, 792–798.
- Parrish, J. (1826). Observations on a peculiar catarrhal complaint in children. *North American Medical and Surgical Journal* *1*, 24–31.
- Phung, E., Chang, L.A., Morabito, K.M., Kanekiyo, M., Chen, M., Nair, D., Kumar, A., Chen, G.L., Ledgerwood, J.E., Graham, B.S., and Ruckwardt, T.J. (2019). Epitope-specific serological assays for RSV: conformation matters. *Vaccines (Basel)* *7*, E23.
- Piedra, P.A., Jewell, A.M., Cron, S.G., Atmar, R.L., and Glezen, W.P. (2003). Correlates of immunity to respiratory syncytial virus (RSV) associated-hospitalization: establishment of minimum protective threshold levels of serum neutralizing antibodies. *Vaccine* *21*, 3479–3482.
- Piedra, P.A., Wyde, P.R., Castleman, W.L., Ambrose, M.W., Jewell, A.M., Speelman, D.J., and Hildreth, S.W. (1993). Enhanced pulmonary pathology

- associated with the use of formalin-inactivated respiratory syncytial virus vaccine in cotton rats is not a unique viral phenomenon. *Vaccine* 17, 1415–1423.
- Plotnicky-Gilquin, H., Goetsch, L., Huss, T., Champion, T., Beck, A., Haeuw, J.F., Nguyen, T.N., Bonnefoy, J.Y., Corvaia, N., and Power, U.F. (1999). Identification of multiple protective epitopes (protectopes) in the central conserved domain of a prototype human respiratory syncytial virus G protein. *J. Virol.* 73, 5637–5645.
- Pneumonia Etiology Research for Child Health (PERCH) Study Group (2019). Causes of severe pneumonia requiring hospital admission in children without HIV infection from Africa and Asia: the PERCH multi-country case-control study. *Lancet*. Published online June 27, 2019. [https://doi.org/10.1016/S0140-6736\(19\)30721-4](https://doi.org/10.1016/S0140-6736(19)30721-4).
- Polack, F.P., Teng, M.N., Collins, P.L., Prince, G.A., Exner, M., Regele, H., Lirman, D.D., Rabold, R., Hoffman, S.J., Karp, C.L., et al. (2002). A role for immune complexes in enhanced respiratory syncytial virus disease. *J. Exp. Med.* 196, 859–865.
- Poletti, P., Merler, S., Ajelli, M., Manfredi, P., Munywoki, P.K., Nokes, D., and Melegaro, A. (2015). Evaluating vaccination strategies for reducing infant respiratory syncytial virus infection in low-income settings. *BMC Med.* 13, 49.
- Power, U.F., Nguyen, T.N., Rietveld, E., de Swart, R.L., Groen, J., Osterhaus, A.D., de Groot, R., Corvaia, N., Beck, A., Bouveret-Le-Cam, N., and Bonnefoy, J.Y. (2001). Safety and immunogenicity of a novel recombinant subunit respiratory syncytial virus vaccine (BBG2Na) in healthy young adults. *J. Infect. Dis.* 184, 1456–1460.
- The PREVENT Study Group (1997). Reduction of respiratory syncytial virus hospitalization among premature infants and infants with bronchopulmonary dysplasia using respiratory syncytial virus immune globulin prophylaxis. *Pediatrics* 99, 93–99.
- Prince, G.A., Horswood, R.L., and Chanock, R.M. (1985). Quantitative aspects of passive immunity to respiratory syncytial virus infection in infant cotton rats. *J. Virol.* 55, 517–520.
- Puthothu, B., Krueger, M., Forster, J., and Heinzmann, A. (2006). Association between severe respiratory syncytial virus infection and IL13/IL4 haplotypes. *J. Infect. Dis.* 193, 438–441.
- Rima, B., Collins, P., Easton, A., Fouchier, R., Kurath, G., Lamb, R.A., Lee, B., Maisner, A., Rota, P., and Wang, L.; Ictv Report Consortium (2017). ICTV virus taxonomy profile: pneumoviridae. *J. Gen. Virol.* 98, 2912–2913.
- Roberts, S.R., Lichtenstein, D., Ball, L.A., and Wertz, G.W. (1994). The membrane-associated and secreted forms of the respiratory syncytial virus attachment glycoprotein G are synthesized from alternative initiation codons. *J. Virol.* 68, 4538–4546.
- Rostad, C.A., Stobart, C.C., Todd, S.O., Molina, S.A., Lee, S., Blanco, J.C.G., and Moore, M.L. (2018). Enhancing the thermostability and immunogenicity of a respiratory syncytial virus (RSV) live-attenuated vaccine by incorporating unique RSV line19f protein residues. *J. Virol.* 92, e01568–17.
- Ruckwardt, T.J., Morabito, K.M., and Graham, B.S. (2016). Determinants of early life immune responses to RSV infection. *Curr. Opin. Virol.* 16, 151–157.
- Russell, C.J., and Hurwitz, J.L. (2016). Sendai virus as a backbone for vaccines against RSV and other human paramyxoviruses. *Expert Rev. Vaccines* 15, 189–200.
- Schepens, B., Sedeyn, K., Vande Ginste, L., De Baets, S., Schotsaert, M., Roose, K., Houspie, L., Van Ranst, M., Gilbert, B., van Rooijen, N., et al. (2014). Protection and mechanism of action of a novel human respiratory syncytial virus vaccine candidate based on the extracellular domain of small hydrophobic protein. *EMBO Mol. Med.* 6, 1436–1454.
- Schittny, J.C. (2017). Development of the lung. *Cell Tissue Res.* 367, 427–444.
- Schmidt, M.E., and Varga, S.M. (2018). The CD8 T cell response to respiratory virus infections. *Front. Immunol.* 9, 678.
- Shaw, C.A., Galarnau, J.R., Bowenkamp, K.E., Swanson, K.A., Palmer, G.A., Palladino, G., Markovits, J.E., Valiante, N.M., Dormitzer, P.R., and Otten, G.R. (2013). The role of non-viral antigens in the cotton rat model of respiratory syncytial virus vaccine-enhanced disease. *Vaccine* 31, 306–312.
- Shi, T., Denouel, A., Tietjen, A.K., Campbell, I., Moran, E., Li, X., Campbell, H., Demont, C., Nyawanda, B.O., Chu, H.Y., et al. (2019). Global disease burden estimates of respiratory syncytial virus-associated acute respiratory infection in older adults in 2015: a systematic review and meta-analysis. *J. Infect. Dis.* Published online March 18, 2019. <https://doi.org/10.1093/infdis/jiz059>.
- Shi, T., McAllister, D.A., O'Brien, K.L., Simoes, E.A.F., Madhi, S.A., Gessner, B.D., Polack, F.P., Balsells, E., Acacio, S., Aguayo, C., et al.; RSV Global Epidemiology Network (2017). Global, regional, and national disease burden estimates of acute lower respiratory infections due to respiratory syncytial virus in young children in 2015: a systematic review and modelling study. *Lancet* 390, 946–958.
- Shinoff, J.J., O'Brien, K.L., Thumar, B., Shaw, J.B., Reid, R., Hua, W., Santosham, M., and Karron, R.A. (2008). Young infants can develop protective levels of neutralizing antibody after infection with respiratory syncytial virus. *J. Infect. Dis.* 198, 1007–1015.
- Spann, K.M., Tran, K.C., Chi, B., Rabin, R.L., and Collins, P.L. (2004). Suppression of the induction of alpha, beta, and lambda interferons by the NS1 and NS2 proteins of human respiratory syncytial virus in human epithelial cells and macrophages [corrected]. *J. Virol.* 78, 4363–4369.
- Spann, K.M., Tran, K.C., and Collins, P.L. (2005). Effects of nonstructural proteins NS1 and NS2 of human respiratory syncytial virus on interferon regulatory factor 3, NF-kappaB, and proinflammatory cytokines. *J. Virol.* 79, 5353–5362.
- Srikiatkachom, A., and Braciale, T.J. (1997). Virus-specific CD8+ T lymphocytes downregulate T helper cell type 2 cytokine secretion and pulmonary eosinophilia during experimental murine respiratory syncytial virus infection. *J. Exp. Med.* 186, 421–432.
- Stensballe, L.G., Ravn, H., Kristensen, K., Meakins, T., Aaby, P., and Simoes, E.A. (2009). Seasonal variation of maternally derived respiratory syncytial virus antibodies and association with infant hospitalizations for respiratory syncytial virus. *J. Pediatr.* 154, 296–298.
- Stobart, C.C., Rostad, C.A., Ke, Z., Dillard, R.S., Hampton, C.M., Strauss, J.D., Yi, H., Hotard, A.L., Meng, J., Pickles, R.J., et al. (2016). A live RSV vaccine with engineered thermostability is immunogenic in cotton rats despite high attenuation. *Nat. Commun.* 7, 13916.
- Swedan, S., Musiyenko, A., and Barik, S. (2009). Respiratory syncytial virus nonstructural proteins decrease levels of multiple members of the cellular interferon pathways. *J. Virol.* 83, 9682–9693.
- Taussig, L.M., Wright, A.L., Holberg, C.J., Halonen, M., Morgan, W.J., and Martinez, F.D. (2003). Tucson Children's Respiratory Study: 1980 to present. *J. Allergy Clin. Immunol.* 111, 661–675, quiz 676.
- Trefny, P., Stricker, T., Baerlocher, C., and Sennhauser, F.H. (2000). Family history of atopy and clinical course of RSV infection in ambulatory and hospitalized infants. *Pediatr. Pulmonol.* 30, 302–306.
- Trisram, D.A., Welliver, R.C., Mohar, C.K., Hogerman, D.A., Hildreth, S.W., and Paradiso, P. (1993). Immunogenicity and safety of respiratory syncytial virus subunit vaccine in seropositive children 18–36 months old. *J. Infect. Dis.* 167, 191–195.
- Villafana, T., Falloon, J., Griffin, M.P., Zhu, Q., and Esser, M.T. (2017). Passive and active immunization against respiratory syncytial virus for the young and old. *Expert Rev. Vaccines* 16, 1–13.
- Walsh, E.E., Peterson, D.R., and Falsey, A.R. (2004). Risk factors for severe respiratory syncytial virus infection in elderly persons. *J. Infect. Dis.* 189, 233–238.
- Welliver, T.P., Garofalo, R.P., Hosakote, Y., Hintz, K.H., Avendano, L., Sanchez, K., Velozo, L., Jafri, H., Chavez-Bueno, S., Ogra, P.L., et al. (2007). Severe human lower respiratory tract illness caused by respiratory syncytial virus and influenza virus is characterized by the absence of pulmonary cytotoxic lymphocyte responses. *J. Infect. Dis.* 195, 1126–1136.
- Wittig, H.J., and Glaser, J. (1959). The relationship between bronchiolitis and childhood asthma; a follow-up study of 100 cases of bronchiolitis. *J. Allergy* 30, 19–23.
- Zhang, W., Choi, Y., Haynes, L.M., Harcourt, J.L., Anderson, L.J., Jones, L.P., and Tripp, R.A. (2010). Vaccination to induce antibodies blocking the CX3C-CX3CR1 interaction of respiratory syncytial virus G protein reduces pulmonary inflammation and virus replication in mice. *J. Virol.* 84, 1148–1157.
- Zhu, Q., McLellan, J.S., Kallewaard, N.L., Ulbrandt, N.D., Palaszynski, S., Zhang, J., Moldt, B., Khan, A., Svabek, C., McAuliffe, J.M., et al. (2017). A highly potent extended half-life antibody as a potential RSV vaccine surrogate for all infants. *Sci. Transl. Med.* 9, eaaj1928.